

Universidad de Granada
Programa de Doctorado en Ingeniería Civil



TESIS DOCTORAL

**Materiales Asfálticos Mecanomutables para la
Construcción de Pavimentos Inteligentes**

**Mechanomutable Asphalt Materials for the
Construction of Smart Pavements**

Paulina Leiva Padilla
Granada, octubre 2020

UNIVERSIDAD DE GRANADA
PROGRAMA DE DOCTORADO EN INGENIERÍA CIVIL
LABORATORIO DE INGENIERÍA DE LA CONSTRUCCIÓN



**MATERIALES ASFALTICOS MECANOMUTABLES PARA LA
CONSTRUCCIÓN DE PAVIMENTOS INTELIGENTES**

TESIS DOCTORAL

Paulina de los Ángeles Leiva Padilla

Directores de Tesis:

Dra. María del Carmen Rubio Gámez

Dr. Fernando Moreno Navarro

Granada, octubre 2020

Editor: Universidad de Granada. Tesis Doctorales
Autor: Paulina Leiva Padilla
ISBN: 978-84-1306-682-0
URI: <http://hdl.handle.net/10481/64575>

AGRADECIMIENTOS

Quiero comenzar esta sección agradeciendo a mis directores de tesis, los profesores María del Carmen Rubio Gámez y Fernando Moreno Navarro. En primer lugar, por permitirme ser parte de este maravilloso proyecto, definitivamente esta ha sido una experiencia que ha marcado mi vida en muchos aspectos. Y, en segundo lugar, por el acompañamiento continuo que he recibido de su parte, por su hospitalidad y cariño, por su apoyo constante. Me han hecho sentir en casa y privilegiada por contar con ustedes como directores.

Asimismo, quiero también ofrecer un agradecimiento especial al profesor Guillermo Iglesias Salto. Muchas gracias por su acompañamiento, por su apoyo, por su consejo, pero sobre todo por su capacidad de motivación, logró sacar lo mejor de mí.

En este mismo contexto, quiero agradecer profundamente a mis compañeros del grupo LabIC.UGR. Muchas gracias por tantas horas donde pudimos compartir no solo tareas de trabajo, si no también momentos que en definitiva conservaré como buenos recuerdos, realmente me han hecho sentir también en casa.

Y no me puedo quedar sin agradecer a todas las personas que conforman la Red de Capacitación Europea SMARTI, supervisores y becarios. Muchas gracias por las increíbles experiencias compartidas a lo largo de estos 3 años de enorme aprendizaje. Sin duda esta ha sido una experiencia que de por vida nos seguirá dando motivos para mantenernos en contacto.

Y para terminar esta sección, quiero agradecer a las nuevas amistades encontradas en este camino. Muchas gracias por su apoyo y su cariño, por esa sensación de familia que me han hecho sentir. En este mismo ámbito, quiero agradecer profundamente a aquellos y aquellas que la distancia física no los ha limitado a seguir en contacto: a mi familia y amigos en Costa Rica, han sido definitivamente el soporte para conquistar esta nueva meta.

RESUMEN

A través los años, la ingeniería ha trabajado en la propuesta de soluciones que permitan solventar las necesidades de la sociedad en términos de vivienda, servicios básicos, o comunicaciones, entre otros.

En el área de la ingeniería de carreteras, las labores han evolucionado desde las calzadas y los caminos rústicos, los caminos asfaltados, las carreteras de alta capacidad y más recientemente a la investigación e implementación de las vías sostenibles e inteligentes.

Esta nueva concepción de las carreteras, ha llevado al surgimiento de esfuerzos en la generación de materiales y sistemas inteligentes que, de forma integrada, pretenden reproducir la capacidad de los seres vivos de adaptarse y responder a las solicitaciones físicas del medio en que se encuentran.

Dentro de esta generación de materiales inteligentes se encuentran los materiales asfálticos mecanomutables (MAMs). Los MAMs están compuestos de una matriz bituminosa modificada con materiales con propiedades magnéticas/eléctricas que pueden responder a la aplicación de campos magnéticos.

A partir de esta definición, se ha identificado que los MAMs son ideales para ser potencialmente utilizados en el desarrollo de pavimentos asfálticos con capacidad de: (1) mejorar las propiedades mecánicas del pavimento, (2) emitir señales magnéticas que pueden ayudar en el guiado de los vehículos, y (3) aumentar su temperatura como mecanismo para la definición de nuevas alternativas de mantenimiento de carreteras.

En este sentido, durante la presente tesis doctoral se realizaron aportes a la línea de investigación del Laboratorio de Ingeniería de la Construcción de la Universidad de Granada (LabIC.UGR), en el desarrollo de cada una de estas aplicaciones potenciales de los MAMs a escala de morteros. Los resultados obtenidos permiten sentar las bases de los niveles de maduración tecnológica 1, 2 y 3, asociados a Tecnologías Futuras y Emergentes del Programa Horizonte 2020, del cual el presente proyecto es parte bajo las acciones Marie Skłodowska-Curie para investigación, desarrollo tecnológico y demostración, programa SMARTI ETN y beca n.721493.

Palabras clave: Materiales Asfálticos Mecanomutables, Materiales Electroconductivos, Campos Magnéticos, Pavimentos Inteligentes, Materiales Asfálticos Codificados.

ABSTRACT

Throughout the years, engineers have been working in the proposal of new solutions to meet the society needs in terms of housing, basic services, communications, among others.

In the field of road engineering, efforts have evolved from the roman and rustic roads, passing through paved roads, high capacity highways and more recently the research and implementation of sustainable and smart roads.

This new concept of roads has led to the emergence of important efforts addressed to develop smart materials and systems, which together are trying to reproduce the ability of living beings to adapt their performance to the physical demands of the environment in which they are located.

The Mechanomutable Asphalt Materials (MAMs) are part of this new generation of smart materials for roads. MAMs are composed by a bituminous matrix modified with magnetically/electrically responsive materials, which give them the capacity to respond to the application of magnetic fields.

Based on this concept, it had been identified that MAMs are ideal to be potentially used in the development of flexible pavements with the following capacities: (1) Improvement of the mechanical properties of the pavements, (2) Emission of magnetic field signals to help in the guidance of the vehicles and, (3) Temperature increase which for the proposal of smart maintenance alternatives for roads.

In this sense, during the present doctoral thesis, contributions were made to the research line of the Laboratory of Construction Engineering of the University of Granada (LabIC.UGR), in the development of each of these potential applications of the MAMs at mortar scale. The results obtained have been important steps in the development of the levels 1, 2 and 3, in the scale of Technology Readiness Level (TRL) associated with Future and Emerging Technologies of the Horizon 2020 Program. The present project is part of SMART ETN program, which receives funding from the Marie Skłodowska-Curie actions for research, technological development and demonstration, scholarship n.721493.

Keywords: Mechanomutable Asphalt Materials, Electroconductive Materials, Magnetic Fields, Smart Pavements, Encoded Asphalt Materials.

Tabla de contenido

| | |
|--|----|
| AGRADECIMIENTOS | 5 |
| RESUMEN | 7 |
| ABSTRACT | 9 |
| Tabla de contenido..... | 11 |
| Lista de Figuras | 15 |
| Lista de tablas | 17 |
| Capítulo 1. Introducción | 19 |
| 1.1. Hipótesis y justificación | 21 |
| 1.2. Contenido y Alcance de la investigación..... | 23 |
| Capítulo 2. Estado del arte..... | 25 |
| 2.1. La carretera del futuro..... | 27 |
| 2.2. Los Materiales Asfálticos Mecanomodificables (MAMs)..... | 30 |
| 2.3. Conclusiones del estado del arte. | 38 |
| Capítulo 3. Objetivos | 41 |
| Capítulo 4. Metodología | 45 |
| 4.1. Materiales utilizados en la investigación. | 48 |
| 4.1.1. Áridos. | 49 |
| 4.1.2. Fibras de acero. | 50 |
| 4.1.3. Filler. | 51 |
| 4.1.4. Betón asfáltico..... | 51 |
| 4.2. Plan de trabajo de la tesis doctoral. | 51 |
| 4.2.1. Etapa 1: Evaluación de los MAMs como materiales que podrían mejorar el comportamiento mecánico de los pavimentos (Primer pilar). | 52 |

| | |
|--|-----|
| 4.2.2. Etapa 2: Evaluación de los MAMs como materiales que emiten señales magnéticas que podrían ayudar en el guiado de los vehículos (Segundo pilar)..... | 53 |
| 4.2.3. Etapa 3: Evaluación de los MAMs como materiales que pueden aumentar su temperatura para la definición de nuevas alternativas de mantenimiento de carreteras. | 56 |
| Capítulo 5. Análisis de resultados..... | 65 |
| 5.1. Etapa 1 - MAMs: Materiales que podrían mejorar el comportamiento mecánico de los pavimentos. | 67 |
| 5.2. MAMs: Materiales que emiten señales magnéticas que podrían ayudar en el guiado de los vehículos (Etapa 2). | 69 |
| 5.3. MAMs: Materiales que aumentan su temperatura para su posible utilización en nuevas alternativas de mantenimiento de carreteras (Etapa 3). | 73 |
| 5.3.1. Capacidades de los MAMs para reducir/eliminar el hielo/la nieve de la superficie de la carretera (Subetapa 3.1)..... | 73 |
| 5.3.2. Mejora de las capacidades de autocurado/autorecuperación de los MAMs (Subetapa 3.2)..... | 77 |
| Capítulo 6. Conclusiones..... | 81 |
| Capítulo 7. Futuras líneas de investigación | 85 |
| Referencias | 89 |
| ANEXOS | 107 |
| Anexo 1. "A review of the contribution of mechanomutable asphalt materials towards addressing the upcoming challenges of asphalt pavements"..... | 109 |
| Anexo 2. "Analysis of the mechanical response of asphalt materials manufactured with metallic fibres under the effect of magnetic fields"..... | 125 |
| Anexo 3. "Interpretation of the Magnetic Field Signals Emitted by Encoded Asphalt Pavement Materials"..... | 141 |
| Anexo 4. "Thermal characterization of electroconductive layers for anti-icing and de-snowing applications on roads"..... | 159 |

Anexo 5. "Recovery capacity of electroconductive asphalt mortars under the influence of magnetic fields"165

Lista de Figuras

| | |
|---|----|
| Figura 1. Acoplamiento entre los dominios físicos de los materiales inteligentes..... | 21 |
| Figura 2. Ámbitos clave de una Ciudad Inteligente. | 28 |
| Figura 3. Efecto provocado por la activación de campos magnéticos en ligantes asfálticos mecanomutables..... | 32 |
| Figura 4. Propiedades reológicas de ligantes mecanomutables (matriz B50/70 y 1% y 10% de polvo de hierro carbonilo) y convencionales (a) Angulo de fase y (b) Módulo complejo. | 33 |
| Figura 5. Fotografía de microscopio electrónico de ligantes mecanomutables y sus nano/micro partículas de hierro. | 33 |
| Figura 6. Valor de deformación del ensayo de carga cíclica de ligantes asfálticos mecanomutables. | 34 |
| Figura 7. Módulo de almacenamiento y factor de reducción promedio de probetas fabricadas con polvo de escoria de acero. | 35 |
| Figura 8. Señal magnética detectada en probetas con fibras de acero de neumáticos fuera de uso. | 36 |
| Figura 9. Ejemplo de codificación de una autovía..... | 36 |
| Figura 10. Imagen de infrarrojo de los dos ensayos elaborados para evaluar ligantes modificados con grafeno..... | 37 |
| Figura 11. Pilares fundamentales de la investigación asociada a esta tesis doctoral..... | 47 |
| Figura 12. Curva granulométrica de la arena caliza utilizada para fabricar los morteros. | 49 |
| Figura 13. Detalle de las fibras de acero utilizadas en la fabricación de los morteros. | 50 |
| Figura 14. Esquema del ensayo de frecuencia de resonancia utilizado. | 53 |
| Figura 15. Dispositivo de ensayo para la evaluación de la señal magnética de morteros mecanomutables..... | 54 |
| Figura 16. Protocolo de ensayo para la evaluación de la señal magnética de morteros mecanomutables..... | 55 |
| Figura 17. Prueba de concepto de uso de morteros mecanomutables para la codificación de carreteras..... | 56 |
| Figura 18. Geometría del sistema intercapa evaluado en el ensayo para la reducción/eliminación del hielo/de la nieve de la superficie de la carretera. | 58 |

| | |
|--|----|
| Figura 19. Esquema utilizado en el ensayo para la reducción/eliminación del hielo/de la nieve de la superficie de la carretera..... | 58 |
| Figura 20. Sistema de capa inteligente propuesto para la eliminación del hielo/nieve de la carretera. | 59 |
| Figura 21. Equipo de Análisis Mecánico Dinámico (DMA). | 62 |
| Figura 22. Montaje utilizado para la aplicación de inducción magnética..... | 63 |
| Figura 23. Influencia de temperatura en los valores de módulo dinámico para una intensidad del campo = 210 mT. | 67 |
| Figura 24. Influencia de la altura de la probeta en el cambio de módulo cuando se aplica una intensidad de campo de 210 mT..... | 68 |
| Figura 25. Influencia de la intensidad de campo magnético en los valores de módulo de probetas de mortero mecanomutable. | 69 |
| Figura 26. Influencia de la altura de medición en la señal magnética emitida por probetas con 11% de fibra de acero..... | 70 |
| Figura 27. Influencia de la velocidad de aproximación a la $D = 0$ en la señal magnética emitida por morteros codificados con fibras de acero..... | 71 |
| Figura 28. Influencia de la distancia más cercana a cada sensor en la señal magnética emitida por morteros codificados con fibras de acero, R: sensor rojo, B: sensor azul. | 72 |
| Figura 29. Prueba de concepto de placas de mortero codificado con fibras de acero. | 73 |
| Figura 30. Distribución de temperaturas en la cara lateral de la probeta para 7.0 mT de campo magnético y capa superficial de 20 mm. | 74 |
| Figura 31. Influencia de la intensidad del campo magnético en los valores de temperatura a los 300 s y 1800 s. | 75 |
| Figura 32. Influencia del espesor de la capa asfáltica superficial en los valores de temperatura a los 300 s y 1800 s. | 76 |
| Figura 33. Sistema de capa inteligente de mortero mecanomutable vs otras alternativas..... | 76 |
| Figura 34. Resultados del módulo promedio para la evaluación del autocurado/autoreparación de morteros mecanomutables..... | 78 |
| Figura 35. Resultados de recuperación obtenida para la evaluación del autocurado/autoreparación de morteros mecanomutables. | 79 |
| Figura 36. Curvas esfuerzo vs número de ciclos para la evaluación del autocurado/autoreparación de morteros mecanomutables. | 80 |

Lista de tablas

| | |
|---|----|
| Tabla 1. Proporción porcentual de la composición de los morteros evaluados en esta tesis doctoral. | 48 |
| Tabla 2. Caracterización de la arena caliza utilizada para fabricar los morteros. | 50 |
| Tabla 3. Características del betún asfáltico utilizado en la fabricación de los morteros. | 51 |
| Tabla 4. Variables del ensayo de frecuencia de resonancia. | 52 |
| Tabla 5. Variables de ensayo para la evaluación de la señal magnética de morteros codificados. | 54 |
| Tabla 6. Variables de ensayo para la reducción/eliminación del hielo/de la nieve de la superficie de la carretera. | 57 |
| Tabla 7. Sistemas de campo para eliminación de hielo/nieve de la superficie de la carretera mediante aumento de temperatura..... | 60 |
| Tabla 8. Variables del ensayo de autocurado/autorecuperación..... | 62 |

Capítulo 1. Introducción

1.1. Hipótesis y justificación

Con referencia al título de la presente tesis doctoral: “**Materiales Asfálticos Mecanomodificables para la Construcción de Pavimentos Inteligentes**”, es importante detallar dos conceptos básicos de este título, a los que se hará mención a lo largo del documento: **Materiales Asfálticos Mecanomodificables (MAMs)** y **pavimentos inteligentes** (con referencia a las carreteras del futuro).

Los **MAMs** por definición se componen de una matriz asfáltica modificada con partículas con propiedades magnéticas/eléctricas, que reaccionan o pueden ser detectadas por dispositivos asociados a campos magnéticos (imanes permanentes, bobinas de inducción magnética, sensores magnéticos, electroimanes, etc) [1]–[4]. Esta capacidad de reacción a los campos magnéticos, hace que los MAMs tengan la capacidad de adaptar las propiedades mecánicas y térmicas de las capas bituminosas del firme, cuando este se encuentra en servicio. En este sentido, como se muestra en la Figura 1, los MAMs pueden acoplar dos o tres dominios de la física, por tanto pueden ser considerados **materiales inteligentes** [5]–[7].

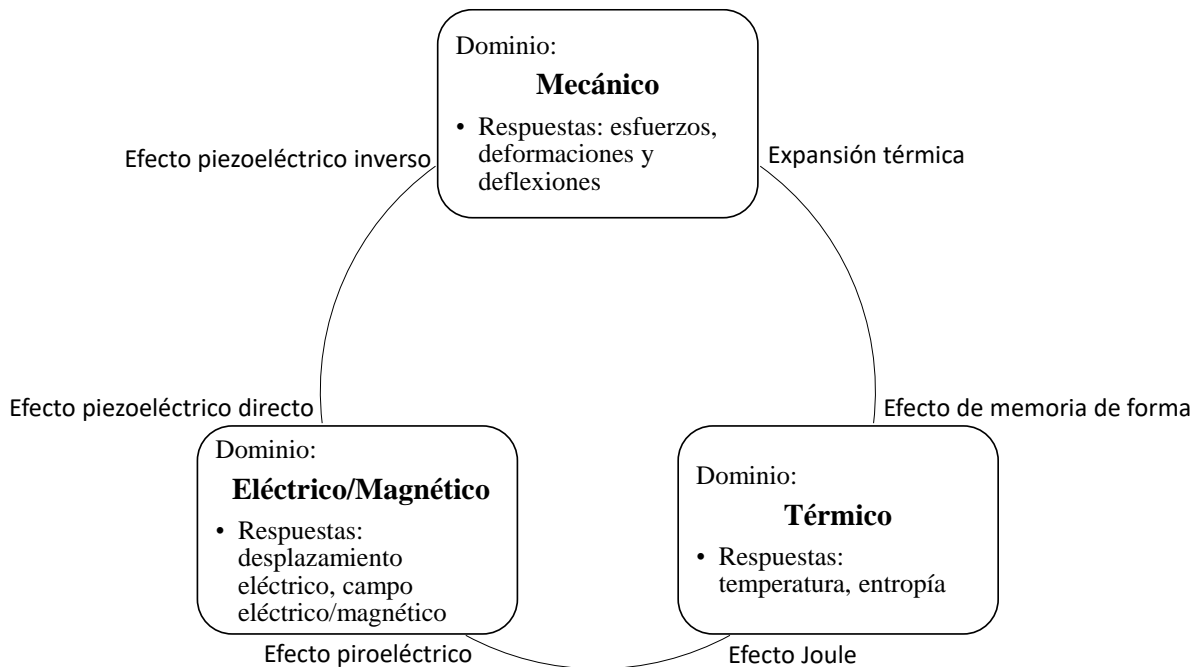


Figura 1. Acoplamiento entre los dominios físicos de los materiales inteligentes.

Nota Figura 1: Tomado de [5]–[7], traducido y adaptado por la autora.

En el campo de la ingeniería de carreteras, los materiales inteligentes han sido principalmente utilizados en la fabricación de sensores y actuadores, empleados en el monitoreo de su salud estructural (SHM: Structural Health Monitoring, de sus siglas al inglés) [8], [9], para la mejora de la respuesta de la estructura en servicio [5]. Los sistemas SHM en la actualidad, han sido complementados con el uso de tecnologías asociadas al internet de las cosas (IoT, de sus siglas al inglés: Internet of Things) y la gestión de tráfico, para el desarrollo de las **carreteras inteligentes** [10], [11].

Considerando que garantizar una **mayor durabilidad a los menores costos de mantenimiento, maximizar la seguridad vial en carretera, control del tráfico, autosuficiencia energética, circulación de vehículos autónomos y comunicación con los usuarios**, son los principales desafíos que estas carreteras inteligentes deben satisfacer. El desarrollo de materiales con nuevas capacidades, como es el caso de los materiales inteligentes, representa una alternativa que es importante desarrollar.

En este contexto, los MAMs extienden el uso de los materiales inteligentes a la construcción de las capas superficiales que componen la estructura de carretera. El concepto MAMs como tal, nace como parte de los proyectos de investigación del **Laboratorio de Ingeniería de la Construcción de la Universidad de Granada (LabIC.UGR)**. Los primeros estudios publicados en esta línea, fueron realizados en betunes asfálticos mecanomutables (MABs) fabricados con partículas de hierro carbonilo [1] y escorias de acero [3], con el objetivo de evaluar la capacidad de modificar el valor del módulo dinámico y por tanto desempeño a fatiga y deformación permanente de estos materiales.

Posteriormente, se realizó un estudio adicional en mezclas asfálticas mecanomutables fabricadas con diferentes contenidos de escorias de acero o fibras de acero extraídas de los neumáticos fuera de uso [12], con la finalidad de evaluar la posibilidad de asignar un código magnético a la carretera, de manera de esta pudiese asistir en el guiado de los vehículos. Como resultado de este estudio, se desarrolló la Patente P201631096: Pavimento, y sistema de seguridad que lo comprende [13], la cual presenta las características técnicas de la invención.

Finalmente, en un estudio complementario dirigido al uso de materiales innovadores como es el caso del grafeno, se analizó la posibilidad de mejorar la conductividad térmica y trabajabilidad de

los ligantes asfálticos, con el propósito de proponer nuevas alternativas para eliminar el hielo/nieve de la superficie de la carretera [14].

A causa de los prometedores resultados alcanzados por el LabIC.UGR sobre los MAMs, junto con las necesidades de dar respuesta a los retos a los que se enfrenta la ingeniería de carreteras en los próximos años, es que se justifica la realización de esta tesis doctoral. La investigación asociada a esta tesis, propone como hipótesis probar las siguientes **tres aplicaciones de los MAMs a nivel de morteros**:

1. La mejora de las prestaciones mecánicas de la capa superficial de la estructura del pavimento flexible.
2. La codificación de la carretera para asistir el guiado de los vehículos.
3. La definición de alternativas de mantenimiento de los pavimentos flexibles, específicamente relacionadas con la eliminación de la nieve de la superficie de la carretera y el mejoramiento de las capacidades de recuperación de los materiales asfálticos.

En este contexto se enmarca la presente tesis doctoral, que además forma parte del proyecto de investigación individual nº14 dentro del proyecto **SMARTI_ETN** (siglas en inglés con significado: Infraestructura del Transporte Sostenible, Multifuncional, Automatizada y Resiliente) [15], financiado por la **Unión Europea** en el programa **Horizonte 2020, bajo las acciones Marie Skłodowska-Curie** para investigación, desarrollo tecnológico y demostración (ref n.721493). Proyecto al que se incorporó la doctoranda en 2017 por un periodo de 3 años, con un contrato Marie Skłodowska-Curie (ESR14-SMARTI).

1.2. Contenido y Alcance de la investigación

El presente documento ha sido organizado en **7 capítulos** con la finalidad de mostrar el flujo de trabajo desarrollado en la presente investigación doctoral.

El **capítulo 1** presenta la introducción y se divide en dos apartados, el primer apartado expone la formulación de la hipótesis del estudio y el segundo la descripción del contenido y el alcance de esta tesis doctoral.

En el **capítulo 2** se detalla el estado del arte que contiene los aspectos relevantes del conocimiento que conducen al desarrollo de los avances expuestos en la presente investigación. Dicha revisión inicia con una introducción al capítulo, seguida de dos importantes apartados

dirigidos a la descripción de las carreteras del futuro y a la definición de los Materiales Asfálticos Mecanomutables. El capítulo termina con un apartado donde se reúnen las conclusiones obtenidas del estado del arte, las cuales sirven como base para la formulación de los objetivos de la tesis.

Por tanto, en el **capítulo 3** se formula el objetivo general de la investigación y los objetivos específicos asociados a 3 pilares fundamentales que constituyen la presente tesis doctoral y que están respectivamente relacionados con las etapas de desarrollo de la metodología expuesta en el **capítulo 4**. El capítulo 4 en este sentido, expone la información asociada a los materiales utilizados en el estudio y un plan de trabajo de tres etapas sobre el cual, se desarrollan los objetivos planteados en esta tesis.

Siguiendo el diagrama metodológico expuesto en el capítulo 4, el **capítulo 5** inicia con una breve introducción, seguida de los resultados experimentales obtenidos a lo largo de las tres etapas del estudio.

Las conclusiones generales del documento son recopiladas en el **capítulo 6**, definiendo a partir de ellas las futuras líneas de investigación expuestas en el **capítulo 7**.

El documento termina mostrando la **bibliografía** de la tesis, seguida de la sección de **anexos** donde se muestran los artículos de investigación que sirven al compendio de esta tesis doctoral.

Capítulo 2. Estado del arte

En el presente capítulo se describen **aspectos relevantes del conocimiento, que conducen a los avances de la investigación de esta tesis doctoral**. En este sentido, el capítulo ha sido dividido en **tres secciones**.

La **primera** sección se refiere a la carretera del futuro, esta sección inicia describiendo el proceso evolutivo que ha tenido la carretera a lo largo de la historia, hasta llegar a las carreteras inteligentes, para las cuales se desarrollan los Materiales Asfálticos Mecanomodificables (MAMs).

La **segunda** sección se refiere a la definición de los MAMs y las aplicaciones potenciales que resultan de su uso en la construcción de firmes flexibles inteligentes de carretera. En esta sección se detallan los principales hallazgos obtenidos en estudios previos a esta tesis doctoral y que permitieron sentar las bases para la definición de los objetivos de esta tesis, la cual se encuentra dentro de los esfuerzos definidos por el LabIC.UGR para el desarrollo de esta línea de investigación.

Finalmente, la **tercera** sección resume las principales conclusiones obtenidas en este capítulo, como punto de partida en la definición de los objetivos desarrollados en esta tesis.

2.1. La carretera del futuro.

A lo largo de la historia, los ingenieros han trabajado en proponer soluciones que permitan solventar las necesidades de la sociedad en términos de vivienda, servicios básicos, comunicaciones, entre otros. En el área de las carreteras, los esfuerzos desarrollados pueden ser asociados a un proceso evolutivo que inicia con las calzadas y caminos rústicos (carreteras de **primera generación**), que posteriormente fueron asfaltados (carreteras de **segunda generación**) y extendidos a carreteras de alta capacidad como las autovías y autopistas (carreteras de **tercera generación**).

En la actualidad, estos esfuerzos han sido ampliados hasta el desarrollo de una **cuarta generación** de carreteras, que se encuentra comprometida con el desarrollo de prácticas sostenibles de construcción, como es el caso de la reutilización y reciclado de materiales, la reducción de emisiones y ruido, entre otras. A pesar de que las investigaciones ya han mostrado un gran avance en los primeros niveles de desarrollo tecnológico de esta cuarta generación, aún quedan pasos por realizar para poder considerar una implementación completa de esta generación.

En traslape con esta cuarta generación y como resultado de la revolución tecnológica del siglo veintiuno, recientemente se habla también de una **quinta generación** de carreteras: las **carreteras inteligentes**. Esta nueva generación de carreteras forma parte de los ejes 4 y 5, referentes a Entorno Inteligente y Movilidad Inteligente, que han sido definidos por el Parlamento Europeo [16]¹ para el desarrollo de las Ciudades Inteligentes, conocidas hoy en día con la etiqueta “smart” (Figura 2).

| 1. Economía inteligente | 2. Gobernanza Inteligente | 3. Entorno inteligente | 4. Movilidad inteligente | 5. Sociedad inteligente | 6. Bienestar inteligente |
|---|--|--|--|--|---|
| <ul style="list-style-type: none"> • Eficiencia • Innovación • Sostenibilidad económica • Nuevos modelos de negocio | <ul style="list-style-type: none"> • Buen gobierno • Transparencia • Gobierno electrónico • Protección de la información | <ul style="list-style-type: none"> • Infraestructuras eficientes • Sostenibilidad medioambiental | <ul style="list-style-type: none"> • Infraestructuras viarias inteligentes • Transporte y tráfico inteligente • Infraestructuras y conectividad TIC | <ul style="list-style-type: none"> • Educación inteligente • Inclusión social • Participación ciudadana | <ul style="list-style-type: none"> • Bienestar ambiental • Bienestar social |

Figura 2. Ámbitos clave de una Ciudad Inteligente.

Nota Figura 2: Tomado de [17].

De acuerdo con esta normativa y en referencia a estos dos ejes, debe entenderse respectivamente el Entorno Inteligente y la Movilidad Inteligente como:

“la gestión eficiente del conjunto de elementos físicos (estructuras) que permiten a los ciudadanos obtener los recursos que necesitan o que permiten la gestión de los mismos dentro de la ciudad”.

“la gestión segura, eficiente y sostenible de los sistemas logísticos y de transporte para facilitar a los ciudadanos el acceso, uso y disfrute del espacio urbano, promoviendo la movilidad eficiente de las personas y el acceso a todos los servicios, especialmente a los ciudadanos con discapacidad”.

En este sentido, se hace importante definir los siguientes elementos¹:

¹ El documento completo puede visitarse en: <http://www.smartcities.at/assets/Publikationen/Weitere-Publikationen-zum-Thema/mappingsmartcities.pdf> [visitado 12/08/2020].

- Infraestructuras eficientes: *"comprenden los elementos necesarios para la prestación de los servicios y mejora de la vida de los ciudadanos"*.
- Sostenibilidad medioambiental: *"una ciudad sostenible es capaz de obtener los recursos necesarios del entorno y mantener los adecuados niveles de calidad medioambiental sin comprometer los recursos y posibilidades futuras"*.
- Infraestructuras viarias inteligentes: *"comprenden los elementos necesarios para la prestación segura, eficiente y accesible de los servicios de movilidad, incluyendo la interconexión entre los diferentes sistemas de transporte: autobuses, vehículos, metros, tren, bicicletas o a pie"*.
- Transporte y tráfico inteligente: *"comprende la gestión eficiente de los recursos proporcionados por las infraestructuras viarias para minimizar los tiempos de desplazamiento de los usuarios y ofrecer mejores servicios e información en tiempo real a los ciudadanos"*.
- Infraestructuras y conectividad TIC: *"las TIC en una Ciudad Inteligente configuran la infraestructura lógica de información. Su papel es crucial a su capacidad para actuar como una plataforma de captación, manejo de información y gestión global del conocimiento ... Las TIC poseen la capacidad de proporcionar soluciones sostenibles y económicamente viables para las ciudades en multitud de áreas que afectan al entorno y a la sociedad ..."*

En este contexto, se identifica que las **necesidades que deben satisfacer las carreteras a futuro**, están relacionadas con garantizar una mayor durabilidad a los menores costos de mantenimiento, maximizar la seguridad vial en carretera, apuntar por la autosuficiencia energética, así como el monitoreo inteligente de la condición del firme, definir sistemas de control del tráfico, que impulsen la resiliencia del sistema y permitan la implementación de medios más eficientes de transporte y gestión, como podría ser el caso de la conducción autónoma, entre otros.

En este sentido, las investigaciones a nivel mundial de los últimos años contemplan el estudio de nuevos sistemas como es el caso de la integración de paneles solares y tuberías para la captación del calor atrapado en el pavimento como producto de la radiación solar [18]–[32] o sistemas piezoeléctricos [33]–[51], que ofrecen nuevas fuentes de energía que a su vez pretenden reducir el efecto de isla en las ciudades. En esta misma línea se encuentran los sistemas para la eliminación de hielo/nieve de la superficie de la carretera, como las bombas de calor

geotérmico/geotermoeléctrico, calor por infrarojo, sistemas hidrónicos y varillas conductivas embebidas en el pavimento [52]–[61]. Las señales inteligentes de tráfico y sistemas que producen energía por vibración, radiofrecuencia y ondas electromagnéticas [62]–[74], que a su vez ayudan en la gestión de tráfico y reducción de accidentes, la mejora de los sistemas de conteo vehicular y las comunicaciones de los diferentes elementos de la vía.

Así mismo se podrían mencionar alternativas innovadoras para la gestión automatizada de la carretera, como es el caso de la imaginería basada en la fotogrametría con drones u otras opciones de menor costo que utilizan teléfonos móviles, los sistemas de posicionamiento global, el uso de sensores y transductores de diferentes tipos (ultrasonido, laser, etc), el procesamiento de información mediante el uso de inteligencia artificial (machine learning, deep learning, big data) y tecnologías asociadas al internet de las cosas (en inglés IoT: Internet of Things), simulación, realidad virtual, etc [75]–[98]. Y por qué no, vinculado a la cuarta generación de carreteras sostenibles, nuevas metodologías relacionadas con la evaluación del ciclo de vida (LCA, LCCA) y economía circular [89], [99]–[111].

En lo que concierne a esta tesis doctoral, se hace importante agregar el desarrollo de materiales inteligentes con nuevas capacidades como lo son la auto-reparación, emisión y recepción de energía desde y hacia el medio, para la comunicación de la vía con el ser humano y el vehículo (texturas, colores, sonidos, señales eléctricas/magnéticas, etc) mejoras en la seguridad vial, la gestión de tráfico, la calidad de viaje del usuario en carretera, así como también, la implementación de nuevos sistemas que permitan asistir el guiado de los vehículos [46], [112]–[123].

Considerando que los MAMs pueden ser parte de esta nueva generación de materiales inteligentes, la siguiente sección se enfoca en describir su definición, así como las potenciales aplicaciones en las que podrían ser utilizados en carreteras y que están vinculadas a esta tesis doctoral.

2.2. Los Materiales Asfálticos Mecanomodificables (MAMs).

Los **Materiales Asfálticos Mecanomodificables (MAMs)** por definición están compuestos de una matriz bituminosa modificada con materiales con propiedades magnéticas y/o eléctricas que responden a la acción de dispositivos relacionados con campos magnéticos (imanes permanentes, bobinas de inducción magnética, sensores de campo magnético, electroimanes, etc) [1]–[4].

El término “mecanmutable” es una palabra compuesta por el prefijo “mecano”, que hace referencia a la mecánica o los mecanismos asociados a las propiedades del material asfáltico, que pueden ser modificadas “mutadas” por medio de la activación de campos magnéticos. La idea de proponer esta nueva generación de materiales, parte de la observación de aplicaciones en otros campos de la ciencia como es el caso de la medicina o la ingeniería industrial [124]–[128], donde se utilizan fluidos magneto-reológicos, cuyas matrices se basan en aceites que ante la acción de campos magnéticos, tienden a aumentar su viscosidad y por tanto, modificar su comportamiento newtoniano a viscoelástico de manera temporal [129][130]. Esta respuesta está relacionada con: la intensidad de campo magnético aplicado, la cantidad de partículas magnéticas, su forma, distribución y tipo [129].

El primer estudio desarrollado por el equipo de investigación del LabIC.UGR en esta línea, fue realizado en betunes asfálticos modificados con partículas de hierro carbonilo [1], [4]. Para este objetivo se utilizó un magneto-reómetro MCR-300 Physica-Aton Parr, con el cual se midieron los valores de módulo de ligantes mecanmutables y convencionales, durante barridos de frecuencia a deformación controlada, para distintas temperaturas e intensidades de campo magnético.

Los resultados mostraron que conforme aumenta la intensidad de campo magnético, la elasticidad y rigidez de los ligantes mecanmutables aumenta, lo que significa la modificación de sus propiedades reológicas. De acuerdo con este estudio, esto podría deberse a que las partículas magnéticas utilizadas en los MAMs, en condiciones en que la consistencia de la matriz asfáltica sea lo suficientemente fluida y el campo magnético lo suficientemente fuerte, tienden a moverse y formar una estructura interna alineada con las líneas de campo. Por otro lado, en condiciones en que la matriz tiene una consistencia que impide el movimiento de estas partículas, es posible que esto ocurra por la producción de un tensor interno de esfuerzos que, bajo el principio de acción-reacción, finalmente genera un aumento en la rigidez del material (Figura 3).

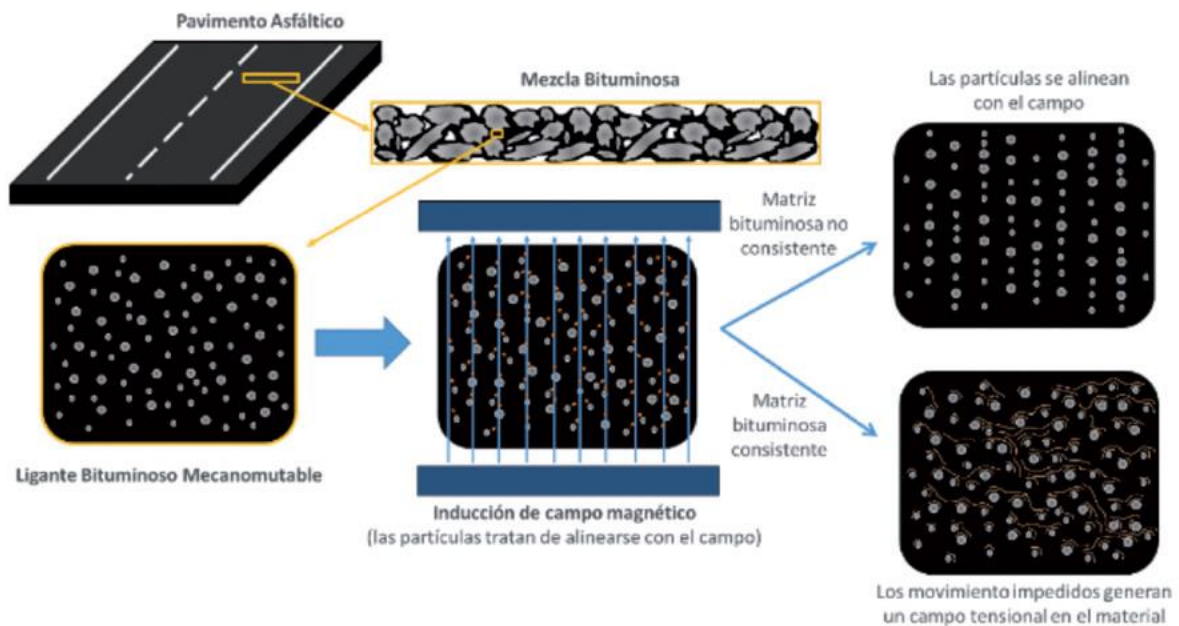


Figura 3. Efecto provocado por la activación de campos magnéticos en ligantes asfálticos mecanomutables.

Nota Figura 3: Tomado de [1], [4].

En este sentido, en dicho estudio se compararon los resultados de ligantes mecanomutables con betunes convencionales de distinta penetración (B 20/30 y B50/70) y como se muestra en la Figura 4 se comprobó que los primeros, pueden modificar su comportamiento mecánico mediante la activación de campos magnéticos, comportándose de una manera inclusive más rígida que los betunes de alto módulo. La fotografía de microscopía electrónica de la Figura 5, muestra el detalle de uno de los ligantes mecanomutables estudiados y sus nano/micro partículas de hierro.

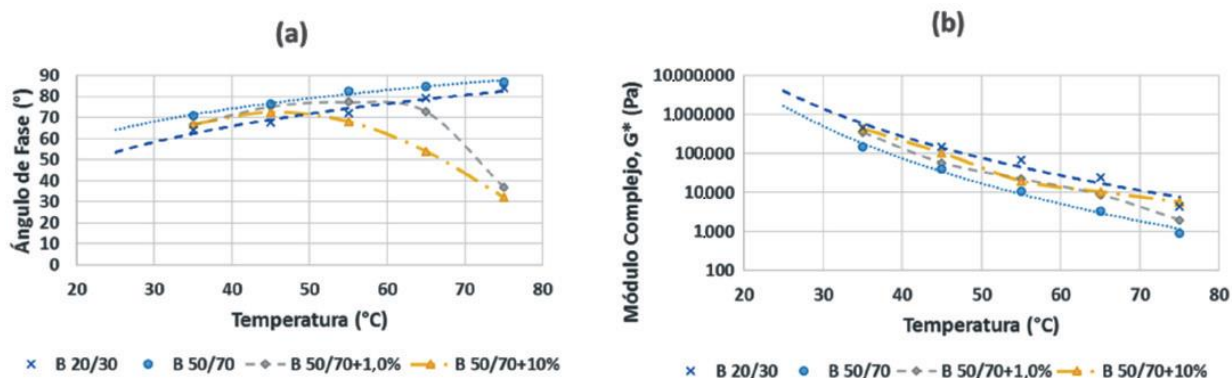


Figura 4. Propiedades reológicas de ligantes mecanomutables (matriz B50/70 y 1% y 10% de polvo de hierro carbonilo) y convencionales (a) Ángulo de fase y (b) Módulo complejo.

Nota Figura 4: Tomado de [1], [4].

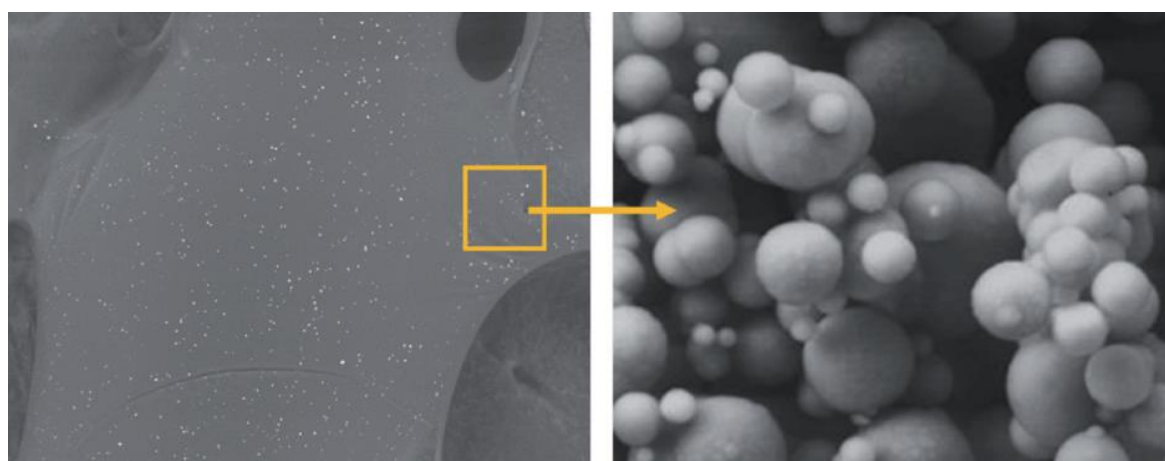


Figura 5. Fotografía de microscopio electrónico de ligantes mecanomutables y sus nano/micro partículas de hierro.

Nota Figura 5: Tomado de [1], [4].

Posteriormente, en un segundo estudio dirigido a la representación del efecto cíclico y con períodos de descanso de las cargas reales de tráfico [2], se estableció un protocolo de ensayo que consistía en considerar la posibilidad de activar campos magnéticos siguiendo el mismo patrón que las cargas. Para esto se realizaron ensayos a 60°C de 30 ciclos tipo "creep and recovery" que consistían en la aplicación de 1 segundo de carga (0.1 kPa para los 15 primeros ciclos y 3.2 kPa para los 15 ciclos restantes) y activación de campo magnético (430 mT de

intensidad), seguido de 9 segundos de descanso. Como se observa en la Figura 6, los resultados obtenidos muestran que la activación del campo magnético reduce el nivel de deformación del material, lo que significa una mayor resistencia ante las cargas.

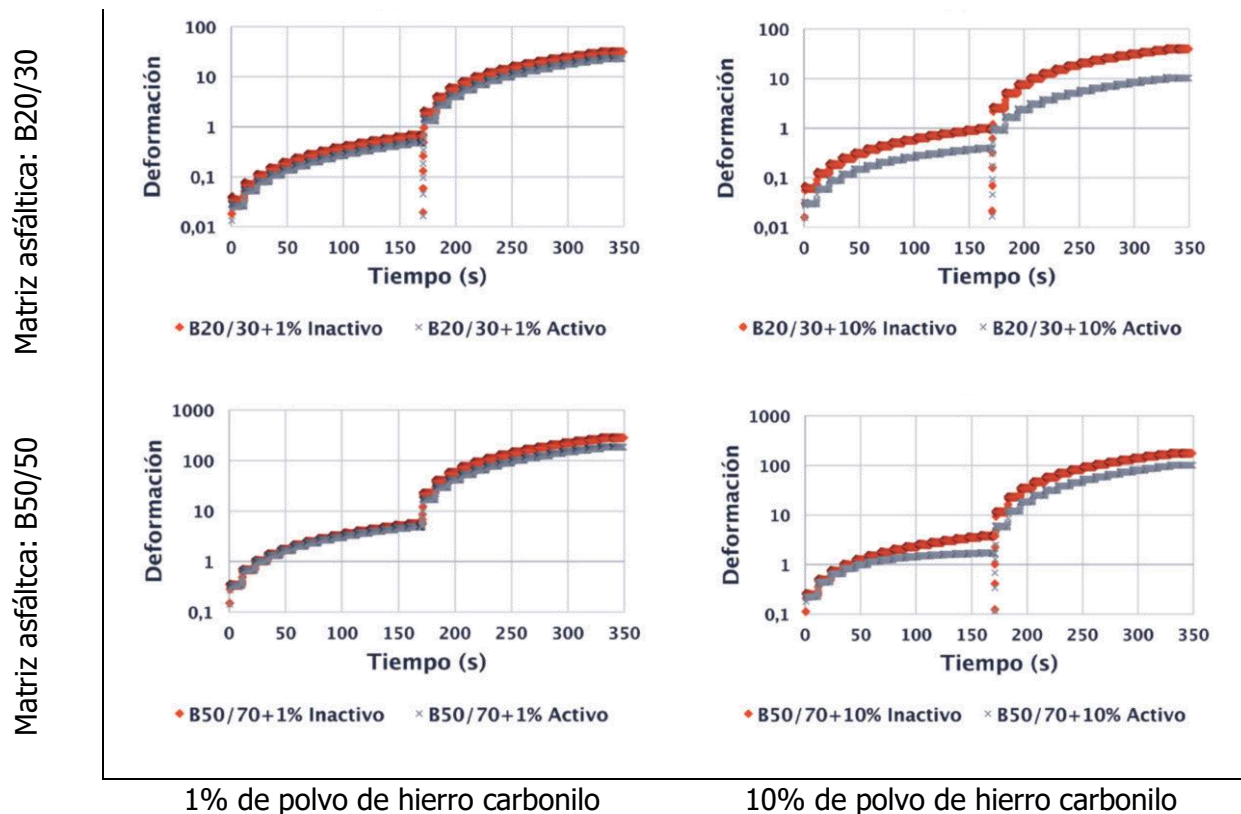


Figura 6. Valor de deformación del ensayo de carga cíclica de ligantes asfálticos mecanomutables.

Nota Figura 6: Tomado de [2], [4].

El siguiente estudio en esta línea consistió en la evaluación de másticos asfálticos mecanomutables [3] fabricados con escorias de acero pulverizadas (SSS, de sus siglas al inglés: stainless steel slag) en proporciones de 10%, 20% y 30% de sobre el peso del ligante. El tamaño de partícula del polvo de escoria utilizado varió en los siguientes tres rangos de tamaño: 0.250 a 0.125 mm, 0.125 a 0.063 mm y 0.063 mm a 0 mm. El objetivo del estudio fue evaluar el efecto del tamaño de partícula y la concentración de material magnético, en las propiedades mecanomutables de los morteros. En este sentido se realizaron dos tipos de ensayos: (1) un barrido de temperatura (a 5Hz y 1% de deformación) y (2) múltiples ciclos “creep and recovery” (a 60°C, con una configuración de 1 s de carga y campo seguido de 9 s de descanso, para 15 ciclos de 0.1 kPa seguidos de 15 ciclos de 3.2 kPa y un campo magnético de 430 mT). Como se

muestra en la Figura 7, los resultados mostraron que ante la activación del campo magnético los másticos estudiados se comportan más elásticamente, aumentando el valor de módulo de almacenamiento y reduciendo el factor de pérdida, lo que significa que se puede reducir su susceptibilidad al desarrollo de deformaciones plásticas permanentes y otros tipos de daños asociados. Adicionalmente se comprobó que el tamaño de la partícula de escoria de acero no tiene un efecto aparentemente importante en esta respuesta, pero si la concentración de hierro en este material.

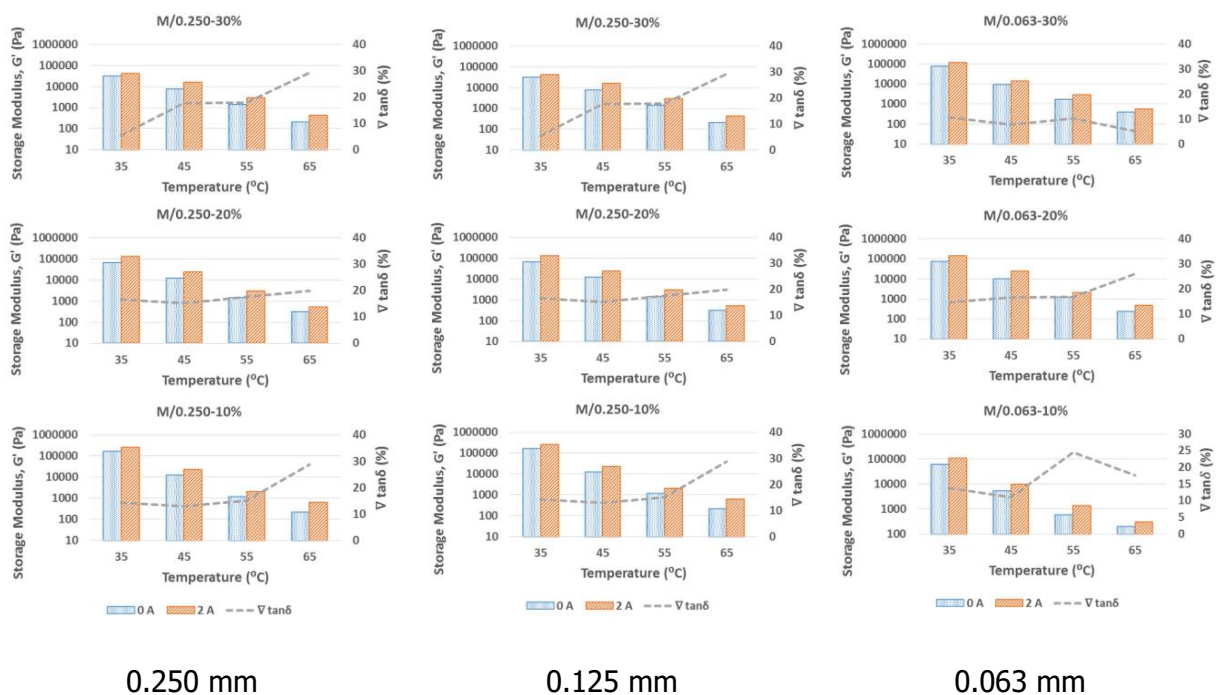


Figura 7. Módulo de almacenamiento y factor de reducción promedio de probetas fabricadas con polvo de escoria de acero.

Nota Figura 7: Tomado de [3].

Posteriormente, contemplando dos patentes [131], [132] que proponen la instalación de diferentes patrones de imanes e imanes poliméricos (materiales magnetizados) en el pavimento, los cuales pueden ser detectados por sensores de campo magnético instalados en vehículos en movimiento, pero que por ser alternativas costosas no se ha continuado su desarrollo, desde el LabIC.UGR, se analizó la posibilidad de utilizar mezclas asfálticas codificadas con diferentes porcentajes de fibras de acero y escoria de acería [12], [13] para ofrecer un sistema económicamente más accesible, con el cual codificar la capa superficial de la carretera.

Los resultados del estudio mostraron que la detección de la señal magnética de estos materiales es sensible a variaciones pequeñas en el contenido de material ferromagnético, siendo posible la utilización de materiales procedentes de residuos siderúrgicos como es el caso de las fibras de acero (ver Figura 8). Este tipo de sistemas podrían ser utilizados como herramientas para asistir el guiado de los vehículos, mediante la emisión de mensajes en tiempo real o en condiciones climáticas difíciles. De esta manera se podría mejorar la seguridad vial en carretera, así como la gestión de tráfico, con la finalidad de generar resiliencia en el uso de la infraestructura vial. La Figura 9 muestra un ejemplo esquemático de la posible codificación de distintos tramos o zonas de una autovía.

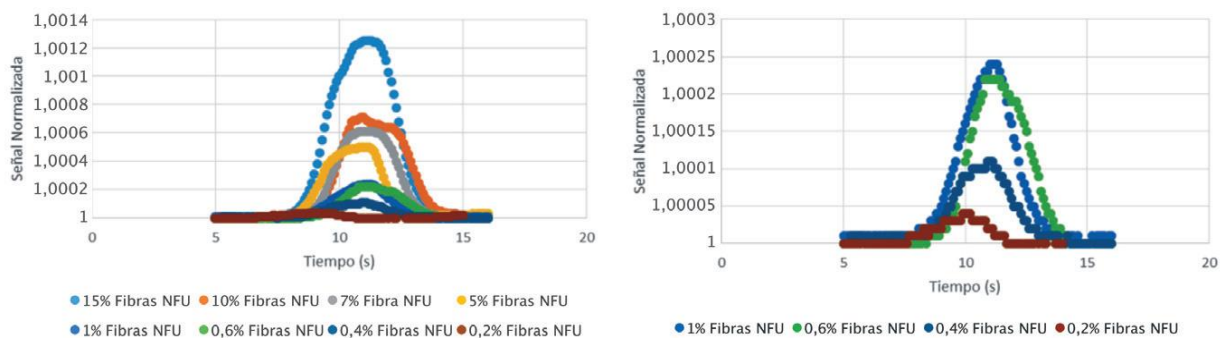


Figura 8. Señal magnética detectada en probetas con fibras de acero de neumáticos fuera de uso.

Nota Figura 8: Tomado de [4], [12].

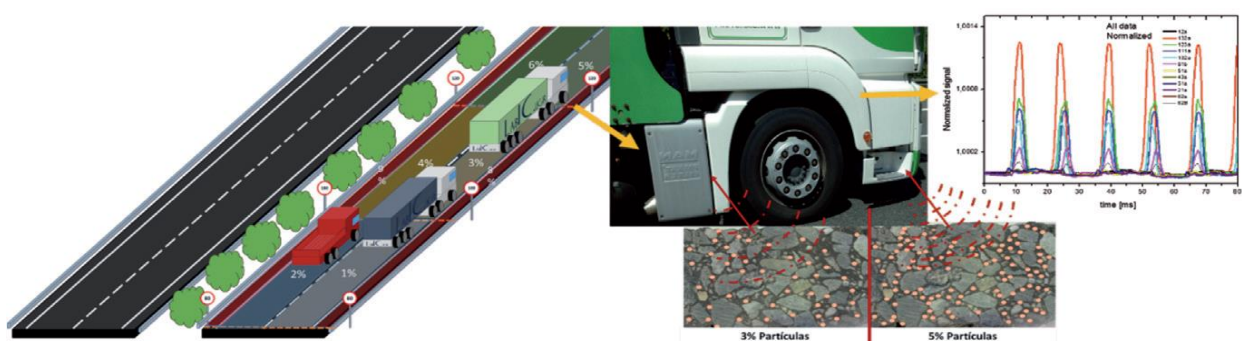


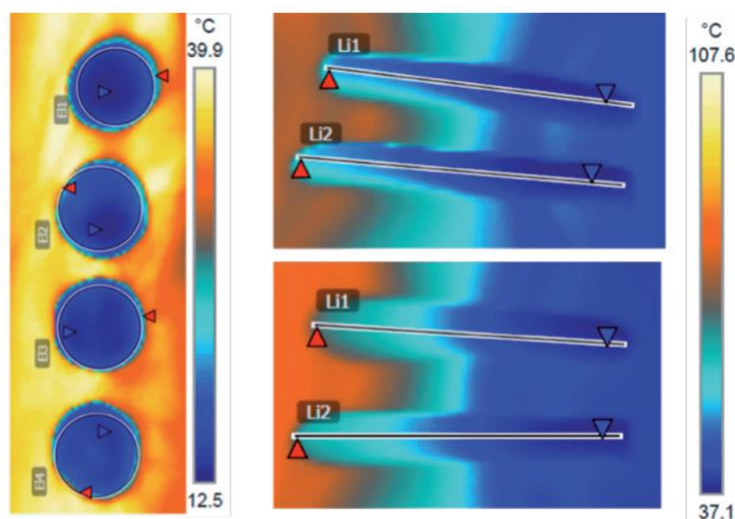
Figura 9. Ejemplo de codificación de una autovía.

Nota Figura 9: Tomado de [4], [12].

En esta misma línea de desarrollo de materiales inteligentes, contemplando la promoción de uso de materiales innovadores en la ingeniería civil como es el caso del grafeno, el LabIC.UGR en conjunto con el Laboratorio de Grafeno y Materiales Bi-dimensionales de la Universidad de

Granada, propuso un nuevo estudio complementario en esta línea de investigación [4], [14], en el que se consideró la posibilidad de mejorar la conductividad térmica y trabajabilidad de los ligantes asfálticos, para la propuesta de nuevas alternativas de eliminación del hielo/nieve de la superficie de la carretera [4]. En el estudio se fabricaron partículas de grafeno tipo "flakes", que luego fueron utilizadas en la producción de ligantes bituminosos con contenidos de grafeno por peso de ligante de 0.1%, 0.5% y 1%.

La capacidad de calentamiento y conductividad térmica de estos materiales fue evaluada respectivamente siguiendo dos protocolos de ensayo distintos (Figura 10): (1) la medición de la variación de la temperatura que podía producirse en probetas de 10 mm de espesor y 25 mm de diámetro, que fueron previamente acondicionadas a una temperatura de 10°C, al ser colocadas sobre una placa metálica con una temperatura constante de 40°C durante un período de 240 segundos; y (2) la medición del tiempo requerido para alcanzar una temperatura de 5°C en un extremo de probetas de 40 mm de longitud y 5 mm de diámetro, las cuales fueron previamente acondicionadas a 35°C y sometidas a una temperatura constante de 100°C en su extremo opuesto. Los resultados del ensayo mostraron que agregar grafeno a los ligantes aumentaba su capacidad y velocidad de calentamiento en 20% y 35% con respecto a los mismos ligantes sin modificar.



Ensayo 1

Ensayo 2

Figura 10. Imagen de infrarrojo de los dos ensayos elaborados para evaluar ligantes modificados con grafeno.

Nota Figura 10: Tomado de [4], [14].

En este punto, es importante agregar como antecedente de los MAMs, las investigaciones realizadas en la inducción de campos magnéticos variables dirigidos al aumento de la temperatura de materiales asfálticos electroconductivos fabricados con desechos de acero (fibras de neumáticos fuera de uso, lana de acero, granallas y virutas, escorias) [121] [119], [133], materiales a base de carbón (nanotubos, fibras, grafito) [134], [135] y restos pulverizados de ferrita y magnetita [119], [136]. Estos estudios han sido principalmente enfocados en el estudio de la posibilidad de potenciar la capacidad de “healing” (autocurado/autorecuperación) de estos materiales [113]–[115], [118]–[123] o su uso en la definición de sistemas destinados a la eliminación del hielo/nieve de la carretera [14], [118], [137]–[142].

En este sentido, considerando esta potencialidad adicional, los estudios asociados a esta línea de investigación del LabIC.UGR están adicionalmente siendo dirigidos a la combinación de las capacidades de conductividad térmica aportadas por materiales como el grafeno y la conductividad eléctrica y por tanto aumento de temperatura, que es generado por el uso de materiales semiconductivos y conductivos.

El Anexo 1 del presente documento contiene el artículo de revisión bibliográfica titulado: “A Review of the Contribution of Mechanomutable Asphalt Materials Towards Addressing the Upcoming Challenges of Asphalt Pavements”, donde se pueden encontrar más detalles acerca de los aspectos expuestos en esta sección.

2.3. Conclusiones del estado del arte.

Las secciones anteriores constituyen la base sobre la cual se han logrado establecer los aspectos relevantes del conocimiento que sustentan el desarrollo de la presente tesis doctoral. Como resultado de este capítulo se logra identificar que los MAMs podrían ser utilizados en la resolución de los siguientes puntos:

1. La necesidad de comprobar que las propiedades mecánicas de los ligantes asfálticos mecanomutables pueden ser escaladas a morteros asfálticos mecanomutables.
2. La necesidad de comprobar que las señales magnéticas emitidas por morteros asfálticos mecanomutables pueden ser afectadas por la altura de medición, la distancia de medición y la velocidad de aproximación del vehículo.

3. La necesidad de comprobar que, a escala de mortero, los materiales asfálticos mecanomutables pueden funcionar para transferir temperatura al pavimento.

Estas necesidades permiten definir los objetivos que sustentan el desarrollo de esta tesis doctoral.

Capítulo 3. Objetivos

En el capítulo anterior se describió el proceso evolutivo que han tenido las carreteras a través de la historia, llegando al contexto del estado actual de las investigaciones en torno a las carreteras inteligentes. Este proceso ayudó a comprender, la necesidad de desarrollar una nueva generación de materiales con capacidad de adaptarse y dar respuesta a las diversas condiciones a las que tendrá que enfrentarse la carretera durante su vida de servicio: los materiales inteligentes. Dentro de esta generación de materiales, se identifica a los materiales asfálticos mecanomutables (MAMs) que constituyen el objeto de estudio de esta tesis doctoral.

En este escenario, el principal objetivo de investigación asociado a esta tesis es la evaluación de los materiales asfálticos mecanomutables para su uso en la construcción de carreteras inteligentes. Se trata de estudiar la aportación de los MAMs (en la escala de morteros) a la mejora de las propiedades mecánicas del pavimento asfáltico, la posibilidad de asistir en el guiado de los vehículos, así como su capacidad de transmisión de calor al pavimento y posibles usos.

De este modo, los objetivos específicos que surgen del objetivo general y que permiten el flujo del desarrollo de esta investigación son los siguientes:

- Comprobar que el aumento en el valor de módulo que se produce por la activación de campos magnéticos en ligantes asfálticos mecanomutables, puede ser escalado a morteros asfálticos mecanomutables, para el desarrollo de materiales inteligentes que pueden adaptar su capacidad mecánica durante su puesta en servicio.
- Caracterizar la forma en que la altura de medición, la distancia de medición y la velocidad de aproximación del vehículo, pueden afectar la señal magnética emitida por morteros asfálticos codificados, que podrían ser utilizados para asistir el guiado de los vehículos.
- Determinar los cambios de temperatura que pueden ser producidos por la activación de campos magnéticos variables, en morteros asfálticos confeccionados con diferentes contenidos de materiales electroconductivos, como mecanismo para la transferencia de temperatura al pavimento.

Capítulo 4. Metodología

En este capítulo se expone la metodología de investigación desarrollada en la presente tesis doctoral. Como se muestra en la Figura 11, esta metodología ha sido diseñada con la finalidad de desarrollar los **tres pilares fundamentales de investigación**, que se encuentran directamente asociados a los objetivos planteados en el capítulo 3 de esta tesis.

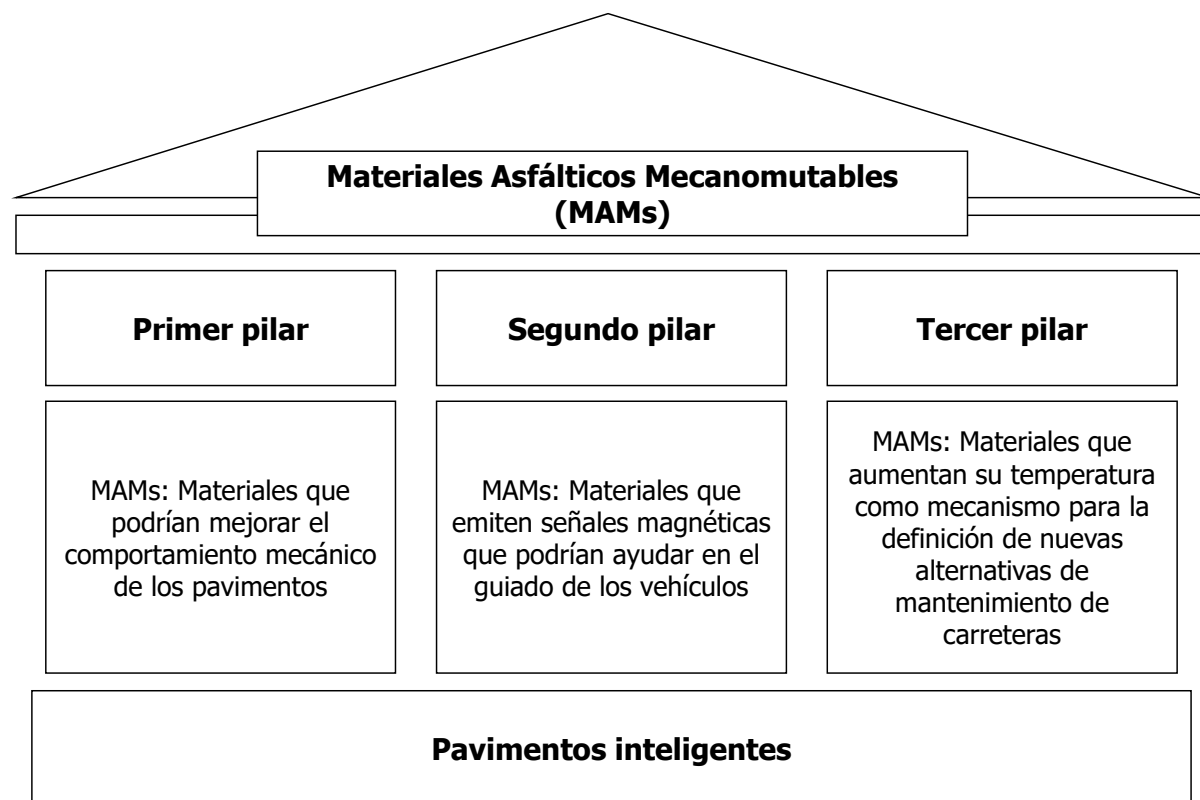


Figura 11. Pilares fundamentales de la investigación asociada a esta tesis doctoral.

A continuación, se describen los **materiales** que fueron utilizados en la confección de los morteros, que fueron evaluados en esta tesis doctoral. Es importante mencionar que el mismo tipo y proporción de materiales ha sido utilizado a lo largo de la tesis, por lo que esta sección aplica para los tres pilares de investigación definidos. Seguidamente se muestra el **plan de trabajo** que describe la metodología de investigación asociada a cada pilar. Considerando que cada pilar está relacionado con 1 o 2 de los artículos de investigación que componen este compendio, se describe la metodología que correspondientemente ha sido definida en cada artículo.

4.1. Materiales utilizados en la investigación.

Debido a que este estudio se centra en la evaluación de los MAMs, y tomando en cuenta que investigaciones previas referentes a este tipo de materiales fueron desarrolladas por el LabIC.UGR en mezclas, másticos y betunes mecanomutables, en esta tesis se decidió abordar el estudio de morteros mecanomutables. Los morteros mecanomutables que se describen en esta sección, fueron utilizados en la confección de las probetas evaluadas en cada uno de los pilares de la investigación, por lo que los detalles de los materiales que se muestran en esta sección, aplican para los tres pilares.

La Tabla 1 muestra las proporciones porcentuales resultantes del diseño de materiales asociado a los cuatro morteros definidos. El diseño de estos morteros estuvo basado en su posible utilización para la construcción de las capas intermedias o de interposición, tipo arena-betún, de los sistemas anti-reflexión de fisuras de firmes flexibles de carretera (capas bituminosas finas de 10 a 20 mm de espesor, con contenidos de betún entre el 8% y el 12% [143] y constituidas por agregados con tamaño de partícula entre los 0/2 mm y los 0/6 mm, con porcentaje de finos entre el 10 y el 15%).

Tabla 1. Proporción porcentual de la composición de los morteros evaluados en esta tesis doctoral.

| Tipo de mortero | Proporción por tipo de material (Por peso total de la mezcla) | | | |
|------------------------|--|-----------------------|-----------------------|--------------------|
| | Arena caliza (tmax=6 mm) | Fibra de acero | Filler cemento | Betún 50/70 |
| M1 - 0%F | 83% | 0% | 9% | 8% |
| M2 - 5%F | 78% | 5% | 9% | 8% |
| M3 - 11%F | 72% | 11% | 9% | 8% |
| M4 - 17%F | 66% | 17% | 9% | 8% |

La finalidad de enfocar la investigación a la construcción de este sistema intercapa, se basó en ofrecer un sistema de protección para los neumáticos de los vehículos que transitan sobre la superficie de ruedo del pavimento. Ya que colocar estos materiales en la superficie, podría dejar fibras de acero expuestas, que tenderían a incrustarse en los neumáticos.

Adicionalmente, y como consecuencia de la ubicación de la capa dentro de la estructura, se decidió reforzar el cumplimiento de las dos principales funciones de las capas arena-betón en sistemas anti-reflexión de fisuras: (1) permitir el desarrollo de grandes deformaciones horizontales de las capas superiores de la estructura sin llegar a la rotura y absorbiendo a su vez los movimientos que se producen en las caras de la grieta, para de esta manera retardar su reflexión y (2) impermeabilizar el pavimento de forma que el agua y otros agentes dañinos no logren ingresar a sus capas inferiores.

A continuación, se describe cada uno de los materiales utilizados para la producción de estos morteros.

4.1.1. Áridos.

Como se observa en la Figura 12, el esqueleto mineral que constituye la mayor porción del mortero, está constituido por una arena caliza con un tamaño máximo de partícula de 6 mm. Las propiedades correspondientes a la densidad de partículas y absorción de agua de esta arena se muestran en la Tabla 2.

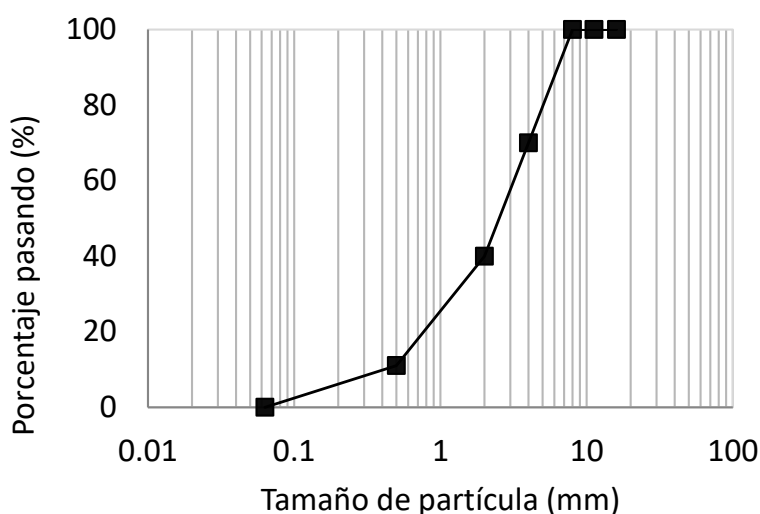


Figura 12. Curva granulométrica de la arena caliza utilizada para fabricar los morteros.

Nota Figura 12: Tomado de [144].

Tabla 2. Caracterización de la arena caliza utilizada para fabricar los morteros.

| Propiedades | Valor | Norma |
|---|--------------|--------------|
| Densidad aparente de las partículas (Mg/m ³) | 3.01 | UNE-EN 1097 |
| Densidad de partículas tras secado en estufa (Mg/m ³) | 2.96 | UNE-EN 1098 |
| Densidad de partículas saturadas con superficie seca (Mg/m ³) | 2.97 | UNE-EN 1099 |
| Absorción de agua tras inmersión por 24h (%) | 0.56 | UNE-EN 1100 |

4.1.2. Fibras de acero.

Con la finalidad de promover el uso de materiales de desecho, los morteros fabricados en este estudio fueron confeccionados con fibras de acero obtenidas de los neumáticos de los vehículos fuera de uso. El detalle de la forma de estas fibras se muestra en la Figura 13.

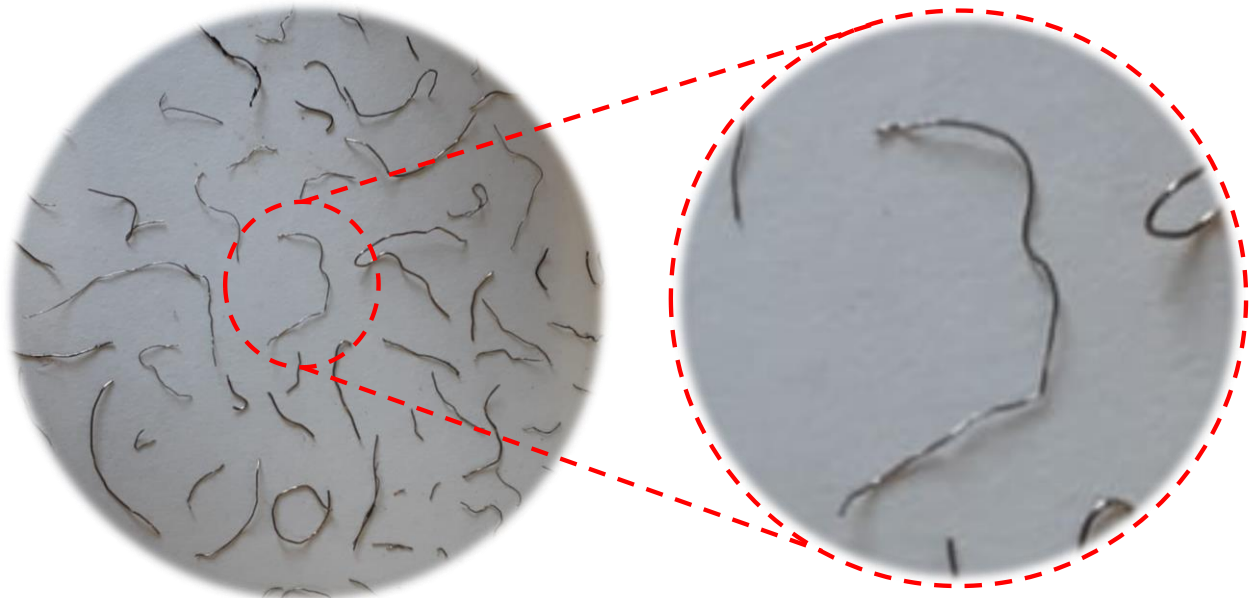


Figura 13. Detalle de las fibras de acero utilizadas en la fabricación de los morteros.

Nota Figura 13: Tomado de [145].

Con la finalidad de ofrecer la suficiente homogeneidad a la mezcla y pensando en desarrollar prácticas de producción que pudiesen ser accesibles en campo, se solicitó a la planta de reciclaje cortar las fibras a manera de representar los menores tamaños que pudiesen ser resultado de su procesamiento. Tomando una muestra de 50 fibras del producto, se obtuvieron longitudes promedio de 4.79 mm con coeficiente de variación de 0.481 mm y diámetros de 0.281 mm con coeficiente de variación de 0.253 mm.

4.1.3. Filler.

Para dar resistencia al mortero, el filler de aportación utilizado fue un cemento portland, CEM II/B-L 32,5 N (EN-197-1-2011). El 95% de este filler tiene un tamaño de partícula menor que 0.063 mm, con una densidad aparente en tolueno (NTL 176/92) de 0.7 Mg/m³ y densidad real (EN 196-6-2019) de 2.95 Mg/m³.

4.1.4. Betún asfáltico.

Finalmente, el ligante bituminoso seleccionado fue un betún asfáltico convencional B50/70, cuyas características se muestran en la Tabla 3.

Tabla 3. Características del betún asfáltico utilizado en la fabricación de los morteros.

| Características | Valor | Norma |
|---------------------------|--------------|--------------|
| Penetración (25°C) | 65 mm | EN 1426 |
| Punto de reblandecimiento | 51 °C | EN 1427 |
| Punto de rotura Fraass | -8 °C | EN 12593 |

4.2. Plan de trabajo de la tesis doctoral.

Como fue mencionado al principio del capítulo, esta tesis doctoral ha sido desarrollada en torno a tres pilares fundamentales, que se encuentran asociados a tres potenciales usos de los MAMs en la construcción de pavimentos inteligentes. A continuación, siguiendo este esquema de los

tres pilares, se describe la metodología asociada a cada una de las publicaciones que componen este compendio de tesis.

4.2.1. Etapa 1: Evaluación de los MAMs como materiales que podrían mejorar el comportamiento mecánico de los pavimentos (Primer pilar).

El propósito de esta etapa fue evaluar la posibilidad de escalar los resultados obtenidos en ligantes asfálticos, donde se logró modificar los valores de módulo por medio de la aplicación de campos magnéticos. En este sentido, en este artículo se evaluaron los valores de módulo (**cambios de módulo**) de probetas de mortero mecanomutable ante variaciones de su altura (8 cm y 12 cm), la intensidad de campo magnético aplicado (de 0 mT, 80 mT, 140 mT, 210 mT) y la temperatura de ensayo (25°C y 45°C). La configuración respectiva de las variables de ensayo se muestra en la Tabla 4. Para esta finalidad, se utilizó el esquema de ensayo de frecuencia de resonancia que se muestra en la Figura 14.

Tabla 4. Variables del ensayo de frecuencia de resonancia.

| Variable de ensayo | Valor |
|---|--|
| Largo y espesor de las probetas | Largo: 0.4 m y Ancho: 0.05 m |
| Altura de las probetas | 0.08 m, 0.12 m |
| Contenido de fibra (por peso de los áridos) | 0%, 5%, 11% |
| Temperatura de acondicionamiento | 25°C, 45°C |
| Intensidad de campo magnético | 0 mT, 80 mT, 140 mT, 210 mT (campo magnético constante, para evitar producción de calor) |

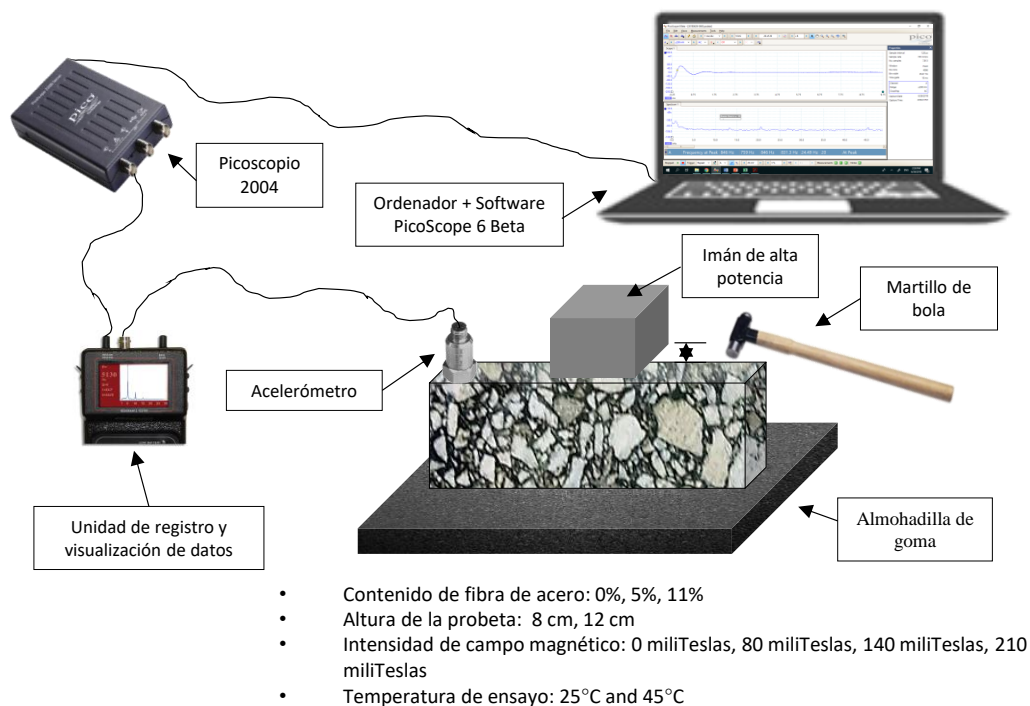


Figura 14. Esquema del ensayo de frecuencia de resonancia utilizado.

Nota Figura 14: Tomado de [146].

Más detalles de esta metodología pueden ser encontrados en el artículo: "Analysis of the mechanical response of asphalt materials manufactured with metallic fibres under the effect of magnetic fields", que se encuentra en el Anexo 2 de este documento.

4.2.2. Etapa 2: Evaluación de los MAMs como materiales que emiten señales magnéticas que podrían ayudar en el guiado de los vehículos (Segundo pilar).

La Etapa 2 consistió en la evaluación de la señal magnética emitida por probetas con distintos contenidos de fibras de acero (**cambios en señal magnética**), ante variaciones (Tabla 5) en la distancia de los sensores (0.05 m, 0.1 m, 0.3 m, 0.4 m), la velocidad de aproximación (0.1 m/s, 0.2 m/s, 0.4 m/s) y distancia de medición (0.250 m, 0.125 m, 0 m). Para la evaluación de la señal magnética de las probetas, fue necesario diseñar y construir el dispositivo de ensayo que se muestra en la Figura 15, que consiste en un sistema ajustable para la medición de los datos, un sistema para el respectivo registro y envío al paquete de aplicaciones de resguardo y procesamiento de la información. El protocolo de ensayo definido para esta Etapa 2 se muestra en la Figura 16, que presenta un esquema de los parámetros evaluados en el estudio.

Tabla 5. Variables de ensayo para la evaluación de la señal magnética de morteros codificados.

| Variables de ensayo | Valor |
|---|-----------------------------|
| | Largo: 0.12 m |
| Dimensiones de las probetas | Ancho: 0.08 m |
| | Espesor: 0.02 m |
| Contenido de fibra de acero | 0%, 5%, 11%, 17% |
| Altura de colocación de los sensores de campo magnético | 0.05 m, 0.1 m, 0.3 m, 0.4 m |
| Velocidad de aproximación | 0.1 m/s, 0.2 m/s, 0.4 m/s |
| Distancia de medición | 0.250 m, 0.125 m, 0 m |

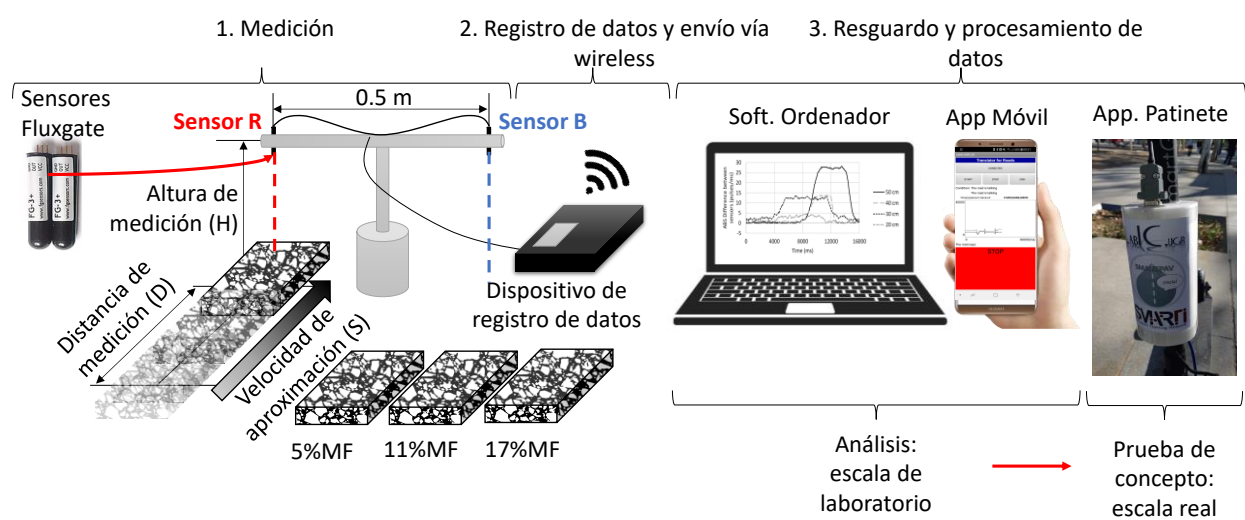


Figura 15. Dispositivo de ensayo para la evaluación de la señal magnética de morteros mecanomutables.

Nota Figura 15: Tomado de [145].

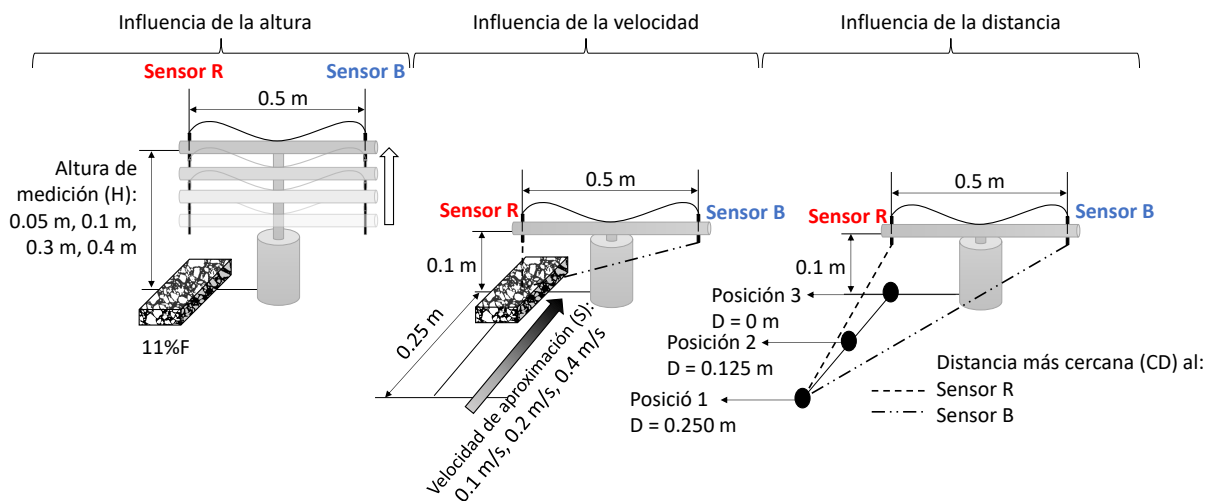


Figura 16. Protocolo de ensayo para la evaluación de la señal magnética de morteros mecanomutables.

Nota Figura 16: Tomado de [145].

Con la finalidad de establecer la configuración de un sistema que permita probar integralmente el concepto asociado al uso de los morteros mecanomutables como materiales que pueden ser codificados para interactuar con los vehículos, se adaptó el sistema de la Figura 15 a la prueba de concepto (PoC, de sus siglas al inglés: Proof of Concept) que se muestra en la Figura 17.

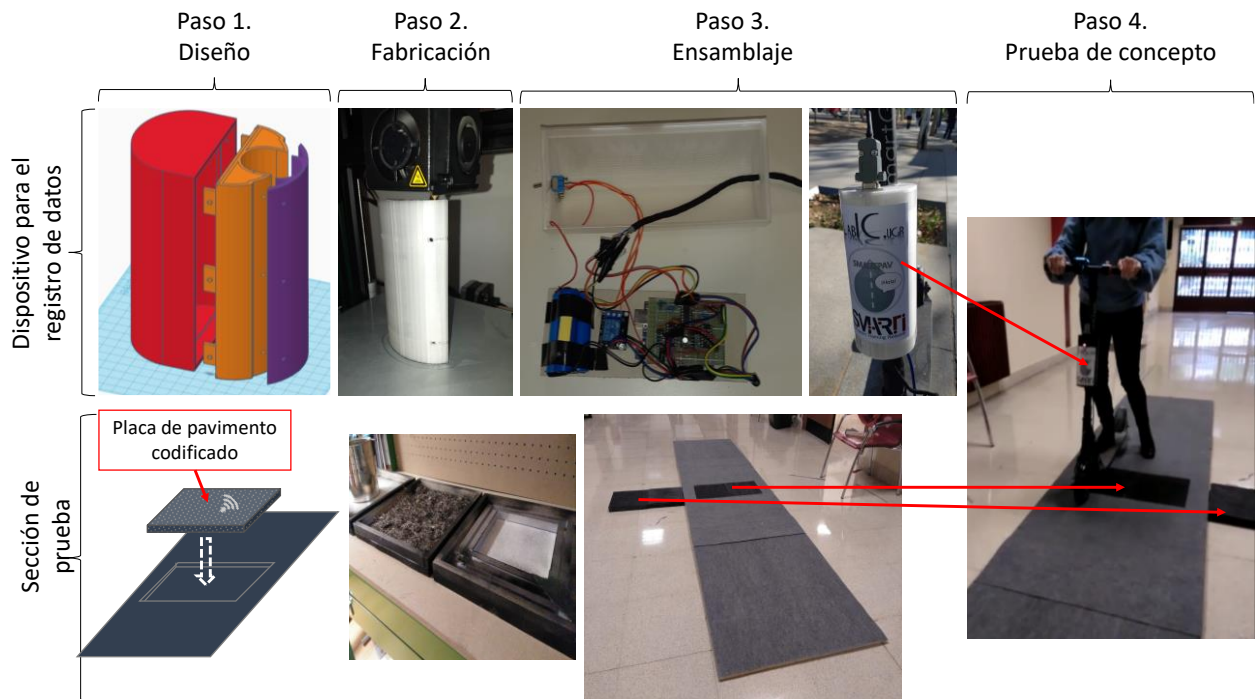


Figura 17. Prueba de concepto de uso de morteros mecanomutables para la codificación de carreteras.

Nota Figura 17: Tomado de [145].

Este sistema se compone de: (1) una sección de prueba desarmable, que permite probar bloques con diferentes codificaciones de materiales con propiedades magnéticas y (2) un patinete eléctrico, que contiene el dispositivo para la interpretación de la señal y facilita la comunicación de la sección de prueba con el patinete.

Más detalles de esta metodología pueden ser encontrados en el artículo: "Interpretation of the magnetic field signal emitted by encoded asphalt materials", que se encuentra en Anexo 3 de este documento.

4.2.3. Etapa 3: Evaluación de los MAMs como materiales que pueden aumentar su temperatura para la definición de nuevas alternativas de mantenimiento de carreteras.

La tercera y última etapa, se desarrolló con la finalidad de evaluar la posibilidad de utilizar los morteros mecanomutables, en la definición de alternativas de mantenimiento que podrían servir tanto para, eliminar el hielo/nieve de la superficie de la carretera, como para, potenciar la

capacidad de autocurado/autoreparación de los morteros asfálticos. Atendiendo a ambas posibilidades, esta etapa se dividió en las dos subetapas que se muestran a continuación.

4.2.3.1. Subetapa 3.1: Capacidades de los MAMs para reducir/eliminar el hielo/la nieve de la superficie de la carretera.

La primera subetapa consistió en la evaluación de los **cambios de temperatura** que pueden ser producidos en una intercapa de mortero mecanomutable, cuando se varía el contenido de fibra de acero, el espesor de la capa superficial colocada sobre este sistema y la intensidad del campo magnético. La Tabla 6 muestra los valores de las variables que fueron utilizadas durante el ensayo y la Figura 18 el detalle de la configuración geométrica del sistema intercapa propuesto.

Tabla 6. Variables de ensayo para la reducción/eliminación del hielo/de la nieve de la superficie de la carretera.

| Variables de ensayo | Valor |
|--------------------------------|--|
| Largo y ancho de las probetas | Largo: 0.08 m Ancho: 0.12 m |
| Espesor de la capa superficial | 0.02 m, 0.03 m, 0.04 m |
| Temperatura de ensayo | -10°C |
| Espesor de la capa de MAMs | 0.02 m |
| Contenido de fibra | 0%, 5%, 11% |
| Intensidad de campo magnético | 4.1 mT, 5.3 mT, 7.0 mT (campo variable en el tiempo, para la inducción de calor) |

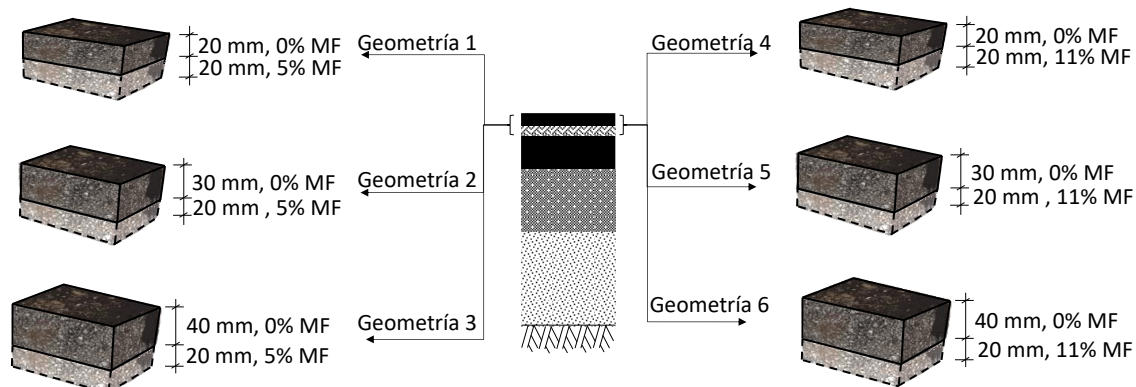


Figura 18. Geometría del sistema intercapa evaluado en el ensayo para la reducción/eliminación del hielo/de la nieve de la superficie de la carretera.

Nota Figura 18: Tomado de [147].

El esquema del protocolo de ensayo y el equipo utilizado en esta subetapa se muestra en la Figura 19, donde se puede observar que el ensayo consiste en la ejecución de tres pasos: (1) el acondicionamiento de la probeta, (2) la activación y (3) la desactivación de la inducción magnética. Los resultados obtenidos fueron procesados en cuatro análisis: (1) diagramas de distribución de temperatura, (2) influencia de la intensidad de campo magnético aplicado, (3) propuesta de un sistema de operación y (4) la influencia del espesor de la capa superficial.

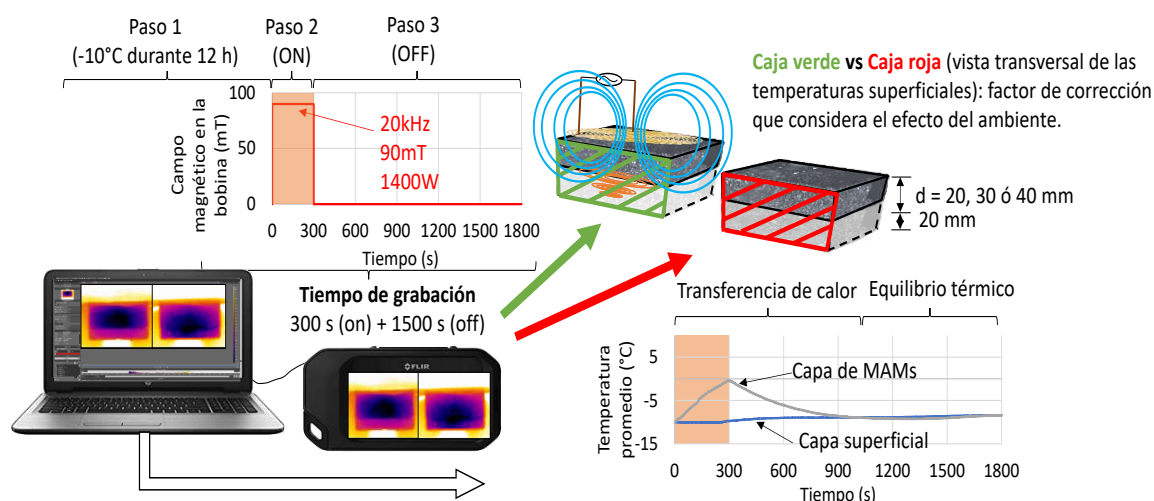


Figura 19. Esquema utilizado en el ensayo para la reducción/eliminación del hielo/de la nieve de la superficie de la carretera.

Nota Figura 19: Tomado de [147].

Finalmente, los resultados obtenidos se utilizaron para analizar la posible operación de un sistema en el que se propuso la adaptación de un camión quitanieve convencional, equipado con una parrilla de bobinas similares a las utilizadas en el ensayo (Figura 20). Los valores de desempeño obtenidos fueron comparados con los de sistemas similares, que han sido propuestos para eliminar el hielo/nieve de la superficie de la carretera, mediante el uso de estrategias de aumento de temperatura (Tabla 7).

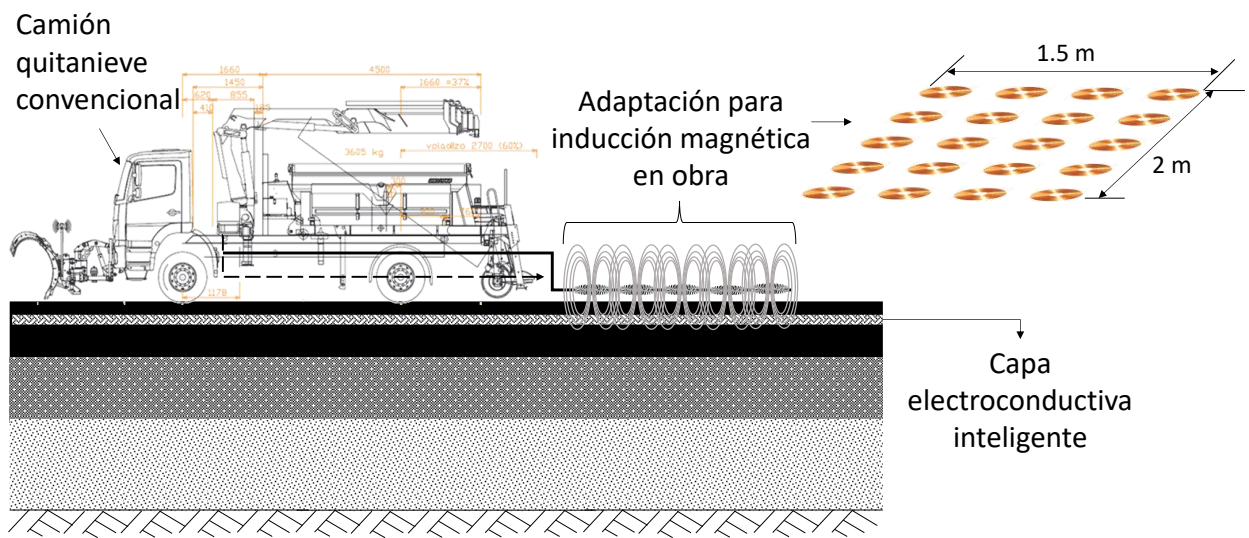
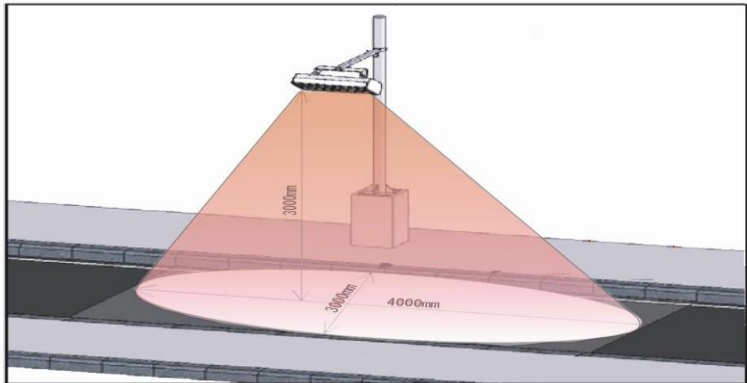
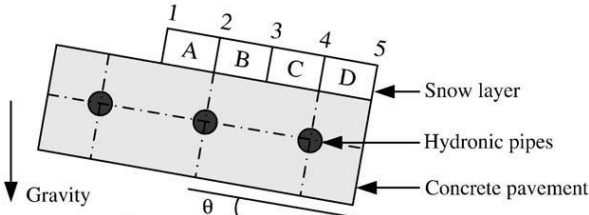
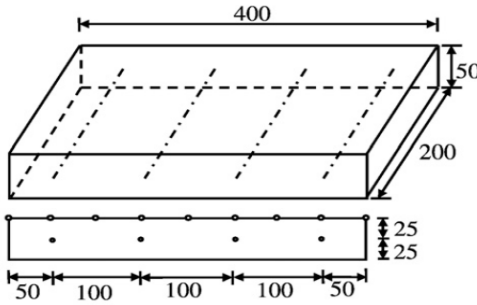
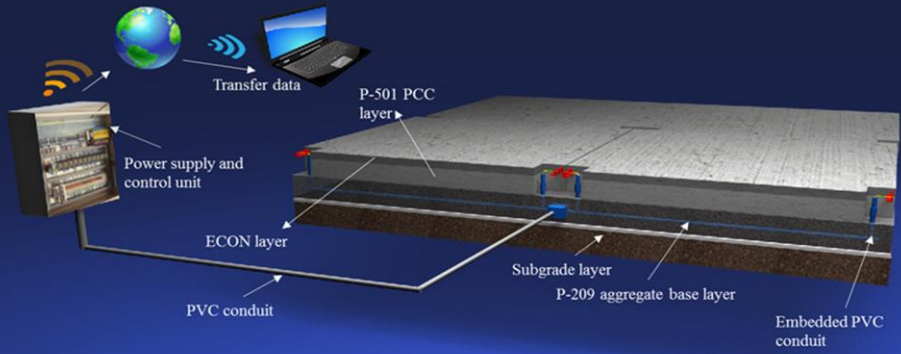


Figura 20. Sistema de capa inteligente propuesto para la eliminación del hielo/nieve de la carretera.

Nota Figura 20: Tomado de [147], el esquema del camión quitanieve fue tomado de los modelos Mercedes Benz.

Tabla 7. Sistemas de campo para eliminación de hielo/nieve de la superficie de la carretera mediante aumento de temperatura.

Nota Tabla 7: Tomado de [147].

| Sistema | Configuración |
|---|--|
| <p>Calefacción por infrarojo [59]–[61].</p> |  |
| <p>Sistemas hidrónicos (500 mm de largo, 400 mm de ancho y 300 mm de espesor) [53].</p> |  |
| <p>Varillas electroconductoras embebidas (valores en mm) [56].</p> |  |
| <p>Materiales electroconductoros [148].</p> |  <p>Power supply and control unit consist of :</p> <ul style="list-style-type: none"> - Power meter (current and voltage monitoring unit) - Circuit breaker - Data acquisition system - Temperature sensors - Power-switching on/off unit |

Más detalles de esta metodología pueden ser encontrados en el artículo: "Thermal characterization of electroconductive layers for anti-icing and de-snowing applications on roads", que se encuentra en el Anexo 4 de este documento.

4.2.3.1. Subetapa 3.2: Mejora de las capacidades de autocurado/autorecuperación de los MAMs. Esta segunda subetapa, se basó en la evaluación de la capacidad de autocurado/autorecuperación de los morteros mecanomutables, debido a la generación de un aumento de su valor de temperatura (**cambios de temperatura**) sobre el valor de su punto de reblandecimiento. Estas condiciones de temperatura son óptimas para generar el flujo del material asfáltico que compone los morteros, permitiendo de esta manera llenar las grietas producidas durante la puesta en servicio de estos materiales.

En este sentido, se utilizó el equipo de Análisis Mecánico Dinámico (DMA) que se muestra en la Figura 21 y el equipo de inducción magnética de la Figura 22, para la evaluación de 2 tipos de ensayos asociados a las siguientes condiciones de tratamiento: (1) el tratamiento de autocurado/autorecuperación luego de la falla a fatiga y (2) el tratamiento de autocurado/autorecuperación antes y durante la falla a fatiga. El tratamiento consistió en el aumento de la temperatura de probetas de mortero mecanomutable con contenidos de fibra de 5%, mediante la aplicación de 2.5 min de inducción magnética con un campo de 10 mT, el cual fue seguido de un periodo de descanso de 1 hora. Las variables de la configuración del ensayo se muestran en la Tabla 8.

Tabla 8. Variables del ensayo de autocurado/autorecuperación

| Variables de ensayo | Valor |
|-------------------------------|---|
| Dimensiones de las probetas | Largo: 50 mm |
| | Ancho y alto: 8.62 mm |
| Contenido de fibra | 0%, 5% |
| Temperatura de ensayo | 35°C |
| Intensidad de campo magnético | 10 mT (campo variable en el tiempo, para la inducción de calor) |
| Aplicación de campo | Única al (final del ensayo) y múltiple (cuatro veces a lo largo del ensayo) |



Figura 21. Equipo de Análisis Mecánico Dinámico (DMA).

Nota Figura 21: Tomado de [147].



Figura 22. Montaje utilizado para la aplicación de inducción magnética.

Nota Figura 22: Tomado de [147].

Más detalles de esta metodología pueden ser encontrados en el artículo: "Recovery capacity of electroconductive asphalt mortars under the influence of magnetic fields", que se encuentra en el Anexo 5 de este documento.

Capítulo 5. Análisis de resultados

En este capítulo se muestran los resultados obtenidos en cada uno de los estudios asociados a los artículos que comprenden este compendio de tesis. El capítulo se divide en las tres etapas asociadas a los tres pilares fundamentales descritos en el capítulo de la metodología.

5.1. Etapa 1 - MAMs: Materiales que podrían mejorar el comportamiento mecánico de los pavimentos.

Como se ha mencionado en secciones anteriores, esta primera etapa estuvo dirigida a determinar la posibilidad de escalar los resultados obtenidos en ligantes asfálticos mecanomutables, a morteros asfálticos.

En este sentido, la Figura 23 muestra los valores de módulo dinámico obtenidos del ensayo de frecuencia de resonancia ejecutado a 25°C y 45°C, sobre probetas con contenido de fibras de acero de 5% y 11%, que fueron sometidas a la acción de un campo magnético de 210 mT. Los resultados muestran tasas de aumento de módulo de 0.81 GPa/°C y 0.92 GPa/°C para 25°C y 45°C respectivamente (15% mayores a 45°C), con una reducción en la tasa de módulo por intensidad de campo magnético que pasa del 0.012 GPa/mT al 0.0016 GPa/mT, para estas temperaturas de ensayo.

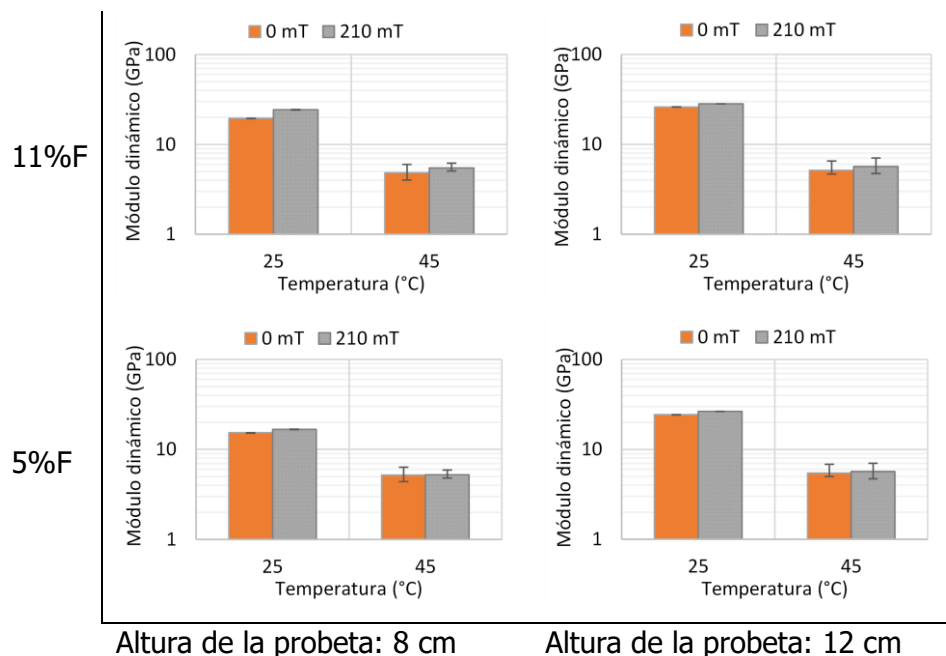


Figura 23. Influencia de temperatura en los valores de módulo dinámico para una intensidad del campo = 210 mT.

Nota Figura 23: Tomado de [146].

Los valores del cambio porcentual de módulo que se obtienen de la figura anterior se muestran en la Figura 24. A partir de estos resultados se observa que los valores son mayores a 45°C, pero se producen más rápidamente a 25°C. El análisis MANOVA de los datos permite determinar con un 95% de confianza (valor $p < 0.05$), que la altura de la probeta no tiene una influencia significativa en estos valores.

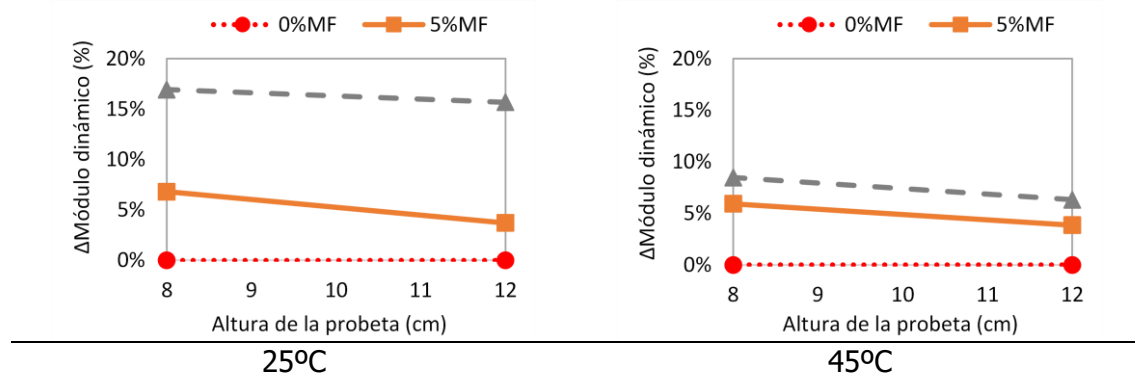


Figura 24. Influencia de la altura de la probeta en el cambio de módulo cuando se aplica una intensidad de campo de 210 mT.

Nota Figura 24: Tomado de [146].

Seguidamente, como resultado de evaluar la variación en el valor de intensidad de campo magnético, la Figura 25 muestra que conforme este parámetro aumenta, aumenta también el valor de cambio de módulo obtenido. El análisis MANOVA de estos resultados revela que con un 95% de confianza (valor $p < 0.05$), no hay evidencia de que este valor sea significativamente distinto al considerar el contenido de fibra de acero y la intensidad de campo magnético aplicada.

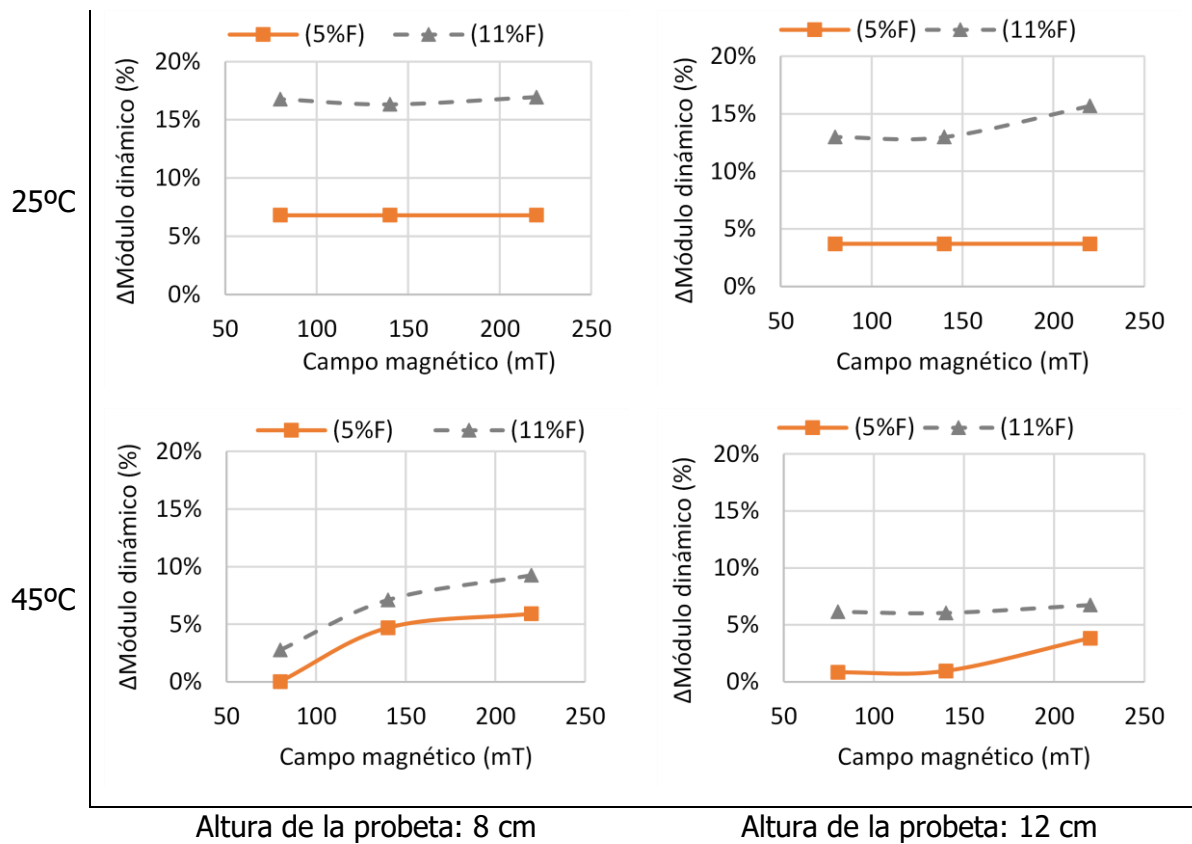


Figura 25. Influencia de la intensidad de campo magnético en los valores de módulo de probetas de mortero mecanomutable.

Nota Figura 25: Tomado de [146].

Para más detalles acerca los resultados obtenidos, revisar el Anexo 2 de este documento, donde se muestra el correspondiente artículo de investigación publicado en el Journal "Smart Materials and Structures".

5.2. MAMs: Materiales que emiten señales magnéticas que podrían ayudar en el guiado de los vehículos (Etapa 2).

En esta segunda etapa, se evaluó la señal magnética emitida por probetas de material asfáltico codificado con porcentajes de fibras de acero de 5%, 11% y 17%, para tres diferentes parámetros: (1) la altura de medición, (2) la velocidad de aproximación y (3) la distancia de medición más cercana.

Como se muestra en la Figura 26, para el primer parámetro asociado a la variación en la altura de medición de los sensores de campo magnético, la señal puede ser percibida por debajo de una altura de 0.11 m.

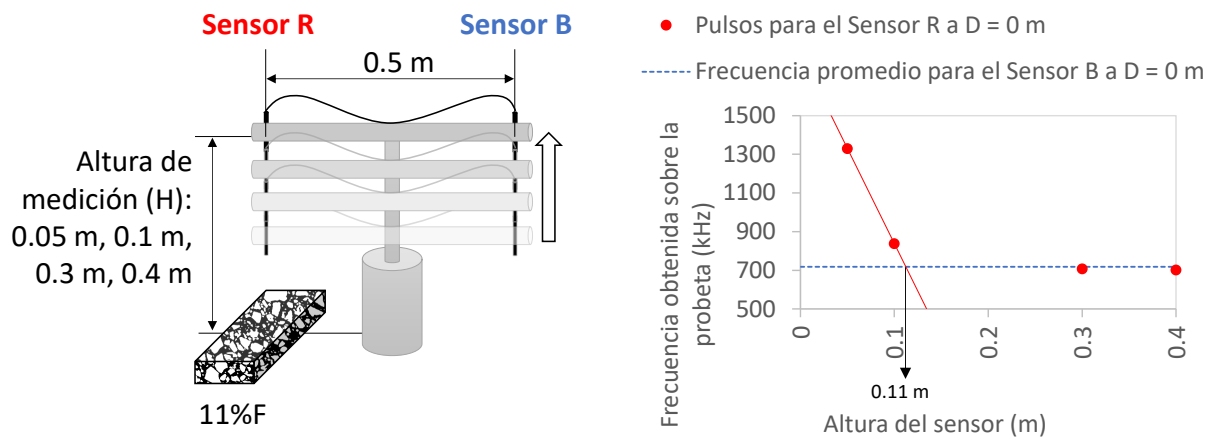
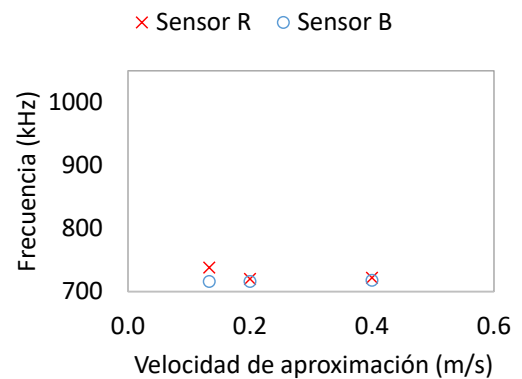
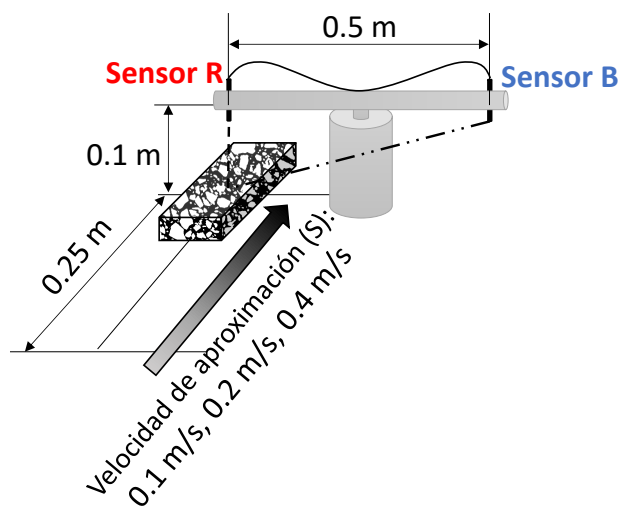


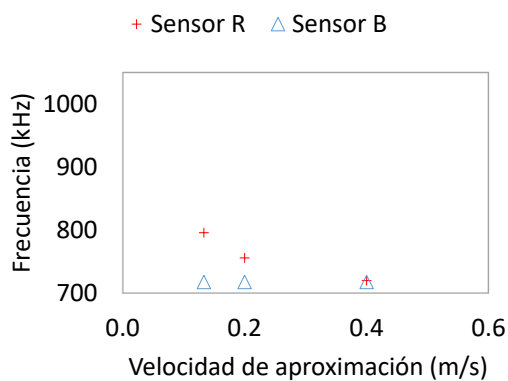
Figura 26. Influencia de la altura de medición en la señal magnética emitida por probetas con 11% de fibra de acero.

Nota Figura 26: Tomado de [145].

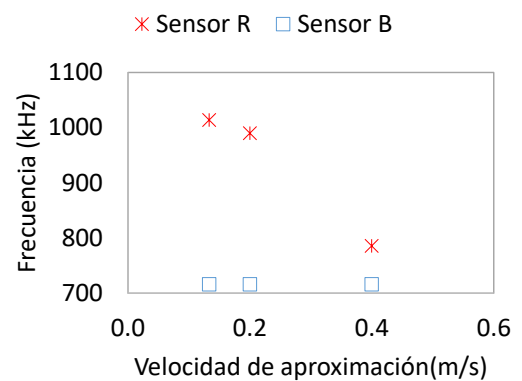
Considerando estos resultados y tal como se muestra en la Figura 27, seguidamente se evaluó la influencia de la velocidad de aproximación de la probeta (equivalente a la velocidad de aproximación del vehículo). Los resultados demostraron que, con el aumento del valor de la velocidad, los sensores utilizados reducen su capacidad de percibir la señal magnética emitida por las probetas codificadas. Esta capacidad puede ser aumentada con el aumento en el contenido de material magnético de la probeta.



5%F



11%F



17%F

Figura 27. Influencia de la velocidad de aproximación a la $D = 0$ en la señal magnética emitida por morteros codificados con fibras de acero.

Nota Figura 27: Tomado de [145].

Como último punto de análisis de esta etapa, se evaluó la distancia de aproximación de la probeta a cada sensor, mediante la evaluación de tres posiciones específicas de la probeta que se muestran en la Figura 28. Los resultados revelan que sobre valores de 0.4 m, los sensores dejan de percibir la probeta, alcanzándose los valores máximos cuando la probeta se ubica debajo del sensor. La señal magnética emitida incrementa con el contenido de fibras de acero de la probeta.

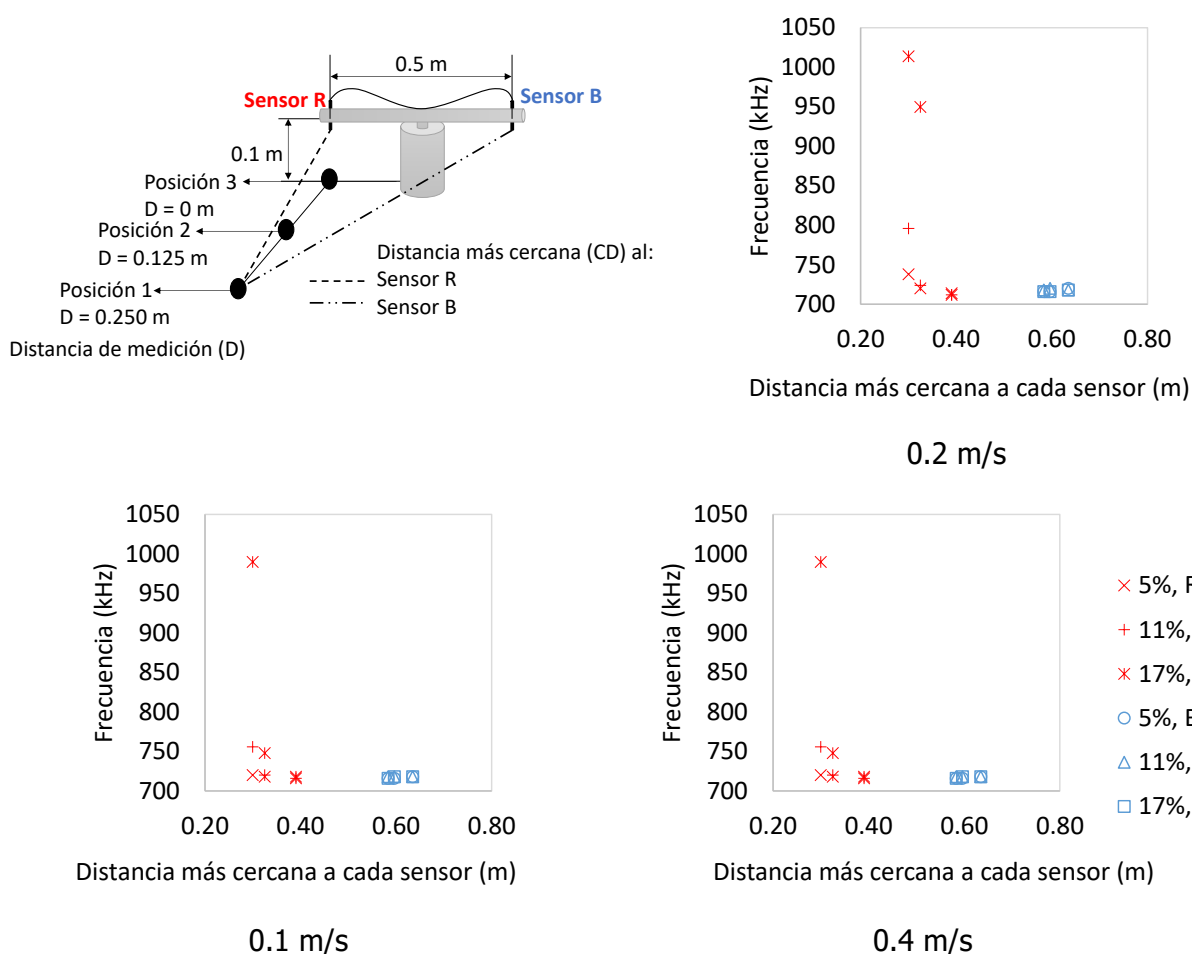


Figura 28. Influencia de la distancia más cercana a cada sensor en la señal magnética emitida por morteros codificados con fibras de acero, R: sensor rojo, B: sensor azul.

Nota Figura 28: Tomado de [145].

Los resultados obtenidos de esta evaluación demuestran que hay una configuración para la cual, es posible realizar la codificación del pavimento. En este sentido, se realizó una prueba de concepto, para la cual se confeccionó una sección de prueba donde se colocaron placas de material asfáltico codificado. Como se muestra en la Figura 29, la prueba de concepto consistió en la desactivación de las funciones del patinete cuando el sensor detecta una señal superior a los 740 kHz, valor establecido como límite, lo que sucede al pasar sobre la placa de material magnético que ha sido colocada en la sección de ensayo.

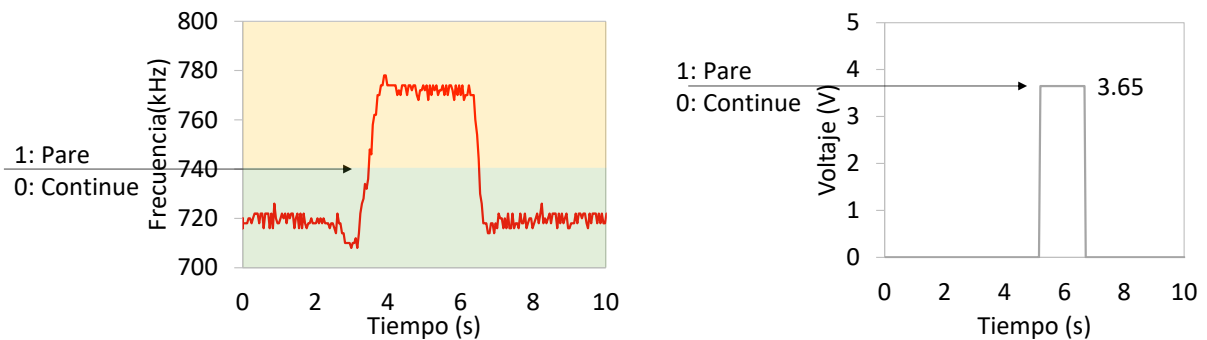


Figura 29. Prueba de concepto de placas de mortero codificado con fibras de acero.

Nota Figura 29: Tomado de [145].

Para más detalles acerca los resultados obtenidos, revisar Anexo 3 de este documento, donde se muestra el correspondiente artículo de investigación publicado en el Journal: "Sustainability".

5.3. MAMs: Materiales que aumentan su temperatura para su posible utilización en nuevas alternativas de mantenimiento de carreteras (Etapa 3).

Esta etapa se subdivide en dos subetapas relacionadas con este pilar fundamental de aplicación de los MAMs. La primera subetapa se refiere a la capacidad de los MAMs para ayudar a reducir/eliminar el hielo/nieve de la superficie de la carretera, mientras que la segunda, se dirige a estudiar la posibilidad de potenciar la capacidad de autocurado/autorecuperación de los MAMs.

5.3.1. Capacidades de los MAMs para reducir/eliminar el hielo/la nieve de la superficie de la carretera (Subetapa 3.1).

Para esta primera subetapa, se evaluaron los cambios de temperatura producidos en los morteros mecanomutables en estudio, como materiales electroconductivos que, ante la aplicación de campos magnéticos variables, generan un campo secundario con corrientes de Foucault que generan calor por el efecto de Joule.

Como se muestra en la Figura 30, la distribución de la temperatura en la superficie transversal del sistema, tanto al inicio, como a los 300 s (tiempo final de aplicación de inducción magnética) y a los 1800 s (final del ensayo, cuando se alcanza el equilibrio térmico), muestra que el aumento de temperatura por el efecto de inducción magnética, inicia en la capa de morteros mecanomutables, que posteriormente por el mecanismo de conducción de calor, aumentan la temperatura general del sistema.

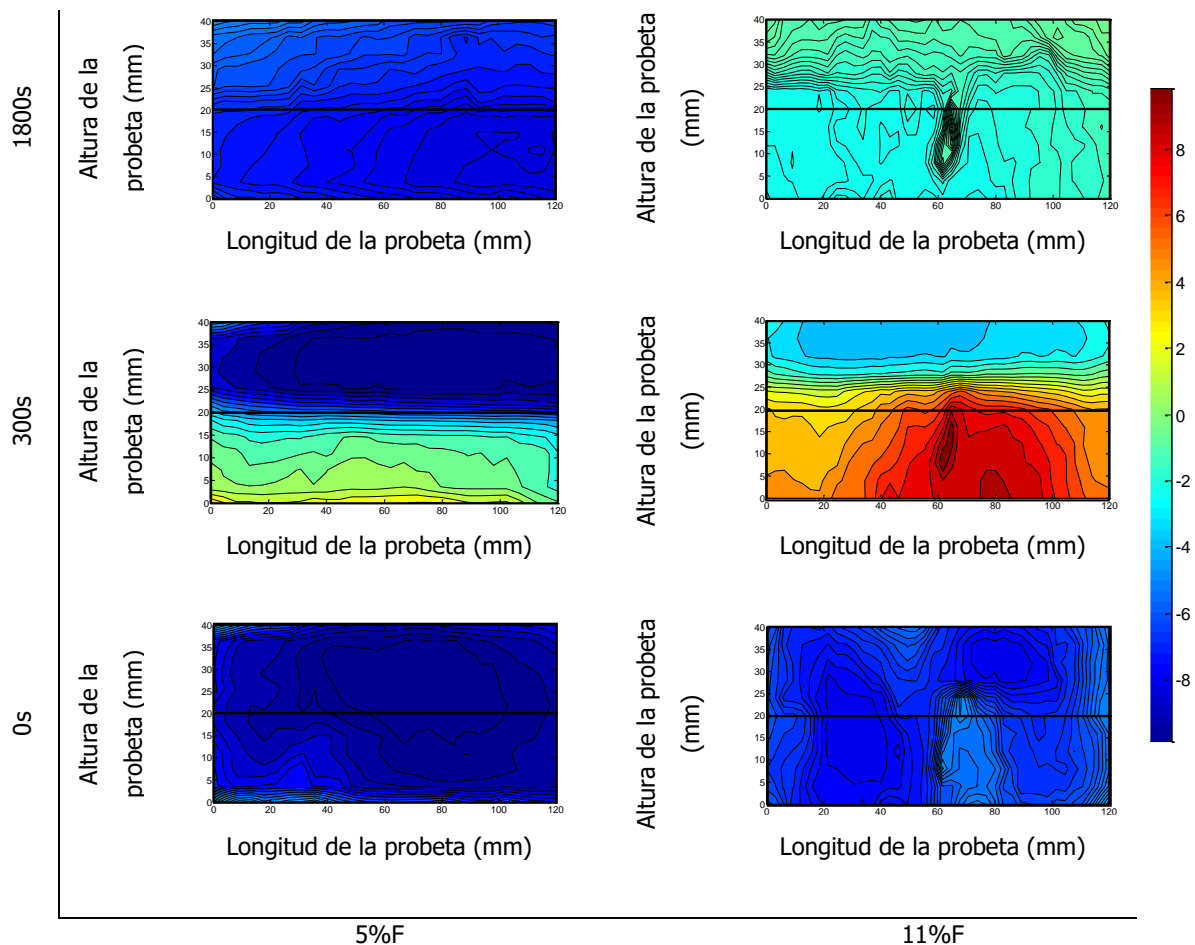


Figura 30. Distribución de temperaturas en la cara lateral de la probeta para 7.0 mT de campo magnético y capa superficial de 20 mm.

Nota Figura 30: Tomado de [147].

La Figura 31 muestra los valores del promedio de cambio de temperatura, que son producidos en la superficie lateral de cada capa de las probetas de la figura anterior, así como los resultados obtenidos cuando la intensidad de campo magnético es reducida a 5.3 mT y 4.0 mT. Los resultados indican que los cambios de temperatura obtenidos en la capa de mortero mecanomutable son dependientes de la intensidad de campo magnético aplicada y la dosis de fibra de acero utilizada, obteniendo un valor máximo de 16.71°C para el campo de 7.0 mT y menores resultados con la reducción del valor de este parámetro. El análisis estadístico correspondiente al diseño de bloques aleatorizados de estos datos muestra que, con un 95% de confianza, el contenido de fibra de acero y la intensidad de campo magnético, tienen influencia significativa en los resultados obtenidos a los 300 s. La figura también muestra que el aumento

de temperatura logrado a los 300 s en la capa de mortero mecanomutable, permite que, por el mecanismo de conducción de calor, se logre aumentar la temperatura del sistema. Una vez desactivado el campo, esta transferencia de calor continúa hasta alcanzar el equilibrio térmico entre las dos capas (aproximadamente 1800 s).

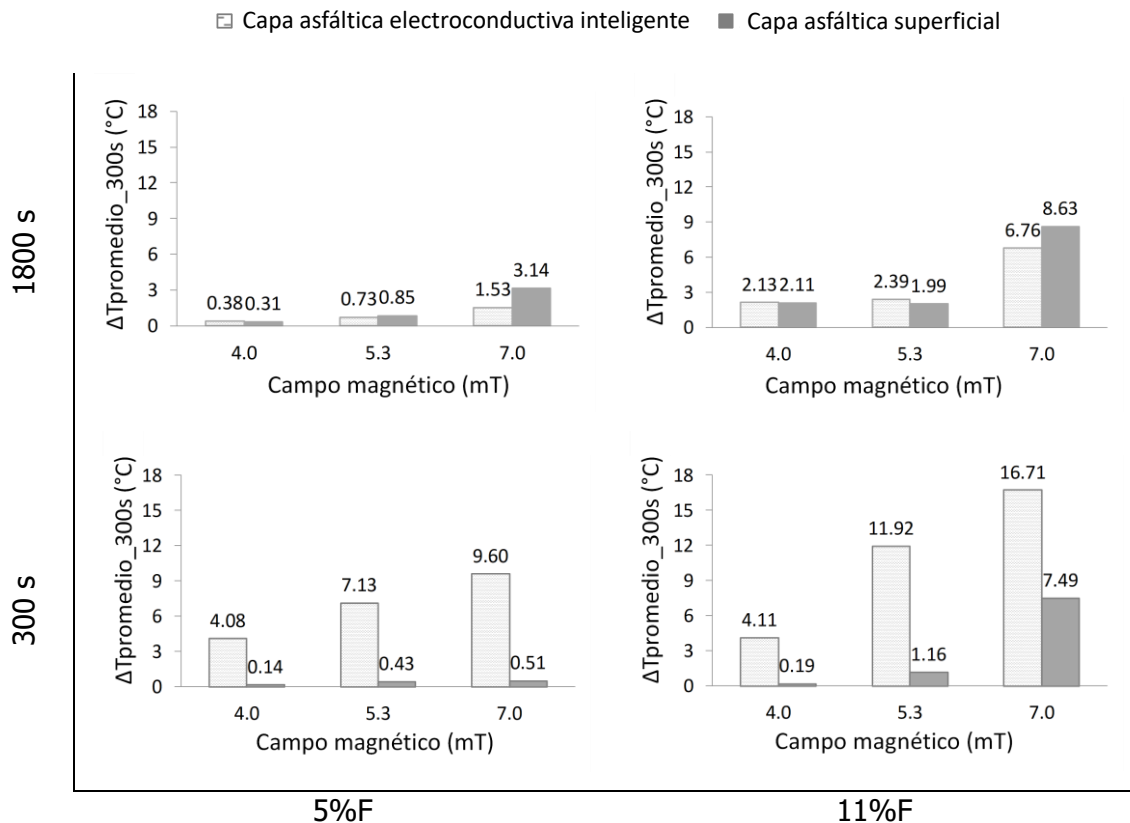


Figura 31. Influencia de la intensidad del campo magnético en los valores de temperatura a los 300 s y 1800 s.

Nota Figura 31: Tomado de [147].

Posteriormente, la Figura 32 muestra los valores de cambio de temperatura alcanzados al aumentar el espesor de capa superficial, cuando la intensidad de campo magnético es de 4.0 mT. Los resultados revelan que los cambios de temperatura son 10%-25% menores por cm aumentado y se deben a que hay una mayor cantidad de material. El análisis estadístico correspondiente al diseño de bloques aleatorizados de estos datos muestra que, con un 95% de confianza, el espesor de la capa superficial afecta significativamente los resultados obtenidos en la capa de mortero mecanomutable a los 300 s, pero no los de la capa superficial.

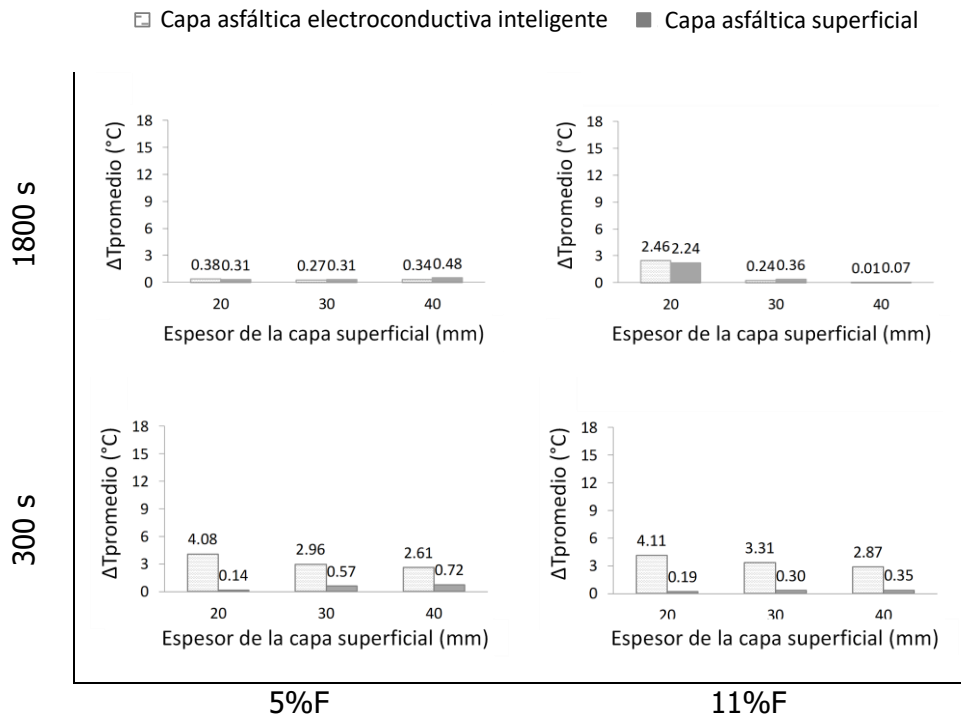


Figura 32. Influencia del espesor de la capa asfáltica superficial en los valores de temperatura a los 300 s y 1800 s.

Nota Figura 32: Tomado de [147].

La Figura 33 muestra que a pesar de que el flujo de calor del sistema depende del contenido de fibra de acero, el sistema puede presentar un desempeño parecido al de otros sistemas que proponen también el aumento de temperatura.

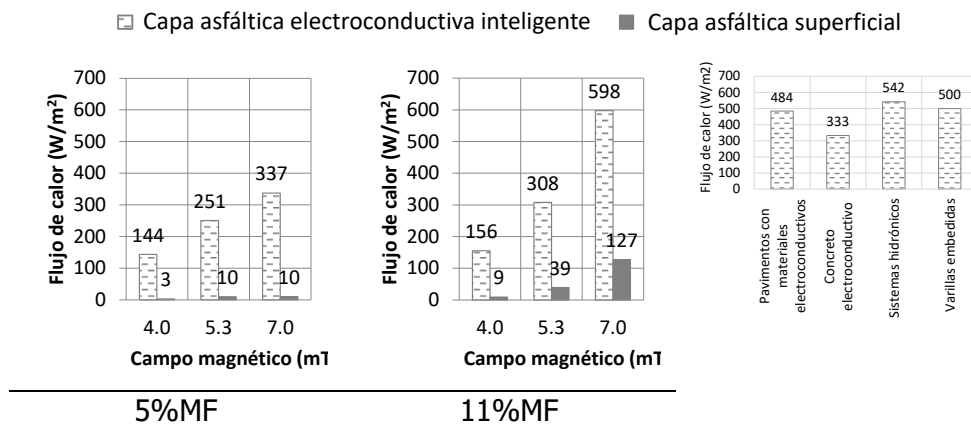


Figura 33. Sistema de capa inteligente de mortero mecanomutable vs otras alternativas.

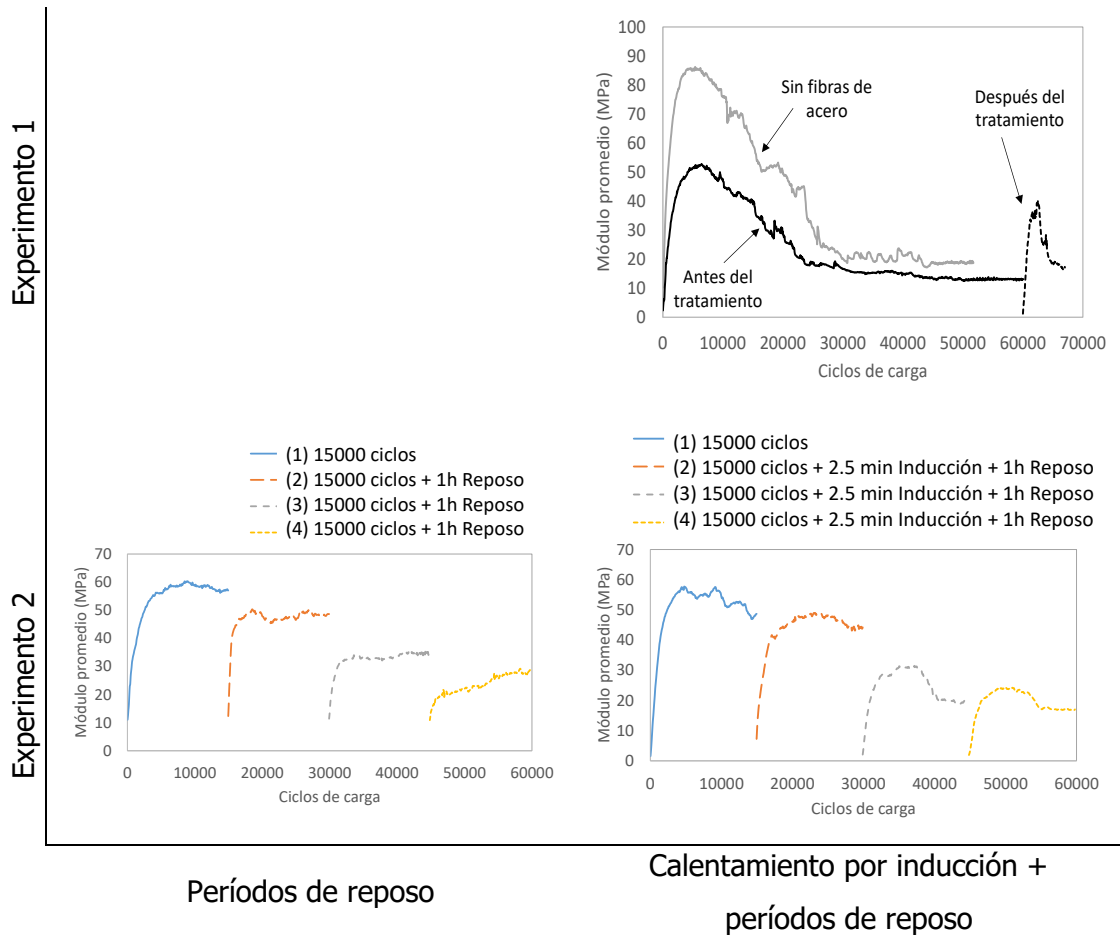
Nota Figura 33: Tomado de [147].

Estos resultados están en proceso de publicación en el Journal "Road Materials and Pavements Desing".

5.3.2. Mejora de las capacidades de autocurado/autorecuperación de los MAMs (Subetapa 3.2).

Para segunda subetapa, al igual en que el apartado anterior, se evaluaron los cambios de temperatura producidos por el efecto de la aplicación de inducción magnética. En este caso, el estudio estuvo dirigido a evaluar la capacidad de mejorar o potenciar, la capacidad de autocurado/autorecuperación de los materiales asfálticos, cuando están a temperaturas sobre su punto de reblandecimiento. Este principio se basa en las propiedades viscoelásticas termodependientes de los materiales asfálticos, que sobre la temperatura asociada a su punto de reblandecimiento [149], empiezan a fluir y en consecuencia llenar las grietas formadas por fatiga, mediante el mecanismo de capilaridad [149][150]–[152].

La Figura 34 muestra los resultados del valor de módulo promedio de los dos experimentos realizados en este estudio: (1) único tratamiento de 2.5 minutos de calor por inducción, seguido de 1 hora de reposo y (2) múltiples tratamientos de 1 hora de reposo o 2.5 minutos de calor por inducción, seguido de 1 hora de reposo. Como se puede ver en la figura, a pesar de que para el primer experimento, el valor de módulo promedio máximo es reducido por la incorporación de las fibras de acero, la vida a fatiga se aumenta en 8% con respecto a los morteros sin fibras. Los correspondientes valores de porcentaje de recuperación, obtenidos de la relación de las áreas bajo la curva de módulo vs ciclo de carga se muestran en la Figura 35. Tal como se puede observar, en el Experimento 1, se obtuvo una recuperación total de 14%, mientras que en el Experimento 2 se obtuvo un valor total de 32%. En el caso del Experimento 2, se puede observar que entre el 14% y 19% de la recuperación, es producida por el efecto de los períodos de descanso, lo que significa que el porcentaje restante corresponde al efecto de la inducción de calor, que principalmente ocurre durante la etapa de microagrietamiento de la probeta.



Períodos de reposo

Calentamiento por inducción +
períodos de reposo

Figura 34. Resultados del módulo promedio para la evaluación del autocurado/autoreparación de morteros mecanomutables.

Nota Figura 34: Tomado de [153].

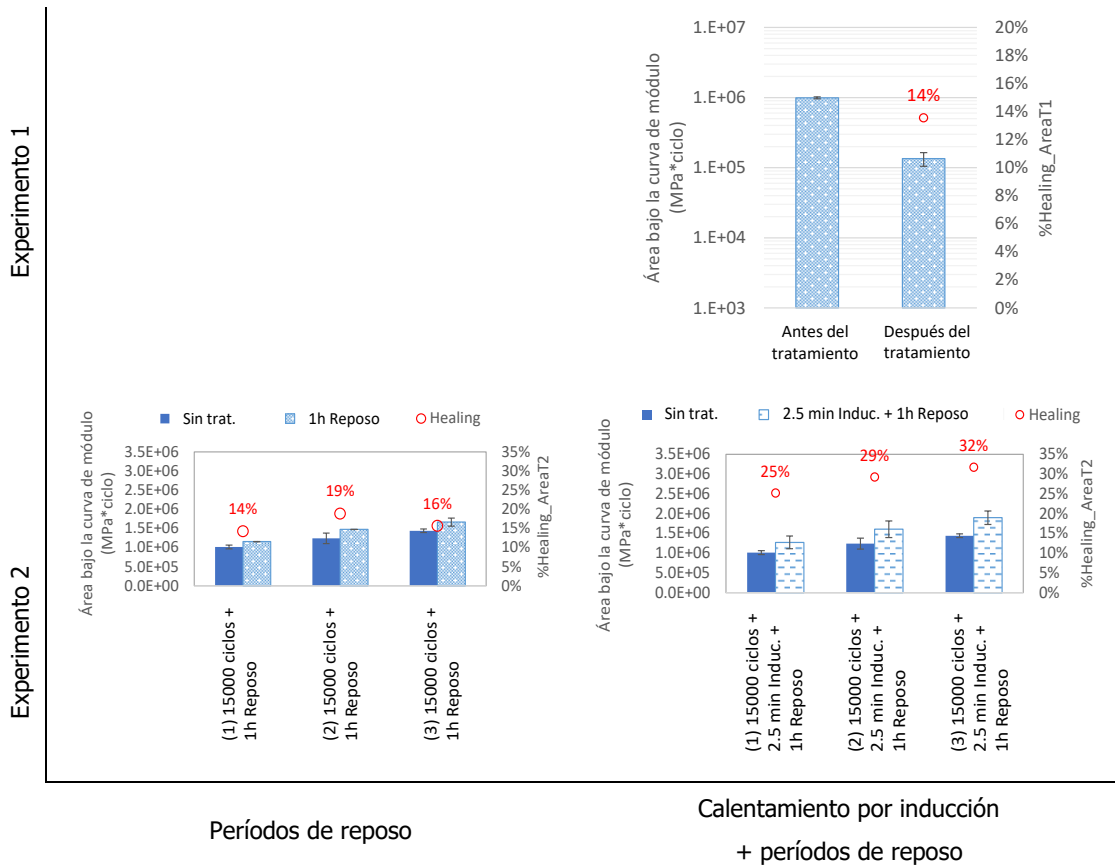


Figura 35. Resultados de recuperación obtenida para la evaluación del autocurado/autoreparación de morteros mecanomodificables.

Nota Figura 35: Tomado de [153].

El esfuerzo de flexión por cada ciclo de carga se muestra en la Figura 36. A partir de la determinación del valor de fatiga de bajo ciclo (LCF) del Experimento 1, fue que se determinaron los ciclos para tratamiento del Experimento 2 (15000 ciclos). La comparación de los ciclos correspondientes a un esfuerzo de flexión de 0.16MPa, demuestra que el tratamiento con períodos de descanso, aumenta la vida a fatiga en 17%, mientras que, para la inducción seguida de períodos de descanso, este valor aumenta al 40%.

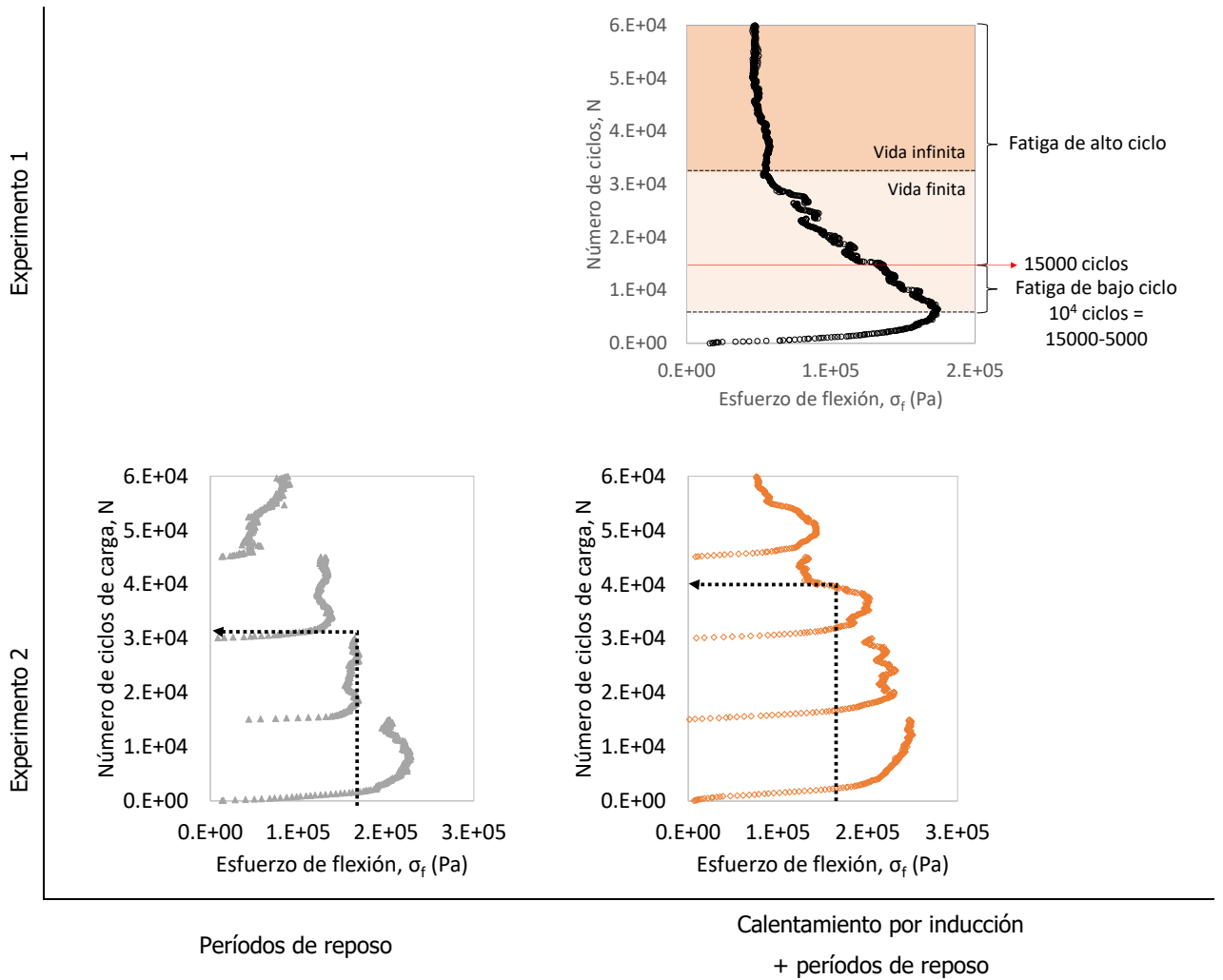


Figura 36. Curvas esfuerzo vs número de ciclos para la evaluación del autocurado/autoreparación de morteros mecanomutables.

Nota Figura 36: Tomado de [153].

Para más detalles acerca los resultados obtenidos, revisar el Anexo 5 de este documento, donde se muestra el correspondiente artículo de investigación publicado en el Journal "Materials Today Communications".

Capítulo 6. Conclusiones

La presente tesis doctoral se enfoca en analizar a nivel de laboratorio, la viabilidad de uso de los MAMs como materiales para la construcción de pavimentos inteligentes. En este sentido, se modificaron y definieron protocolos de ensayo existentes y nuevos, con la finalidad de permitir la activación de campos magnéticos sobre los MAMs y producirles tres efectos: cambios en el valor de módulo, cambios en la señal magnética que emiten y cambios de temperatura.

A partir de estos tres efectos, es que en esta tesis se proponen tres aplicaciones de uso de los MAMs: mejoramiento del comportamiento mecánico de los pavimentos, codificación de las carreteras para asistencia en el guiado de los vehículos y definición de nuevas alternativas de mantenimiento que utilizan el aumento de su temperatura como mecanismo en la eliminación del hielo/nieve de la carretera o el mejoramiento de capacidad de autorecuperación/autocurado de los materiales asfálticos.

Con base en los resultados obtenidos a lo largo de este compendio de tesis, las principales conclusiones obtenidas son las siguientes:

1. El aumento en el valor de módulo que se produce en ligantes asfálticos mecanomutables ante la activación de campos magnéticos constantes, puede ser escalado a nivel superior en morteros asfálticos mecanomutables. En este caso, la incorporación del agregado reduce el efecto logrado a escala de ligante, siendo este igualmente dependiente de la intensidad de campo magnético aplicada, el contenido de material magnético utilizado en la fabricación del mortero y la temperatura a la que se realiza el ensayo.
2. Los MAMs pueden emitir señales magnéticas detectables por sensores de campo magnético. La intensidad de la señal registrada por los sensores depende del contenido de material con propiedades magnéticas que es utilizado en la producción de los MAMs, así como, la altura de ubicación de los sensores en el vehículo, su velocidad y distancia de aproximación a la sección con MAMs. Esta capacidad de los MAMs puede ser utilizada para asistir el guiado de los vehículos y en consecuencia mejorar la seguridad vial de la carretera.
3. Las propiedades eléctricas de las fibras de acero, reaccionan a la acción de campos magnéticos variables, generando corrientes de Foucault que finalmente por el efecto de Joule, aumentan la temperatura de los morteros mecanomutables. Este aumento de temperatura, permite que sea posible la definición de un sistema de capa inteligente de

morteros mecanomutables, que puede ser instalada dentro de las capas bituminosas del pavimento, de forma que puede ser utilizada como alternativa para reducir/eliminar el hielo/nieve de la superficie de la carretera. Esta alternativa ofrece de esta manera una nueva forma aumentar la seguridad vial de la carretera en condiciones de clima adversas como lo son las intensas nevadas.

4. El mecanismo de generación de calor mencionado en la conclusión anterior, puede también ser utilizado para potenciar la capacidad de autocurado/autorecuperación de los morteros asfálticos mecanomutables, principalmente durante la fase de microagrietamiento.

Con base en los resultados presentados en esta tesis, se puede decir que los morteros asfálticos mecanomutables son materiales inteligentes con capacidades potenciales para ofrecer soluciones nuevas e innovadoras, a las necesidades presentes y futuras de la carretera.

Capítulo 7. Futuras líneas de investigación

A lo largo del desarrollo de la presente tesis doctoral, se han identificado esfuerzos adicionales que podrían llevarse a cabo en investigaciones futuras para la consolidación de esta línea de investigación y una mejor comprensión de los materiales asfálticos mecanomutables en la construcción de pavimentos inteligentes. A continuación, se describen algunos de estos posibles esfuerzos, que ya están siendo o que serán abordados por el LabIC.UGR como desarrollador y promotor de este tema de investigación:

- Estudios de los MAMs en laboratorio a escala micro y macro donde se permita trasladar los resultados obtenidos en esta investigación desde el nivel de morteros, al nivel de las mezclas asfálticas.
- Estudios a escala real donde se pongan a prueba los hallazgos obtenidos en el laboratorio y que permitan determinar los factores de ajuste idóneos, para definir guías que faciliten y expongan el uso adecuado de los MAMs, como materiales que adaptan sus capacidades mecánicas y térmicas a condiciones específicas de servicio, ofreciendo características de resiliencia a la carretera.
- Estudio de laboratorio a las diferentes escalas, de los MAMs como sistemas con capacidad de aliviar los esfuerzos y servir de refuerzo en rehabilitaciones relacionadas con la colocación de sobrecapas asfálticas.
- Considerando que esta tesis doctoral ha estado enfocada al estudio de MAMs producidos con fibras de acero obtenidas de los neumáticos fuera de uso y tras la identificación del resto de materiales que podrían ser utilizados en la producción de MAMs. Se recomienda elaborar estudios adicionales que además de permitir la comparación de los resultados obtenidos en esta investigación, permitan contemplar las capacidades de estos materiales, de acuerdo con sus respectivas capacidades magnéticas/eléctricas.
- Evaluación de diferentes escenarios de ciclo de vida de los MAMs, para las diferentes aplicaciones identificadas en esta tesis doctoral, considerando no solo los procesos relacionados con su producción, sino que también aquellos asociados a su uso a lo largo de la vida de la carretera.

Referencias

- [1] F. Moreno-Navarro, G. R. Iglesias, y M. C. Rubio-Gómez, «Development of mechanomutable asphalt binders for the construction of smart pavements», *Mater. Des.*, vol. 84, pp. 100-109, nov. 2015, doi: 10.1016/J.MATDES.2015.06.098.
- [2] F. Moreno-Navarro, G. R. Iglesias, y M. C. Rubio-Gómez, «Mechanical performance of mechanomutable asphalt binders under cyclic creep and recovery loads», *Constr. Build. Mater.*, vol. 113, pp. 506-512, jun. 2016, doi: 10.1016/J.CONBUILDMAT.2016.03.042.
- [3] F. Moreno-Navarro, G. R. Iglesias, y M. C. Rubio-Gómez, «Experimental evaluation of using stainless steel slag to produce mechanomutable asphalt mortars for their use in smart materials», *Smart Mater. Struct.*, 2016, doi: 10.1088/0964-1726/25/11/115036.
- [4] F. Moreno-Navarro y M. C. Rubio-Gómez, «Desarrollo de nuevos materiales inteligentes para pavimentos del futuro», *Carreteras Rev. técnica la Asoc. Española la Carret.*, n.º 217, pp. 56-65, 2018.
- [5] V. L. Junior, V. Steffen, y M. A. Savi, *Dynamics of Smart Systems and Structures*. Springer International Publishing, Switzerland, 2016.
- [6] D. J. Inman, «Smart Materials and Structures», en *CISM International Centre for Mechanical Sciences, Courses and Lectures*, 2007.
- [7] D. J. Leo, *Engineering Analysis of Smart Material Systems*. 2008.
- [8] G. Park, H. H. Cudney, y D. J. Inman, «Impedance-based health monitoring of civil structural components», *J. Infrastruct. Syst.*, 2000, doi: 10.1061/(ASCE)1076-0342(2000)6:4(153).
- [9] G. Park y D. J. Inman, «Structural health monitoring using piezoelectric impedance measurements», *Philosophical Transactions of the Royal Society A: Mathematical, Physical and Engineering Sciences*. 2007, doi: 10.1098/rsta.2006.1934.
- [10] A. Fernández-Isabel, R. Fuentes-Fernández, y I. Martín de Diego, «Modeling multi-agent systems to simulate sensor-based Smart Roads», *Simul. Model. Pract. Theory*, vol. 99, p. 101994, feb. 2020, doi: 10.1016/J.SIMPAT.2019.101994.
- [11] B. C. Chifor, I. Bica, y V. V. Patriciu, «Sensing service architecture for smart cities using

- social network platforms», *Soft Comput.*, 2017, doi: 10.1007/s00500-016-2053-x.
- [12] F. Moreno-Navarro, G. R. Iglesias, y M. C. Rubio-Gómez, «Encoded asphalt materials for the guidance of autonomous vehicles», *Autom. Constr.*, vol. 99, pp. 109-113, mar. 2019, doi: 10.1016/j.autcon.2018.12.004.
- [13] F. Moreno-Navarro, M. C. Rubio-Gómez, y G. Iglesias, «Pavimento, y sistema de seguridad que lo comprende», P201631096, 2018.
- [14] F. Moreno-Navarro, M. Sol-Sánchez, F. Gámiz, y M. C. Rubio-Gómez, «Mechanical and thermal properties of graphene modified asphalt binders», *Constr. Build. Mater.*, vol. 180, pp. 265-274, ago. 2018, doi: 10.1016/J.CONBUILDMAT.2018.05.259.
- [15] «Sustainable Multifunctional Automated and Resilient Transport Infrastructures, European Training Network», *Programa Europeo Horizonte 2020, financiado por acciones Marie Skłodowska-Curie para investigación, desarrollo tecnológico y demostración, beca No.721493.*, 2017. <http://www.smartietn.eu/> (accedido sep. 08, 2020).
- [16] C. Manville *et al.*, «Mapping Smart Cities in the EU», 2014. [En línea]. Disponible en: <http://www.europarl.europa.eu/studies>.
- [17] «UNE 178201 - Ciudades Inteligentes. Definición, atributos y requisitos», 2016.
- [18] Z. Bi *et al.*, «Life cycle assessment and tempo-spatial optimization of deploying dynamic wireless charging technology for electric cars», *Transp. Res. Part C Emerg. Technol.*, 2019, doi: 10.1016/j.trc.2019.01.002.
- [19] A. S. Dezfooli, F. M. Nejad, H. Zakeri, y S. Kazemifard, «Solar pavement: A new emerging technology», *Sol. Energy*, 2017, doi: 10.1016/j.solener.2017.04.016.
- [20] J. Hu, Q. Gao, y X. Yu, «Characterization of the optical and mechanical properties of innovative multifunctional thermochromic asphalt binders», *J. Mater. Civ. Eng.*, vol. 27, n.º 5, 2015, doi: 10.1061/(ASCE)MT.1943-5533.0001132.
- [21] M. Ouria y H. Sevinc, «Evaluation of the potential of solar energy utilization in Famagusta, Cyprus», *Sustain. Cities Soc.*, vol. 37, pp. 189-202, 2018, doi: 10.1016/j.scs.2017.10.036.
- [22] A. Chiarelli, A. R. Dawson, y A. García, «Parametric analysis of energy harvesting

- pavements operated by air convection», *Appl. Energy*, vol. 154, pp. 951-958, 2015, doi: 10.1016/j.apenergy.2015.05.093.
- [23] T. Ma, H. Yang, W. Gu, Z. Li, y S. Yan, «Development of walkable photovoltaic floor tiles used for pavement», *Energy Convers. Manag.*, 2019, doi: 10.1016/j.enconman.2019.01.035.
- [24] A. Dawson, R. Mallick, A. G. Hernandez, y P. K. Dehdezi, *Energy harvesting from pavements*, vol. 204. 2014.
- [25] D. Vizzari, E. Chailleux, E. Genesseeux, S. Lavaud, y N. Vignard, «Viscoelastic characterisation of transparent binders for application on solar roads», *Road Mater. Pavement Des.*, 2019, doi: 10.1080/14680629.2019.1588774.
- [26] D. Vizzari, E. Chailleux, S. Lavaud, E. Genesseeux, y S. Bouron, «Fraction factorial design of a novel semi-transparent layer for applications on solar roads», *Infrastructures*, 2020, doi: 10.3390/infrastructures5010005.
- [27] A. García y M. N. Partl, «How to transform an asphalt concrete pavement into a solar turbine», *Appl. Energy*, vol. 119, pp. 431-437, abr. 2014, doi: 10.1016/j.apenergy.2014.01.006.
- [28] N. A. A. Guntor, M. Fadhil, M. Ponraj, y K. Iwao, «Thermal performance of developed coating material as cool pavement material for tropical regions», *J. Mater. Civ. Eng.*, vol. 26, n.º 4, pp. 755-760, 2014, doi: 10.1061/(ASCE)MT.1943-5533.0000859.
- [29] A. Sha, Z. Liu, K. Tang, y P. Li, «Solar heating reflective coating layer (SHRCL) to cool the asphalt pavement surface», *Constr. Build. Mater.*, vol. 139, pp. 355-364, 2017, doi: 10.1016/j.conbuildmat.2017.02.087.
- [30] W. Jiang, J. Xiao, D. Yuan, H. Lu, S. Xu, y Y. Huang, «Design and experiment of thermoelectric asphalt pavements with power-generation and temperature-reduction functions», *Energy Build.*, vol. 169, pp. 39-47, 2018, doi: 10.1016/j.enbuild.2018.03.049.
- [31] G. Guldentops, A. M. Nejad, C. Vuye, W. Van den bergh, y N. Rahbar, «Performance of a pavement solar energy collector: Model development and validation», *Appl. Energy*, vol. 163, pp. 180-189, 2016, doi: 10.1016/j.apenergy.2015.11.010.

- [32] Z. Zhou, X. Wang, X. Zhang, G. Chen, J. Zuo, y S. Pullen, «Effectiveness of pavement-solar energy system - An experimental study», *Appl. Energy*, vol. 138, pp. 1-10, 2015, doi: 10.1016/j.apenergy.2014.10.045.
- [33] S. Do Hong *et al.*, «Enhanced energy-generation performance of a landfilled road-capable piezoelectric harvester to scavenge energy from passing vehicles», *Energy Convers. Manag.*, 2020, doi: 10.1016/j.enconman.2020.112900.
- [34] S. Wang, C. Wang, G. Yu, y Z. Gao, «Development and performance of a piezoelectric energy conversion structure applied in pavement», *Energy Convers. Manag.*, vol. 207, p. 112571, 2020, doi: <https://doi.org/10.1016/j.enconman.2020.112571>.
- [35] H. Xiong y L. Wang, «Piezoelectric energy harvester for public roadway: On-site installation and evaluation», *Appl. Energy*, vol. 174, pp. 101-107, 2016, doi: 10.1016/j.apenergy.2016.04.031.
- [36] H. Roshani, S. Dessouky, A. Montoya, y A. T. T. Papagiannakis, «Energy harvesting from asphalt pavement roadways vehicle-induced stresses: A feasibility study», *Appl. Energy*, vol. 182, pp. 210-218, 2016, doi: 10.1016/j.apenergy.2016.08.116.
- [37] C. Wang, S. Wang, Q. J. Li, X. Wang, Z. Gao, y L. Zhang, «Fabrication and performance of a power generation device based on stacked piezoelectric energy-harvesting units for pavements», *Energy Convers. Manag.*, vol. 163, pp. 196-207, 2018, doi: 10.1016/j.enconman.2018.02.045.
- [38] C. Wang, J. Zhao, Q. Li, y Y. Li, «Optimization design and experimental investigation of piezoelectric energy harvesting devices for pavement», *Appl. Energy*, vol. 229, pp. 18-30, 2018, doi: 10.1016/j.apenergy.2018.07.036.
- [39] H. Roshani, P. Jagtap, S. Dessouky, A. Montoya, y A. T. Papagiannakis, «Theoretical and experimental evaluation of two roadway piezoelectric-based energy harvesting prototypes», *J. Mater. Civ. Eng.*, vol. 30, n.º 2, 2018, doi: 10.1061/(ASCE)MT.1943-5533.0002112.
- [40] P. Liu *et al.*, «Numerical study on influence of piezoelectric energy harvester on asphalt pavement structural responses», *J. Mater. Civ. Eng.*, vol. 31, n.º 3, 2019, doi:

10.1061/(ASCE)MT.1943-5533.0002640.

- [41] B. González, F. J. Jiménez, y J. De Frutos, «A Virtual Instrument for Road Vehicle Classification Based on Piezoelectric Transducers», *Sensors (Basel)*, vol. 20, n.º 16, 2020, doi: 10.3390/s20164597.
- [42] H. Yang *et al.*, «Development in stacked-array-type piezoelectric energy harvester in asphalt pavement», *J. Mater. Civ. Eng.*, vol. 29, n.º 11, 2017, doi: 10.1061/(ASCE)MT.1943-5533.0002079.
- [43] C.-H. Wang, S. Chen, Y.-W. Li, X. Shi, y Q. Li, «Design of piezoelectric elements' protection measures and energy output of intelligent power pavement», *Zhongguo Gonglu Xuebao/China J. Highw. Transp.*, vol. 29, n.º 5, pp. 41-49, 2016.
- [44] C. Wang, S. Wang, Z. Gao, y X. Wang, «Applicability evaluation of embedded piezoelectric energy harvester applied in pavement structures», *Appl. Energy*, 2019, doi: 10.1016/j.apenergy.2019.113383.
- [45] N. Zabihi y M. Saafi, «Recent developments in the energy harvesting systems from road infrastructures», *Sustain.*, vol. 12, n.º 17, 2020, doi: 10.3390/SU12176738.
- [46] L. Guo y Q. Lu, «Potentials of piezoelectric and thermoelectric technologies for harvesting energy from pavements», *Renewable and Sustainable Energy Reviews*. 2017, doi: 10.1016/j.rser.2017.01.090.
- [47] F. Duarte y A. Ferreira, «Energy harvesting on road pavements: State of the art», *Proc. Inst. Civ. Eng. Energy*, 2016, doi: 10.1680/jener.15.00005.
- [48] P. Jiao, K.-J. I. Egbe, Y. Xie, A. M. Nazar, y A. H. Alavi, «Piezoelectric sensing techniques in structural health monitoring: A state-of-the-art review», *Sensors (Switzerland)*, vol. 20, n.º 13, pp. 1-21, 2020, doi: 10.3390/s20133730.
- [49] J. Xiao, X. Zou, y W. Xu, «ePave: A self-powered wireless sensor for smart and autonomous pavement», *Sensors (Switzerland)*, vol. 17, n.º 10, 2017, doi: 10.3390/s17102207.
- [50] S. Wang, C. Wang, Z. Gao, y H. Cao, «Design and performance of a cantilever piezoelectric power generation device for real-time road safety warnings», *Appl. Energy*, vol. 276, 2020,

doi: 10.1016/j.apenergy.2020.115512.

- [51] A. Pérez Lepe *et al.*, «Project REC "Roads as Energetic Crops". Energetic roads through piezoelectric harvesting | Proyecto REC "Roads as Energetic Crops" Carreteras energéticas mediante captación piezoeléctrica», *Carreteras*, 2015.
- [52] C. Han, G. Wu, y X. B. Yu, «Performance Analyses of Geothermal and Geothermoelectric Pavement Snow Melting System», *J. Energy Eng.*, 2018, doi: 10.1061/(ASCE)EY.1943-7897.0000585.
- [53] H. Wang, L. Liu, y Z. Chen, «Experimental investigation of hydronic snow melting process on the inclined pavement», *Cold Reg. Sci. Technol.*, 2010, doi: 10.1016/j.coldregions.2010.04.007.
- [54] R. Mirzanimadi, C. E. Hagentoft, P. Johansson, y J. Johnsson, «Anti-icing of road surfaces using Hydronic Heating Pavement with low temperature», *Cold Reg. Sci. Technol.*, 2018, doi: 10.1016/j.coldregions.2017.10.006.
- [55] A. Balbay y M. Esen, «Experimental investigation of using ground source heat pump system for snow melting on pavements and bridge decks», *Sci. Res. Essays*, 2010.
- [56] H. Zhao, Z. Wu, S. Wang, J. Zheng, y G. Che, «Concrete pavement deicing with carbon fiber heating wires», *Cold Reg. Sci. Technol.*, vol. 65, n.º 3, pp. 413-420, mar. 2011, doi: 10.1016/J.COLDREGIONS.2010.10.010.
- [57] Y. Lai, Y. Liu, y D. Ma, «Automatically melting snow on airport cement concrete pavement with carbon fiber grille», *Cold Reg. Sci. Technol.*, 2014, doi: 10.1016/j.coldregions.2014.03.008.
- [58] J. W. Daniels, E. Heymsfield, R. F. Saunders, y M. L. Kuss, «Development of automated electrical heat grid for pavement snowmelt», *Therm. Sci. Eng. Prog.*, vol. 10, pp. 169-178, may 2019, doi: 10.1016/j.tsep.2019.01.004.
- [59] K. Mensah y J. M. Choi, «Review of technologies for snow melting systems», *J. Mech. Sci. Technol.*, 2015, doi: 10.1007/s12206-015-1152-4.
- [60] ASHRAE, *ASHRAE Handbook - HVAC Applications*. 2011.

- [61] Y. Endoh, Y. Yoneda, y K. Mori, «FAR-infrared ray snow melting system». West Nippon Expressway Facilities Company Limited, 2000.
- [62] G. J. Song *et al.*, «Development of a pavement block piezoelectric energy harvester for self-powered walkway applications», *Appl. Energy*, 2019, doi: 10.1016/j.apenergy.2019.113916.
- [63] J. Y. Cho *et al.*, «A multifunctional road-compatible piezoelectric energy harvester for autonomous driver-assist LED indicators with a self-monitoring system», *Appl. Energy*, 2019, doi: 10.1016/j.apenergy.2019.03.075.
- [64] Q. Ren, K. L. Man, M. Li, B. Gao, y J. Ma, «Intelligent design and implementation of blockchain and Internet of things–based traffic system», *Int. J. Distrib. Sens. Networks*, 2019, doi: 10.1177/1550147719870653.
- [65] F. Bhatti, M. A. Shah, C. Maple, y S. Ul Islam, «A novel internet of things-enabled accident detection and reporting system for smart city environments», *Sensors (Switzerland)*, 2019, doi: 10.3390/s19092071.
- [66] O. Tahan, R. Rima, S. Bakri, Z. Merhi, y S. E. Deek, «GoSafe: A power-efficient android application for road events signaling and notification», 2016, doi: 10.1109/MELCON.2016.7495457.
- [67] O. Grembek, A. Kurzhanskiy, A. Medury, P. Varaiya, y M. Yu, «Making intersections safer with I2V communication», *Transp. Res. Part C Emerg. Technol.*, vol. 102, pp. 396-410, may 2019, doi: 10.1016/J.TRC.2019.02.017.
- [68] A. S. M. Bakibillah, M. A. S. Kamal, C. P. Tan, T. Hayakawa, y J.-I. Imura, «Event-Driven Stochastic Eco-Driving Strategy at Signalized Intersections from Self-Driving Data», *IEEE Trans. Veh. Technol.*, vol. 68, n.º 9, pp. 8557-8569, 2019, doi: 10.1109/TVT.2019.2931519.
- [69] A. Buzachis, A. Celesti, A. Galletta, M. Fazio, G. Fortino, y M. Villari, «A multi-agent autonomous intersection management (MA-AIM) system for smart cities leveraging edge-of-things and Blockchain», *Inf. Sci. (Ny)*, vol. 522, pp. 148-163, jun. 2020, doi: 10.1016/J.INS.2020.02.059.

- [70] M. M. A. Momen, H. A. Fayed, M. H. Aly, N. E. Ismail, y A. Mokhtar, «An efficient hybrid visible light communication/radio frequency system for vehicular applications», *Opt. Quantum Electron.*, vol. 51, n.º 11, 2019, doi: 10.1007/s11082-019-2082-7.
- [71] M. A. Vieira, M. Vieira, P. Louro, y P. Vieira, «Cooperative vehicular communication systems based on visible light communication», *Opt. Eng.*, vol. 57, n.º 7, 2018, doi: 10.1117/1.OE.57.7.076101.
- [72] Y. H. Kim y Y. H. O. Chung, «Experimental demonstration of highway I2V using visible light communications», *Appl. Opt.*, vol. 55, n.º 22, pp. 5840-5845, 2016, doi: 10.1364/AO.55.005840.
- [73] R. A. Gheorghiu, I. Bădescu, y R. S. Timnea, «Infrastructure to vehicle communications using inductive loops», *WSEAS Trans. Commun.*, vol. 13, pp. 596-605, 2014.
- [74] J. Rivas, R. Wunderlich, y S. J. Heinen, «Road Vibrations as a Source to Detect the Presence and Speed of Vehicles», *IEEE Sens. J.*, 2017, doi: 10.1109/JSEN.2016.2628858.
- [75] S. S. C. Congress, A. J. Puppala, y C. L. Lundberg, «Total system error analysis of UAV-CRP technology for monitoring transportation infrastructure assets», *Eng. Geol.*, 2018, doi: 10.1016/j.enggeo.2018.11.002.
- [76] L. Inzerillo, G. Di Mino, y R. Roberts, «Image-based 3D reconstruction using traditional and UAV datasets for analysis of road pavement distress», *Autom. Constr.*, 2018, doi: 10.1016/j.autcon.2018.10.010.
- [77] R. Roberts, G. Giancontieri, L. Inzerillo, y G. Di Mino, «Towards low-cost pavement condition health monitoring and analysis using deep learning», *Appl. Sci.*, 2020, doi: 10.3390/app10010319.
- [78] N. Karballaezadeh *et al.*, «Intelligent road inspection with advanced machine learning; Hybrid prediction models for smart mobility and transportation maintenance systems», *Energies*, 2020, doi: 10.3390/en13071718.
- [79] M. M. Naddaf-Sh, S. Hosseini, J. Zhang, N. A. Brake, y H. Zargarzadeh, «Real-Time Road Crack Mapping Using an Optimized Convolutional Neural Network», *Complexity*, 2019, doi: 10.1155/2019/2470735.

- [80] E. Romero-Chambi, S. Villarroel-Quezada, E. Atencio, y F. M. La Rivera, «Analysis of optimal flight parameters of unmanned aerial vehicles (UAVs) for detecting potholes in pavements», *Appl. Sci.*, 2020, doi: 10.3390/APP10124157.
- [81] M. Arbabpour Bidgoli, A. Golroo, H. Sheikhzadeh Nadjar, A. Ghelmani Rashidabad, y M. R. Ganji, «Road roughness measurement using a cost-effective sensor-based monitoring system», *Autom. Constr.*, 2019, doi: 10.1016/j.autcon.2019.04.007.
- [82] J.-R. Chang, «Asphalt pavement performance analysis using “big data” computing approaches», *J. Test. Eval.*, vol. 47, n.º 3, 2019, doi: 10.1520/JTE20170772.
- [83] H. C. Chung, G. Choi, y M. Azam, «Effects of Initial Starting Distance and Gap Characteristics on Children’s and Young Adults’ Velocity Regulation When Intercepting Moving Gaps», *Hum. Factors*, 2019, doi: 10.1177/0018720819867501.
- [84] T. Fuest, E. Schmidt, y K. Bengler, «Comparison of methods to evaluate the influence of an automated vehicle’s driving behavior on pedestrians: Wizard of Oz, virtual reality, and video», *Inf.*, 2020, doi: 10.3390/INFO11060291.
- [85] L. Thevin, C. Briant, y A. M. Brock, «X-Road: Virtual Reality Glasses for Orientation and Mobility Training of People with Visual Impairments», *ACM Trans. Access. Comput.*, 2020, doi: 10.1145/3377879.
- [86] I. T. Feldstein y G. N. Dyszak, «Road crossing decisions in real and virtual environments: A comparative study on simulator validity», *Accid. Anal. Prev.*, 2020, doi: 10.1016/j.aap.2019.105356.
- [87] R. Roberts, L. Inzerillo, y G. Di Mino, «Exploiting low-cost 3D imagery for the purposes of detecting and analyzing pavement distresses», *Infrastructures*, 2020, doi: 10.3390/infrastructures5010006.
- [88] R. Woodman, K. Lu, M. D. Higgins, S. Brewerton, P. A. Jennings, y S. Birrell, «Gap acceptance study of pedestrians crossing between platooning autonomous vehicles in a virtual environment», *Transp. Res. Part F Traffic Psychol. Behav.*, 2019, doi: 10.1016/j.trf.2019.09.017.
- [89] J. Santos, A. Ferreira, y G. Flintsch, «A multi-objective optimization-based pavement

- management decision-support system for enhancing pavement sustainability», *J. Clean. Prod.*, vol. 164, pp. 1380-1393, 2017, doi: 10.1016/j.jclepro.2017.07.027.
- [90] J. Jang, Y. Yang, A. W. Smyth, D. Cavalcanti, y R. Kumar, «Framework of Data Acquisition and Integration for the Detection of Pavement Distress via Multiple Vehicles», *J. Comput. Civ. Eng.*, vol. 31, n.º 2, 2017, doi: 10.1061/(ASCE)CP.1943-5487.0000618.
- [91] J. Santos, A. Ferreira, G. Flintsch, y V. Cerezo, «A multi-objective optimisation approach for sustainable pavement management», *Struct. Infrastruct. Eng.*, vol. 14, n.º 7, pp. 854-868, 2018, doi: 10.1080/15732479.2018.1436571.
- [92] S. K. Sharma, H. Phan, y J. Lee, «An application study on road surface monitoring using DTW based image processing and ultrasonic sensors», *Appl. Sci.*, 2020, doi: 10.3390/app10134490.
- [93] A. Mahmoudzadeh, A. Golroo, M. R. Jahanshahi, y S. F. Yeganeh, «Estimating pavement roughness by fusing color and depth data obtained from an inexpensive RGB-D sensor», *Sensors (Switzerland)*, 2019, doi: 10.3390/s19071655.
- [94] N. Bahrani, J. Blanc, P. Horny, y F. Menant, «Alternate method of pavement assessment using geophones and accelerometers for measuring the pavement response», *Infrastructures*, 2020, doi: 10.3390/infrastructures5030025.
- [95] H. Teng *et al.*, «A novel code data dissemination scheme for Internet of Things through mobile vehicle of smart cities», *Futur. Gener. Comput. Syst.*, vol. 94, pp. 351-367, may 2019, doi: 10.1016/J.FUTURE.2018.11.039.
- [96] H. Teng, W. Liu, T. Wang, A. Liu, X. Liu, y S. Zhang, «A Cost-Efficient Greedy Code Dissemination Scheme Through Vehicle to Sensing Devices (V2SD) Communication in Smart City», *IEEE Access*, vol. 7, pp. 16675-16694, 2019, doi: 10.1109/ACCESS.2019.2895899.
- [97] H. Teng, W. Liu, T. Wang, X. Kui, S. Zhang, y N. N. Xiong, «A Collaborative Code Dissemination Schemes through Two-Way Vehicle to Everything (V2X) Communications for Urban Computing», *IEEE Access*, vol. 7, pp. 145546-145566, 2019, doi: 10.1109/ACCESS.2019.2940639.

- [98] J. Wang, Y. Cai, Z. Liu, G. Ding, G. Cai, y H. Fu, «Preparation and performance study of a new type of Tile transducer for roadway applications», *J. Intell. Mater. Syst. Struct.*, 2020, doi: 10.1177/1045389X20942571.
- [99] K. Mantalovas y G. Di Mino, «The sustainability of reclaimed asphalt as a resource for road pavement management through a circular economic model», *Sustain.*, 2019, doi: 10.3390/su11082234.
- [100] J.-H. Choi, «Strategy for reducing carbon dioxide emissions from maintenance and rehabilitation of highway pavement», *J. Clean. Prod.*, vol. 209, pp. 88-100, 2019, doi: 10.1016/j.jclepro.2018.10.226.
- [101] Z. Leng, I. L. Al-Qadi, y R. Cao, «Life-cycle economic and environmental assessment of warm stone mastic asphalt», *Transp. A Transp. Sci.*, vol. 14, n.º 7, pp. 562-575, 2018, doi: 10.1080/23249935.2017.1390707.
- [102] A. Umer, K. Hewage, H. Haider, y R. Sadiq, «Sustainability evaluation framework for pavement technologies: An integrated life cycle economic and environmental trade-off analysis», *Transp. Res. Part D Transp. Environ.*, vol. 53, pp. 88-101, 2017, doi: 10.1016/j.trd.2017.04.011.
- [103] K. E. Haslett, E. V. Dave, y W. Mo, «Realistic traffic condition informed life cycle assessment: Interstate 495 maintenance and rehabilitation case study», *Sustain.*, vol. 11, n.º 12, 2019, doi: 10.3390/SU11123245.
- [104] K. Mantalovas y G. Di Mino, «Integrating circularity in the sustainability assessment of asphalt mixtures», *Sustain.*, 2020, doi: 10.3390/su12020594.
- [105] J. T. Harvey, A. Kendall, A. Butt, A. Saboori, M. Lozano, y M. Ostovar, «Supply curves using LCA and LCCA for conceptual evaluation of proposed policies to improve the environment», en *Lecture Notes in Civil Engineering*, 2020.
- [106] Y. Huang, R. Bird, y O. Heidrich, «Development of a life cycle assessment tool for construction and maintenance of asphalt pavements», *J. Clean. Prod.*, 2009, doi: 10.1016/j.jclepro.2008.06.005.
- [107] A. Jullien, M. Dauvergne, y V. Cerezo, «Environmental assessment of road construction

- and maintenance policies using LCA», *Transp. Res. Part D Transp. Environ.*, 2014, doi: 10.1016/j.trd.2014.03.006.
- [108] M. Batouli, M. Bienvenu, y A. Mostafavi, «Putting sustainability theory into roadway design practice: Implementation of LCA and LCCA analysis for pavement type selection in real world decision making», *Transp. Res. Part D Transp. Environ.*, vol. 52, pp. 289-302, 2017, doi: 10.1016/j.trd.2017.02.018.
- [109] J. Kulczycka y M. Smol, «Environmentally friendly pathways for the evaluation of investment projects using life cycle assessment (LCA) and life cycle cost analysis (LCCA)», *Clean Technol. Environ. Policy*, vol. 18, n.º 3, pp. 829-842, 2016, doi: 10.1007/s10098-015-1059-x.
- [110] R. Liu, B. W. Smartz, y B. Descheneaux, «LCCA and environmental LCA for highway pavement selection in Colorado», *Int. J. Sustain. Eng.*, vol. 8, n.º 2, pp. 102-110, 2015, doi: 10.1080/19397038.2014.958602.
- [111] R. Cao, Z. Leng, y S.-C. Hsu, «Comparative eco-efficiency analysis on asphalt pavement rehabilitation alternatives: Hot in-place recycling and milling-and-filling», *J. Clean. Prod.*, vol. 210, pp. 1385-1395, 2019, doi: 10.1016/j.jclepro.2018.11.122.
- [112] J. L. Concha y J. Norambuena-Contreras, «Thermophysical properties and heating performance of self-healing asphalt mixture with fibres and its application as a solar collector», *Appl. Therm. Eng.*, 2020, doi: 10.1016/j.applthermaleng.2020.115632.
- [113] E. Lizasoain-Arteaga, I. Indacochea-Vega, P. Pascual-Muñoz, y D. Castro-Fresno, «Environmental impact assessment of induction-healed asphalt mixtures», *J. Clean. Prod.*, vol. 208, pp. 1546-1556, 2019, doi: <https://doi.org/10.1016/j.jclepro.2018.10.223>.
- [114] I. Pérez, B. Gómez-Meijide, A. R. Pasandín, A. García, y G. Airey, «Enhancement of curing properties of cold in-place recycling asphalt mixtures by induction heating», *Int. J. Pavement Eng.*, 2019, doi: 10.1080/10298436.2019.1609674.
- [115] A. Garcia, S. Salih, y B. Gómez-Meijide, «Optimum moment to heal cracks in asphalt roads by means electromagnetic induction», *Constr. Build. Mater.*, vol. 238, p. 117627, 2020, doi: <https://doi.org/10.1016/j.conbuildmat.2019.117627>.

- [116] J. Kim, S. T. Lee, S. Yang, y J. Lee, «Implementation of thermal-energy-harvesting technology on pavement», *J. Test. Eval.*, 2017, doi: 10.1520/JTE20140396.
- [117] S. Gobee, V. Durairajah, V. Thiruchelvam, A. Imran, Larry, y Shassivan, «Smart pavement: Energy harvesting tile», *Int. J. Adv. Sci. Technol.*, vol. 29, n.º 1, pp. 1380-1389, 2020.
- [118] Y. Sun, S. Wu, Q. Liu, J. Hu, Y. Yuan, y Q. Ye, «Snow and ice melting properties of self-healing asphalt mixtures with induction heating and microwave heating», *Appl. Therm. Eng.*, vol. 129, pp. 871-883, 2018, doi: <https://doi.org/10.1016/j.applthermaleng.2017.10.050>.
- [119] J. Wan, S. Wu, Y. Xiao, Z. Chen, y D. Zhang, «Study on the effective composition of steel slag for asphalt mixture induction heating purpose», *Constr. Build. Mater.*, vol. 178, pp. 542-550, jul. 2018, doi: <https://doi.org/10.1016/j.conbuildmat.2018.05.170>.
- [120] F. Patti, K. Mansour, M. Pannirselvam, y F. Giustozzi, «Mining materials to generate magnetically-triggered induction healing of bitumen on smart road pavements», *Constr. Build. Mater.*, vol. 171, pp. 577-587, may 2018, doi: 10.1016/J.CONBUILDMAT.2018.03.160.
- [121] H. Ajam, B. Gómez-Meijide, I. Artamendi, y A. Garcia, «Mechanical and healing properties of asphalt mixes reinforced with different types of waste and commercial metal particles», *J. Clean. Prod.*, vol. 192, pp. 138-150, ago. 2018, doi: 10.1016/J.JCLEPRO.2018.04.262.
- [122] D. Grosseegger, B. Gomez-Meijide, S. Vansteenkiste, y A. Garcia, «Influence of rheological and physical bitumen properties on heat-induced self-healing of asphalt mastic beams», *Constr. Build. Mater.*, vol. 182, pp. 298-308, 2018, doi: <https://doi.org/10.1016/j.conbuildmat.2018.06.148>.
- [123] E. Jeoffroy, F. Bouville, M. Bueno, A. R. Studart, y M. N. Partl, «Iron-based particles for the magnetically-triggered crack healing of bituminous materials», *Constr. Build. Mater.*, vol. 164, pp. 775-782, mar. 2018, doi: 10.1016/J.CONBUILDMAT.2017.12.223.
- [124] P. P. Phulé, M. P. Mihalcin, y S. Genc, «Role of the dispersed-phase remnant magnetization on the redispersibility of magnetorheological fluids», *J. Mater. Res.*, 1999, doi: 10.1557/JMR.1999.0407.

- [125] M. Zubieta, S. Eceolaza, M. J. Elejabarrieta, y M. M. Bou-Ali, «Magnetorheological fluids: Characterization and modeling of magnetization», *Smart Mater. Struct.*, 2009, doi: 10.1088/0964-1726/18/9/095019.
- [126] G. R. Iglesias, S. Ahualli, J. Echávarri Otero, L. Fernández Ruiz-Morón, y J. D. G. Durán, «Theoretical and experimental evaluation of the flow behavior of a magnetorheological damper using an extremely bimodal magnetic fluid», *Smart Mater. Struct.*, 2014, doi: 10.1088/0964-1726/23/8/085028.
- [127] M. R. Jolly, J. W. Bender, y J. D. Carlson, «Properties and Applications of Commercial Magnetorheological Fluids», *J. Intell. Mater. Syst. Struct.*, 1999, doi: 10.1177/1045389x9901000102.
- [128] D. Baranwal y T. S. Deshmukh, «MR-Fluid Technology and Its Application - A Review», *Int. J. Emerg. Technol. Adv. Eng.*, 2012.
- [129] G. R. Iglesias, M. T. López-López, J. D. G. Durán, F. González-Caballero, y A. V. Delgado, «Dynamic characterization of extremely bidisperse magnetorheological fluids», *J. Colloid Interface Sci.*, 2012, doi: 10.1016/j.jcis.2012.03.077.
- [130] V. Chacón, «Designing a suspension for a motor vehicle based on Magnetorheological dampers», 2009.
- [131] R. Fayling, «Vehicle guidance track of transverse extent», *US Pat. 3,714,625*, 1973.
- [132] R. E. Fayling, «Magnetized means for providing control information to moving vehicles», *US Pat. 3,609,678*, 1971.
- [133] Y. Sun *et al.*, «Self-healing performance of asphalt mixtures through heating fibers or aggregate», *Constr. Build. Mater.*, vol. 150, pp. 673-680, sep. 2017, doi: 10.1016/J.CONBUILDMAT.2017.06.007.
- [134] D. Y. Yoo, S. Kim, M. J. Kim, D. Kim, y H. O. Shin, «Self-healing capability of asphalt concrete with carbon-based materials», *J. Mater. Res. Technol.*, vol. 8, n.º 1, pp. 827-839, ene. 2019, doi: 10.1016/j.jmrt.2018.07.001.
- [135] K. Zhang, X. Gao, Q. Zhang, T. Li, H. Chen, y X. Chen, «Preparation and microwave

- absorption properties of asphalt carbon coated reduced graphene oxide/magnetic CoFe₂O₄ hollow particles modified multi-wall carbon nanotube composites», *J. Alloys Compd.*, vol. 723, pp. 912-921, nov. 2017, doi: 10.1016/J.JALLCOM.2017.06.327.
- [136] K. Liu *et al.*, «Induction heating performance of asphalt pavements incorporating electrically conductive and magnetically absorbing layers», *Constr. Build. Mater.*, vol. 229, p. 116805, 2019, doi: <https://doi.org/10.1016/j.conbuildmat.2019.116805>.
- [137] Á. García, E. Schlangen, M. van de Ven, y Q. Liu, «Electrical conductivity of asphalt mortar containing conductive fibers and fillers», *Constr. Build. Mater.*, vol. 23, n.º 10, pp. 3175-3181, oct. 2009, doi: 10.1016/J.CONBUILDMAT.2009.06.014.
- [138] Y. Rew, X. Shi, K. Choi, y P. Park, «Structural Design and Lifecycle Assessment of Heated Pavement Using Conductive Asphalt», *J. Infrastruct. Syst.*, 2018, doi: 10.1061/(asce)is.1943-555x.0000440.
- [139] P. Pan, S. Wu, M. Chen, y N. Tang, «A Method for Improvement of the Heating Efficiency of Conductive Asphalt Pavement», *J. Test. Eval.*, 2014, doi: 10.1520/jte20130173.
- [140] P. Pan, S. Wu, F. Xiao, L. Pang, y Y. Xiao, «Conductive asphalt concrete: A review on structure design, performance, and practical applications», *J. Intell. Mater. Syst. Struct.*, 2015, doi: 10.1177/1045389X14530594.
- [141] A. Arabzadeh, H. Ceylan, S. Kim, A. Sassani, K. Gopalakrishnan, y M. Mina, «Electrically-conductive asphalt mastic: Temperature dependence and heating efficiency», *Mater. Des.*, vol. 157, pp. 303-313, nov. 2018, doi: 10.1016/j.matdes.2018.07.059.
- [142] P. Lastra-González, I. Indacochea-Vega, M. A. Calzada-Pérez, Á. Vega-Zamanillo, y D. Castro-Fresno, «Assessment of induction heating in the performance of porous asphalt mixtures», *Road Mater. Pavement Des.*, 2019, doi: 10.1080/14680629.2019.1606729.
- [143] A. H. Vanelstraete and Bondt, «Crack Prevention and Use of Overlay Systems», en *RILEM Conference in Prevention of Reflective Cracking in Pavements*, E. by A. V. and L. Francken, Ed. Brussels, 1997, pp. 42-60.
- [144] P. Leiva-Padilla, F. Moreno-Navarro, G. R. Iglesias, y M. C. Rubio-Gámez, «Recovery capacity of electroconductive bituminous mortars under the influence of magnetic fields»,

- Mater. Des.*, p. under review, 2020.
- [145] P. Leiva-Padilla, F. Moreno-Navarro, G. Iglesias, M. C. Rubio-Gómez, y M. C. Rubio-Gamez, «Interpretation of the Magnetic Field Signals Emitted by Encoded Asphalt Pavement Materials», *Sustainability*, vol. 12, n.º 7300, 2020, doi: 10.3390/SU12187300.
- [146] P. Leiva-Padilla, F. Moreno-Navarro, G. R. Iglesias, y M. C. Rubio-Gómez, «Analysis of the mechanical response of asphalt materials manufactured with metallic fibres under the effect of magnetic fields», *Smart Mater. Struct.*, 2019.
- [147] P. Leiva-Padilla, F. Moreno-Navarro, G. Iglesias, y M. C. Rubio-Gómez, «Thermal characterization of electroconductive layers for anti-icing and de-snowing applications on roads (pendiente de publicación)», *Road Mater. Pavement Des.*, 2020.
- [148] H. Abdualla *et al.*, «Design and Construction of the World's First Full-Scale Electrically Conductive Concrete Heated Airport Pavement System at a U.S. Airport», *Transp. Res. Rec.*, 2018, doi: 10.1177/0361198118791624.
- [149] J. Tang, Q. Liu, S. Wu, Q. Ye, Y. Sun, y E. Schlangen, «Investigation of the optimal self-healing temperatures and healing time of asphalt binders», *Constr. Build. Mater.*, vol. 113, pp. 1029-1033, jun. 2016, doi: 10.1016/J.CONBUILDMAT.2016.03.145.
- [150] Á. García, «Self-healing of open cracks in asphalt mastic», *Fuel*, vol. 93, pp. 264-272, mar. 2012, doi: 10.1016/J.FUEL.2011.09.009.
- [151] R. N. Traxler, *Asphalt: Its composition, properties, and uses*. 1961.
- [152] Y. Hou, L. Wang, T. Pauli, y W. Sun, «Investigation of the asphalt self-healing mechanism using a phase-field model», *J. Mater. Civ. Eng.*, 2015, doi: 10.1061/(ASCE)MT.1943-5533.0001047.
- [153] P. Leiva-Padilla, F. Moreno-Navarro, G. Iglesias-Salto, y M. C. Rubio-Gamez, «Recovery capacity of electroconductive asphalt mortars under the influence of magnetic fields», *Mater. Today Commun.*, vol. 25, p. 101527, 2020, doi: <https://doi.org/10.1016/j.mtcomm.2020.101527>.

ANEXOS

Anexo 1. "A review of the contribution of mechanomutable asphalt materials towards addressing the upcoming challenges of asphalt pavements".

Este anexo contiene la **versión del manuscrito preparado por la autora** y que fue publicado en el Journal: "*Infrastructures*". El acceso al documento publicado, debe realizarse a través del DOI de la publicación: <https://doi.org/10.3390/infrastructures5030023>

Debido a que este es un documento de revisión, **se considera un aporte adicional a los artículos del compendio**, que pretende describir de una manera sencilla, los temas asociados a cada uno de los objetivos de esta tesis doctoral.

Leiva-Padilla, P.; Moreno-Navarro, F.; Iglesias, G.; Rubio-Gamez, M.C. A Review of the Contribution of Mechanomutable Asphalt Materials Towards Addressing the Upcoming Challenges of Asphalt Pavements. *Infrastructures* 2020, 5, 23.

DOI: <https://doi.org/10.3390/infrastructures5030023>

Review

A review of the contribution of mechanomutable asphalt materials towards addressing the upcoming challenges of asphalt pavements

Paulina Leiva-Padilla ^{1,*}, Fernando Moreno-Navarro ², Guillermo Iglesias ³ and M^a Carmen Rubio-Gamez ⁴

¹ Laboratory of Construction Engineering of the University of Granada (LabIC.UGR), Granada, Spain; pleiva@ugr.es

² Laboratory of Construction Engineering of the University of Granada (LabIC.UGR), Granada, Spain; fmoreno@ugr.es

³ Department of Applied Physics of the University of Granada, Spain; iglesias@ugr.es

⁴ Laboratory of Construction Engineering of the University of Granada (LabIC.UGR), Granada, Spain; mcrubio@ugr.es

* Correspondence: pleiva@ugr.es

Received: date; Accepted: date; Published: date

Abstract: In the coming years, asphalt materials will face significant challenges due to the demand for smart multifunctional materials in transportation infrastructures, designed under sustainability criteria. Asphalt pavements will not only have to contribute towards the provision of an adequate surface for the transportation of different types of vehicles but will need to do so considering the increased loads that they will have to support, as well as the extreme weather conditions resulting from climate change. These pavements will also need the capacity to interact with autonomous vehicles and provide information to the users and maintenance agencies regarding traffic data or performance levels. This paper describes how mechanomutable asphalt materials (MAMs) could enhance the properties of asphalt materials, enabling their use as a solution for smart infrastructures.

Keywords: mechanomutable asphalt materials, MAMs, smart materials, smart roads, magnetic fields

1. Introduction

Over the years, engineers have worked on developing solutions to meet the needs of society, including housing, basic services and communications. In the area of transport infrastructure, there is an identifiable process of development, which began with the roman roads and continually evolved to produce the improved paved roads that allow for the driving of motorized vehicles. These roads were later transformed into the high-capacity roads (the roads that we know today) that have recently begun to incorporate more sustainable and smarter materials and practices of building and design.

Therefore, roads are beginning to be regarded as more than simply a means of transporting goods and services between cities; they are required to provide extra value for the investments made to build them

Leiva-Padilla, P.; Moreno-Navarro, F.; Iglesias, G.; Rubio-Gamez, M.C. A Review of the Contribution of Mechanomutable Asphalt Materials Towards Addressing the Upcoming Challenges of Asphalt Pavements. *Infrastructures* 2020, 5, 23.

DOI: <https://doi.org/10.3390/infrastructures5030023>

and the spaces that they use. In particular, new trends have emerged in the design and production of advanced materials with the capacity to overcome the challenges associated with recent technological advances, as well as the effects of extreme weather resulting from climate change. One example is the implementation of methodologies for evaluating the environmental impact of traditional processes of production and construction, and for the definition of strategies to make these processes cleaner and more sustainable (e.g., low temperature manufacturing technologies, the use of waste as a substitute for natural resources, and LCA studies). A further example is the design of new materials capable of dealing with extreme temperature changes and the associated problems, including the permanent deformations produced at high temperatures, the aging generated by high exposure to UV rays and chemical pollutants, fatigue cracking produced by freeze-thaw cycles, and thermal cracking caused by the retraction of the material at low temperatures.

In general terms, this new generation of roads could be built using resilient and smart materials that have the capacity to extend the life of the pavement, improve sustainability, reduce maintenance costs and improve road safety in addition to avoiding the traffic disruptions that lead to significant economic losses and therefore the slower development of countries. Additionally, these roads could contribute towards meeting the requirements established by recent technological advances in the autonomous vehicle industry.

Therefore, some of the main characteristics of the materials developed to be included in this new generation of roads include the capacity to: self-heal the cracks developed as a result of traffic-induced fatigue, to show more visible colors at night in order to enhance road safety, to register the level of pressure and strain experienced by the effect of vehicle loads, to capture energy from the environment (wind, solar, hydraulic) in order to feed other components of the traffic system, to communicate with autonomous vehicles to assist in their guidance, as well as send traffic signals to generate an integral system of communications.

Included among this new generation of materials are mechanomutable asphalt materials (MAMs), which are composed of a bituminous matrix with magnetically susceptible materials activated by the effect of external magnetic fields, if needed. MAMs can be used in three main potential applications [1]-[6]: (1) the mechanical control of the modulus of the bituminous matrix, to improve the performance of specific areas of the road; (2) the generation of thermal changes in order to propose alternative solutions for road maintenance and (3) the construction of encoded roads to assist self-guided vehicle systems.

The present paper presents a general description of MAMs, the mechanisms associated with their functioning and use, as well as the specific areas in which they could be most conveniently placed, in order to consider their use as a potential solution for the construction of smart pavements.

2. Mechanomutable Asphalt Materials

Mechanomutable asphalt materials can be defined as a bituminous matrix modified with ferromagnetic materials, which can modify mechanical performance by the effect of magnetic fields produced in permanent magnets [2]-[5],[7]. As shown in Figure 1, this concept can be extended to thermomutable materials due to the thermal changes produced by the effect of magnetic fields generated in induction coils, which can also allow for the construction of encoded roads for Smart Cities (communication with self-driving vehicles, cars, scooters, bikes people with limited mobility, traffic signals, and for collecting traffic count data, among other uses) [6].

Leiva-Padilla, P.; Moreno-Navarro, F.; Iglesias, G.; Rubio-Gamez, M.C. A Review of the Contribution of Mechanomutable Asphalt Materials Towards Addressing the Upcoming Challenges of Asphalt Pavements. *Infrastructures* 2020, 5, 23.

DOI: <https://doi.org/10.3390/infrastructures5030023>

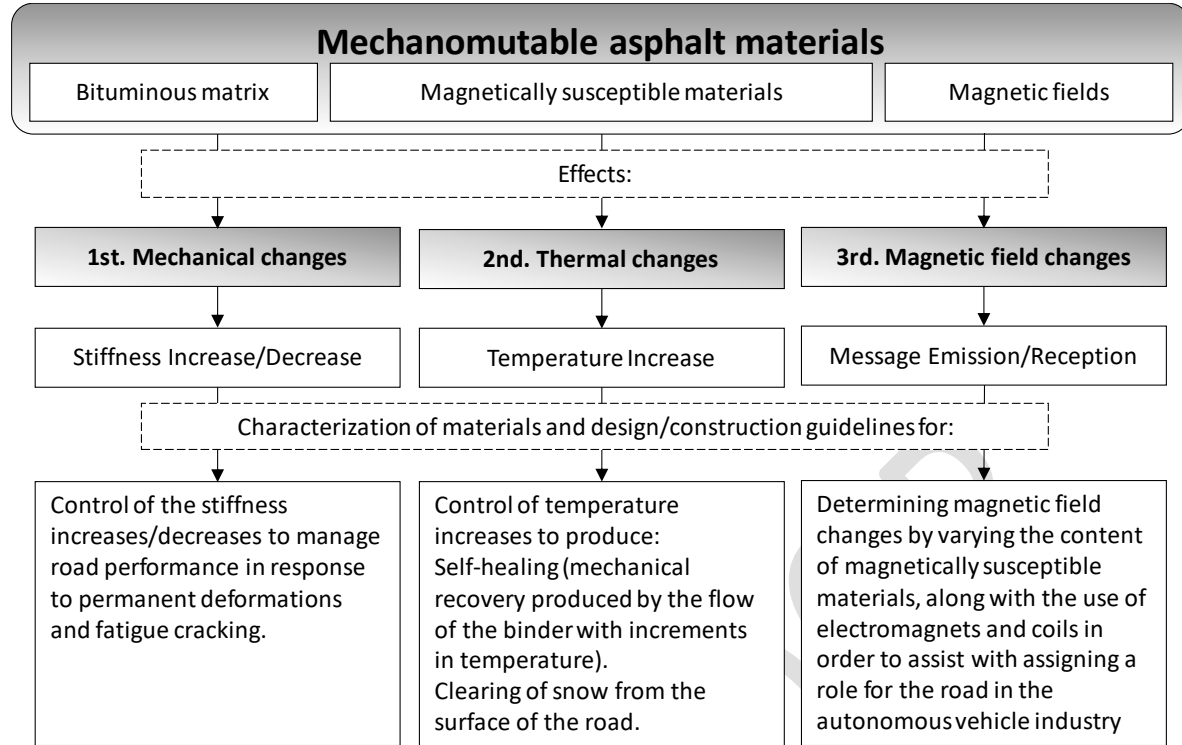


Figure 1. Mechanomutable asphalt materials

Table 1 displays the materials with ferromagnetic properties that have been used until now in the construction of asphalt materials. These can be summarized as: steel slag, steel grit, ferrite fillers, fibers (carbon, steel, steel wood and carbon nanofibers), magnetite (tailings and powered), carbonyl iron powder, graphene, graphite, carbon nanotubes and carbon black. Depending on the type of material, these can serve as total or partial substitutes for the fine/coarse aggregate. The main parameters evaluated in previous studies are associated with the typical distresses developed in the material during practice but without the application of magnetic fields (Table 1). These are: cracking (dynamic and quasi-static tests to represent fatigue and fracture), permanent deformation (Marshall stability and rutting) and moisture damage (stiffness loss).

More recent studies (Table 1) have also evaluated the changes produced by magnetic fields in terms of dynamic modulus values, phase angle, and the healing capacity of these materials (understood as the mechanical recovery of the material following the application of heat and resting periods), as well as susceptibility to detection by magnetic field sensors, a characteristic that makes these materials a viable option for encoding the roads needed for the autonomous vehicle industry.

Leiva-Padilla, P.; Moreno-Navarro, F.; Iglesias, G.; Rubio-Gamez, M.C. A Review of the Contribution of Mechanomutable Asphalt Materials Towards Addressing the Upcoming Challenges of Asphalt Pavements. *Infrastructures* 2020, 5, 23.

DOI: <https://doi.org/10.3390/infrastructures5030023>

Table 1. Ferromagnetic materials used in the construction of asphalt materials

| Material | Parameters studied | Reference |
|---|---|--|
| Steel slag (coarse aggregate and powdered), steel grit. Ferrite fillers. | Permanent deformation, fracture energy, moisture damage, Marshall stability. Permanent deformation, healing, moisture damage, Marshall stability | [8]-[12]. [13]-[16]. |
| Fibers (carbon, steel, steel wood and carbon nanofibers) Magnetite (tailings and powdered) Carbonyl iron powder | Fracture energy, moisture damage, Marshall stability. Moisture damage, Marshall stability. Permanent deformation, fatigue cracking, complex modulus, and phase angle. | [6],[16]-[23]. [24]-[26] [3],[4] |
| Carbon (carbon fiber, flake graphite and exfoliated graphite, graphene, carbon black, and carbon nanotubes) | Electrical resistivity, healing, rheology, electrical conductivity, temperature changes. | [18],[27]-[34] |

2.1. Mechanomutable Asphalt Materials as Improved Materials for Constructing Pavements

Mechanomutable asphalt materials were born from the principle of functioning of the magneto-rheological (MR) fluids, applied to asphalt binders [3], [4]. As shown in Figure 2, the characteristics of magneto-rheological fluids provide a medium (in this case a bituminous matrix) in which to magnetically suspend active particles during the absence of magnetic fields. However, when magnetic fields are present, these materials have the capacity to behave as a quasi-solid material, increasing the apparent viscosity of the material [35], [36], modifying its rheological behavior from Newtonian to viscoelastic [37] and impeding the movement of the magnetically active particles, which produce an internal stress tensor in the mixture [4].

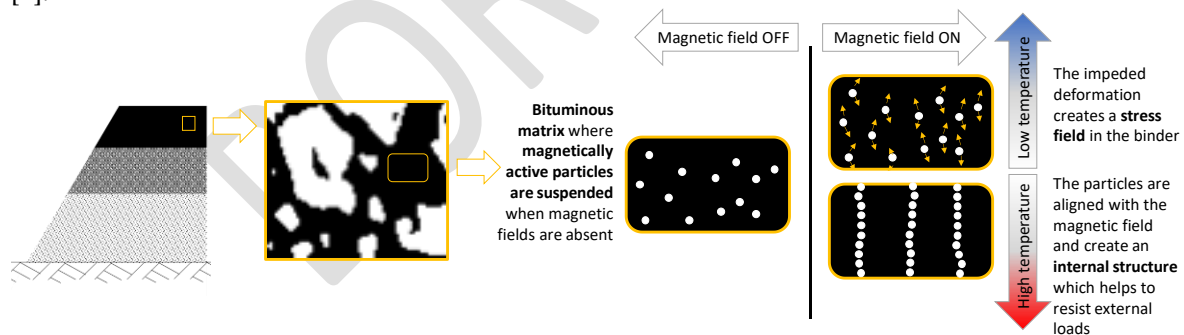


Figure 2. Mechanomutable asphalt materials in the presence of magnetic fields

Research studies that have specifically focused on mechanomutable asphalt materials have confirmed that at the binder scale, higher intensities of magnetic field and higher quantities of magnetically active particles can increase the modulus and decrease the phase angle of the mechanomutable binder [4]. Related studies that have simulated the dynamic demands of traffic (creep and recovery tests) have revealed that

Leiva-Padilla, P.; Moreno-Navarro, F.; Iglesias, G.; Rubio-Gamez, M.C. A Review of the Contribution of Mechanomutable Asphalt Materials Towards Addressing the Upcoming Challenges of Asphalt Pavements. *Infrastructures* 2020, 5, 23.

DOI: <https://doi.org/10.3390/infrastructures5030023>

the cumulative deformations in these materials are due to a decrease in their propensity to deform rather than an increase in their recovery capacity (which is more strongly influenced by the penetration grade of the bitumen) [3]. In order to scale those findings to practice, later studies at mortar scale confirmed the increase in modulus values, depending on the increase in intensity of the magnetic field and the quantity of magnetically susceptible materials [5].

Finally, studies regarding the piezoresistivity of electrically conductive asphalt base composites reveal that there is a correlation between this parameter and the stress-strain responses of the pavement, which could be useful for weighing, traffic monitoring, border monitoring, and structural vibration control [38], [39]. Therefore, the aforementioned capacities of these materials point to their potential use in the construction of airport runways, high loading areas of airports, ports and parking lots; bus stops, and exclusive lanes for heavy traffic.

2.2. Mechanomutable Asphalt Materials for Improving Road Safety and Service Conditions

Mechanomutable asphalt materials are electroconductive; thus, they have the capacity to produce and conduct the parasite currents (Foucault currents) generated from the effect of magnetic fields (Figure 3). These parasite currents are the source of the energy losses transformed into heat through the Joule effect. Thus, mechanomutable asphalt materials can also be regarded as thermomutable materials.

Recent studies [18], [30] have taken advantage of the thermal capacity of these materials to study their potential use in the implementation of alternative systems for clearing ice or snow from the surface of the road (Figure 3). In fact, other similar installations have been shown to operate successfully, such as the electrically heated pavement [18], including Snowfree® [40] (pavement system in Chicago O'Hare International Airport), along with bridges in West Virginia [41] (US 35 over 5 and 20 Creek), South New Jersey [42] (Route 130) and Nebraska [43] (Slat Creek at Roca).

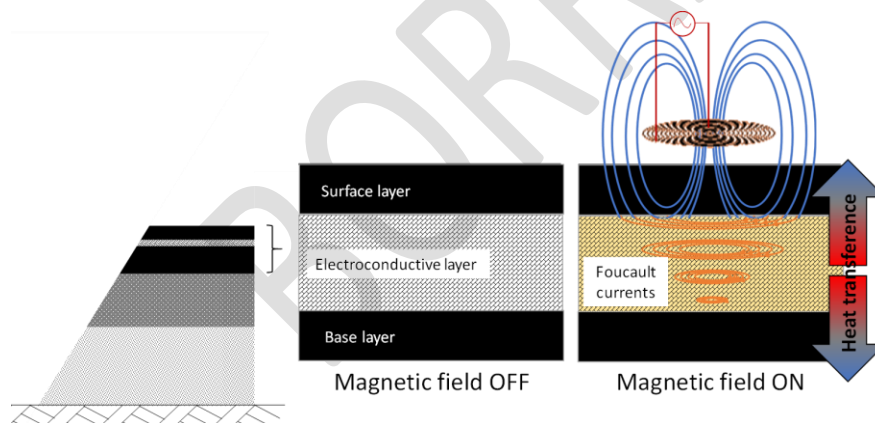


Figure 3. Schema of the thermomutable asphalt materials under magnetic fields for use in de-icing and producing anti-snow roads

Similar studies concerned with the thermal changes generated in electroconductive materials due to the effect of magnetic fields produced by induction [19], [44] and microwaves [19] were conducted to evaluate the healing capacity of these materials (Figure 4) in terms of the mechanical recovery of the

Leiva-Padilla, P.; Moreno-Navarro, F.; Iglesias, G.; Rubio-Gamez, M.C. A Review of the Contribution of Mechanomutable Asphalt Materials Towards Addressing the Upcoming Challenges of Asphalt Pavements. *Infrastructures* 2020, 5, 23.

DOI: <https://doi.org/10.3390/infrastructures5030023>

material by the flow of the binder at temperatures between 30°C and 70°C, and the consequent sealing of the existing cracks [22].

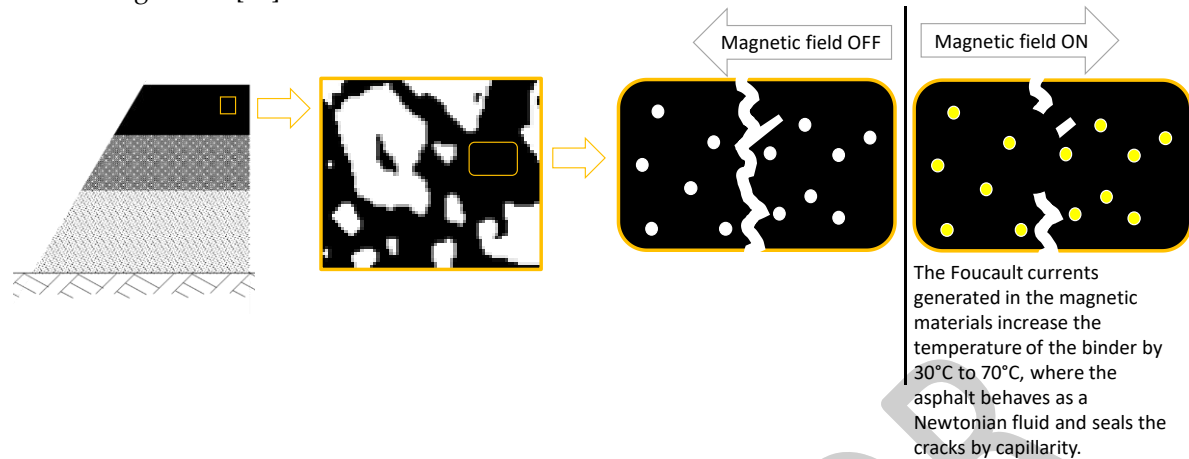


Figure 4. Schema of the healing capacity of thermomutable asphalt binders

Given that weather conditions can increase the number of traffic accidents, with snowfall being a particularly high risk factor in road accidents [45], the thermomutable capacity of these materials can be used in the implementation of environmental-friendly and smart alternatives to the traditional “de-icing salts”, which, despite having been shown to be economically accessible and effective, affect the roadside soil, the underground, the surface water, and the vegetation [46], [47], as well as the vehicles and the infrastructure of the road [48].

2.3. Mechanomutable Asphalt Materials for the Guidance of Autonomous Vehicles

According to the levels established by the US National Highways Traffic Safety Administration (NHTSA), there are 5 levels, ranging from 0 (no automation) to 4 (full self-driving automation) for classifying the autonomy of vehicles [49]. Due to the fact that the majority of the new conventional vehicles have one or more specific control functions that are automated, it can be assumed that Level 1 and Level 2 are now being implemented in real life. Ongoing research by the major vehicle manufacturers is being carried out with the aim of reaching Level 3, where the drivers can concede full control of the safety-critical functions of the vehicle under certain traffic or environmental conditions. Finally, some researchers [6], [50], [51] consider that to fully achieve Level 3 and Level 4, that is, full self-driving automation, it will be essential to incorporate the necessary infrastructure.

If the benefits of assigning a multifunctional character to the road are also considered, the use of mechanomutable asphalt materials can be extended to encoding the road [6] (Figure 5). Encoding the road entails assigning it with a type of language that is easily read by magnetic field sensors, with the aim of processing this signal so that it can be converted into specific functions for the vehicles. Therefore, studies [6] in this field have addressed this issue by evaluating the performance of MAMs to allow for encoded roads, with the aim of establishing design methodologies and guidelines for their real-life implementation.

Figure 5 shows potential areas of application, such as tunnels (where the GPS signal can be weak) and intersections (where the interaction can also involve traffic signals, pedestrians, and personal mobility vehicles).

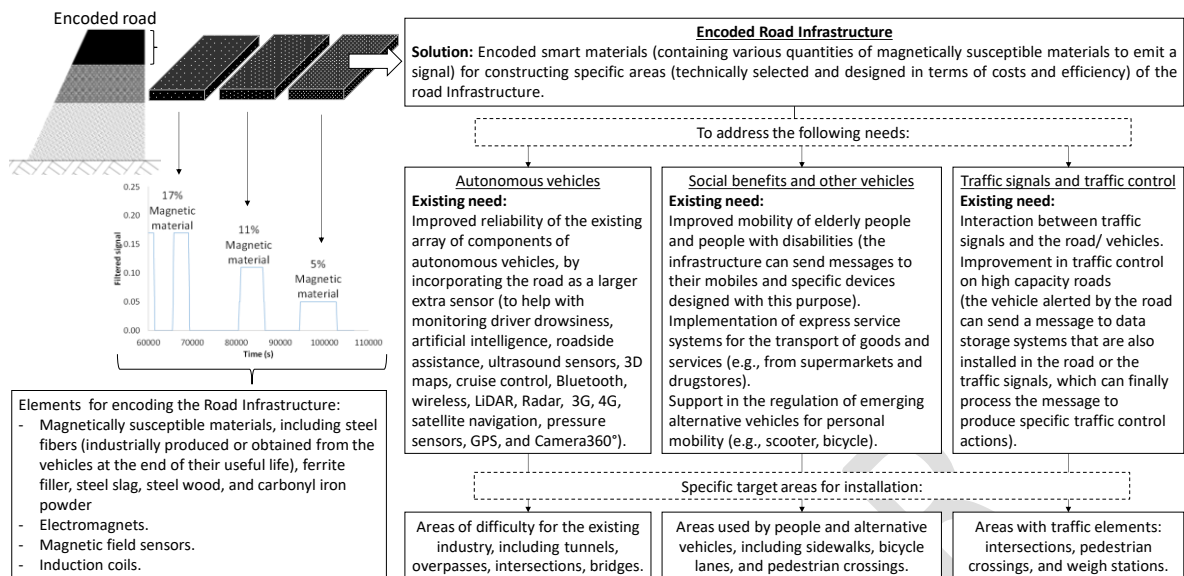


Figure 5. Schema of the applications of the encoded roads

3. Conclusions

The aim of this paper was to describe how mechanomutable asphalt materials (obtained by modifying conventional asphalt materials with magnetically susceptible particles) could contribute towards meeting the challenges faced by asphalt roads. The main conclusions can be summarised as follows:

- The first potential application in which MAMs aim to improve the mechanical performance of asphalt pavements showed that the magnetically susceptible materials tend to be aligned to the forces of activated magnetic fields. This movement improves the mechanical properties of these materials, which depends on the temperature, the amount of magnetically susceptible materials, and the intensity of the magnetic field. The mechanisms of action involved in the process are associated with: (1) the development of an internal structure in the material at high temperatures and (2) the generation of a stress field inside the bituminous matrix at low temperatures.

- In the case of the second application, the concept of MAMs can be extended to their use as thermomutable materials. The electrical properties of the magnetically susceptible materials used in their manufacture allows for the production of parasite currents which produce energy losses and increments in the temperature of the material and the surrounding layers. This thermal capacity could be taken into account when proposing new strategies for improving the safety and service conditions of the road.

- With regard to the third application, the development of a better means of transportation means that the road infrastructure should be prepared to respond to the associated advances in technology, and mechanomutable asphalt materials provide a tool for developing roads that can be used for the guidance of autonomous vehicles.

- Finally, it should be noted that further research is required with regard to the development of these materials. In particular, there is a need is to replicate the results obtained in laboratory in a real-scale study. More results are needed to provide inputs for validating numerical models, which can be useful in the parametrization – and therefore extrapolation – of the uses of MAMs in practice. This will allow for

Leiva-Padilla, P.; Moreno-Navarro, F.; Iglesias, G.; Rubio-Gamez, M.C. A Review of the Contribution of Mechanomutable Asphalt Materials Towards Addressing the Upcoming Challenges of Asphalt Pavements. *Infrastructures* 2020, 5, 23.

DOI: <https://doi.org/10.3390/infrastructures5030023>

validating and adjusting the tested designs, a step that is necessary for the future implementation of MAMs as smart materials that can be used in the construction of smart pavements.

Acknowledgments

The research presented in this paper was carried out as part of the H2020-MSCA-ETN-2016. This project has received funding from the European Union's H2020 Program for research, technological development, and demonstration under grant agreement number 721493.

References

- [1] F. Moreno-Navarro and M. C. Rubio-Gómez, "Development of new smart materials for the pavements of the future," *Carreteras*, 2018.
- [2] F. Moreno-Navarro, G. R. Iglesias, and M. C. Rubio-Gómez, "Experimental evaluation of using stainless steel slag to produce mechanomutable asphalt mortars for their use in smart materials," *Smart Mater. Struct.*, 2016.
- [3] F. Moreno-Navarro, G. R. Iglesias, and M. C. Rubio-Gómez, "Mechanical performance of mechanomutable asphalt binders under cyclic creep and recovery loads," *Constr. Build. Mater.*, vol. 113, pp. 506–512, Jun. 2016.
- [4] F. Moreno-Navarro, G. R. Iglesias, and M. C. Rubio-Gómez, "Development of mechanomutable asphalt binders for the construction of smart pavements," *Mater. Des.*, vol. 84, pp. 100–109, Nov. 2015.
- [5] P. Leiva-Padilla, F. Moreno-Navarro, G. R. Iglesias, and M. C. Rubio-Gómez, "Analysis of the mechanical response of asphalt materials manufactured with metallic fibres under the effect of magnetic fields," *Smart Mater. Struct.*, 2019.
- [6] F. Moreno-Navarro, G. R. Iglesias, and M. C. Rubio-Gómez, "Encoded asphalt materials for the guidance of autonomous vehicles," *Autom. Constr.*, vol. 99, pp. 109–113, Mar. 2019.
- [7] F. Moreno-Navarro, G. R. Iglesias, and M. C. Rubio-Gómez, "Ligante modificado con propiedades mecánicas controlables por campos magnéticos," *PCT/ES2014/071002*, 2016.
- [8] M. Skaf, J. M. Manso, Á. Aragón, J. A. Fuente-Alonso, and V. Ortega-López, "EAF slag in asphalt mixes: A brief review of its possible re-use," *Resour. Conserv. Recycl.*, vol. 120, pp. 176–185, May 2017.
- [9] Z. Chen, S. Wu, J. Wen, M. Zhao, M. Yi, and J. Wan, "Utilization of gneiss coarse aggregate and steel slag fine aggregate in asphalt mixture," *Constr. Build. Mater.*, vol. 93, pp. 911–918, Sep. 2015.
- [10] J. Wan, S. Wu, Y. Xiao, Z. Chen, and D. Zhang, "Study on the effective composition of steel slag for asphalt mixture induction heating purpose," *Constr. Build. Mater.*, vol. 178, pp. 542–550, Jul. 2018.
- [11] B. Gómez-Mejjide, H. Ajam, A. Garcia, and S. Vansteenkiste, "Effect of bitumen properties in the induction healing capacity of asphalt mixes," *Constr. Build. Mater.*, vol. 190, pp. 131–139, Nov. 2018.
- [12] B. Gómez-Mejjide, H. Ajam, P. Lastra-González, and A. Garcia, "Effect of air voids content on asphalt self-healing via induction and infrared heating," *Constr. Build. Mater.*, vol. 126, pp. 957–966, Nov. 2016.

Leiva-Padilla, P.; Moreno-Navarro, F.; Iglesias, G.; Rubio-Gamez, M.C. A Review of the Contribution of Mechanomutable Asphalt Materials Towards Addressing the Upcoming Challenges of Asphalt Pavements. *Infrastructures* 2020, 5, 23.

DOI: <https://doi.org/10.3390/infrastructures5030023>

- [13] H. Zhao, S. Zhong, X. Zhu, and H. Chen, "High-efficiency heating characteristics of ferrite-filled asphalt-based composites under microwave irradiation," *J. Mater. Civ. Eng.*, 2017.
- [14] N. Nabiun and M. M. Khabiri, "Mechanical and moisture susceptibility properties of HMA containing ferrite for their use in magnetic asphalt," *Constr. Build. Mater.*, vol. 113, pp. 691–697, Jun. 2016.
- [15] X. Zhu, Y. Cai, S. Zhong, J. Zhu, and H. Zhao, "Self-healing efficiency of ferrite-filled asphalt mixture after microwave irradiation," *Constr. Build. Mater.*, vol. 141, pp. 12–22, Jun. 2017.
- [16] Á. García, E. Schlangen, M. Van De Ven, and D. Van Vliet, "Induction heating of mastic containing conductive fibers and fillers," *Mater. Struct. Constr.*, 2011.
- [17] Y. Pamulapati, M. A. Elseifi, S. B. Cooper, L. N. Mohammad, and O. Elbagalati, "Evaluation of self-healing of asphalt concrete through induction heating and metallic fibers," *Constr. Build. Mater.*, vol. 146, pp. 66–75, Aug. 2017.
- [18] P. Pan, S. Wu, F. Xiao, L. Pang, and Y. Xiao, "Conductive asphalt concrete: A review on structure design, performance, and practical applications," *J. Intell. Mater. Syst. Struct.*, 2015.
- [19] J. Norambuena-Contreras and A. Garcia, "Self-healing of asphalt mixture by microwave and induction heating," *Mater. Des.*, vol. 106, pp. 404–414, Sep. 2016.
- [20] Q. Dai, Z. Wang, and M. R. Mohd Hasan, "Investigation of induction heating effects on electrically conductive asphalt mastic and asphalt concrete beams through fracture-healing tests," *Constr. Build. Mater.*, vol. 49, pp. 729–737, Dec. 2013.
- [21] A. García, J. Norambuena-Contreras, and M. N. Partl, "Experimental evaluation of dense asphalt concrete properties for induction heating purposes," *Constr. Build. Mater.*, vol. 46, pp. 48–54, Sep. 2013.
- [22] Á. García, E. Schlangen, M. van de Ven, and Q. Liu, "A simple model to define induction heating in asphalt mastic," *Constr. Build. Mater.*, vol. 31, pp. 38–46, Jun. 2012.
- [23] Q. Liu, Á. García, E. Schlangen, and M. van de Ven, "Induction healing of asphalt mastic and porous asphalt concrete," *Constr. Build. Mater.*, vol. 25, no. 9, pp. 3746–3752, Sep. 2011.
- [24] Z. Wang, C. Xu, S. Wang, J. Gao, and T. Ai, "Utilization of magnetite tailings as aggregates in asphalt mixtures," *Constr. Build. Mater.*, vol. 114, pp. 392–399, Jul. 2016.
- [25] Z. Wang, H. Wang, D. An, T. Ai, and P. Zhao, "Laboratory investigation on deicing characteristics of asphalt mixtures using magnetite aggregate as microwave-absorbing materials," *Constr. Build. Mater.*, vol. 124, pp. 589–597, Oct. 2016.
- [26] F. Patti, K. Mansour, M. Pannirselvam, and F. Giustozzi, "Mining materials to generate magnetically-triggered induction healing of bitumen on smart road pavements," *Constr. Build. Mater.*, vol. 171, pp. 577–587, May 2018.
- [27] K. Zhang, X. Gao, Q. Zhang, T. Li, H. Chen, and X. Chen, "Preparation and microwave absorption properties of asphalt carbon coated reduced graphene oxide/magnetic CoFe₂O₄ hollow particles modified multi-wall carbon nanotube composites," *J. Alloys Compd.*, vol. 723, pp. 912–921, Nov. 2017.

Leiva-Padilla, P.; Moreno-Navarro, F.; Iglesias, G.; Rubio-Gamez, M.C. A Review of the Contribution of Mechanomutable Asphalt Materials Towards Addressing the Upcoming Challenges of Asphalt Pavements. *Infrastructures* 2020, 5, 23.

DOI: <https://doi.org/10.3390/infrastructures5030023>

- [28] D. Y. Yoo, S. Kim, M. J. Kim, D. Kim, and H. O. Shin, "Self-healing capability of asphalt concrete with carbon-based materials," *J. Mater. Res. Technol.*, vol. 8, no. 1, pp. 827–839, Jan. 2019.
- [29] J. V. S. de Melo, G. Trichês, and L. T. de Rosso, "Experimental evaluation of the influence of reinforcement with Multi-Walled Carbon Nanotubes (MWCNTs) on the properties and fatigue life of hot mix asphalt," *Constr. Build. Mater.*, vol. 162, pp. 369–382, Feb. 2018.
- [30] A. Arabzadeh, H. Ceylan, S. Kim, A. Sassani, K. Gopalakrishnan, and M. Mina, "Electrically-conductive asphalt mastic: Temperature dependence and heating efficiency," *Mater. Des.*, vol. 157, pp. 303–313, Nov. 2018.
- [31] H. Jahanbakhsh, M. M. Karimi, B. Jahangiri, and F. M. Nejad, "Induction heating and healing of carbon black modified asphalt concrete under microwave radiation," *Constr. Build. Mater.*, 2018.
- [32] Z. Wang, Q. Dai, D. Porter, and Z. You, "Investigation of microwave healing performance of electrically conductive carbon fiber modified asphalt mixture beams," *Constr. Build. Mater.*, 2016.
- [33] B. Chen, B. Li, Y. Gao, T. C. Ling, Z. Lu, and Z. Li, "Investigation on electrically conductive aggregates produced by incorporating carbon fiber and carbon black," *Constr. Build. Mater.*, 2017.
- [34] Z. Wang, Q. Dai, and S. Guo, "Laboratory performance evaluation of both flake graphite and exfoliated graphite nanoplatelet modified asphalt composites," *Constr. Build. Mater.*, 2017.
- [35] G. R. Iglesias, S. Ahualli, J. Echávarri Otero, L. Fernández Ruiz-Morón, and J. D. G. Durán, "Theoretical and experimental evaluation of the flow behavior of a magnetorheological damper using an extremely bimodal magnetic fluid," *Smart Mater. Struct.*, 2014.
- [36] M. Zubieta, S. Eceolaza, M. J. Elejabarrieta, and M. M. Bou-Ali, "Magnetorheological fluids: Characterization and modeling of magnetization," *Smart Mater. Struct.*, 2009.
- [37] P. Skalski and K. Kalita, "Role of magnetorheological fluids and elastomers in today's world," *Acta Mechanica et Automatica*. 2017.
- [38] X. Liu and S. Wu, "Study on the graphite and carbon fiber modified asphalt concrete," *Constr. Build. Mater.*, vol. 25, no. 4, pp. 1807–1811, Apr. 2011.
- [39] X. Liu, S. Wu, Q. Ye, J. Qiu, and B. Li, "Properties evaluation of asphalt-based composites with graphite and mine powders," *Constr. Build. Mater.*, vol. 22, no. 3, pp. 121–126, Mar. 2008.
- [40] D. Derwin, P. Booth, P. Zaleski, W. Marsey, and W. Flood, "Snowfree®, Heated Pavement System to Eliminate Icy Runways," in *SAE Technical Paper Series*, 2010.
- [41] L. Minsk and N. H. Hanover, "Electrically conductive asphaltic concrete," Patent 3573427 A, 1971.
- [42] M. F. Caggiano, "Route 130 Bridge Snowfree Installation Electrical Analysis and Recommendations 1002 AR D," Contract, 1998.
- [43] C. Y. Tuan, "Roca Spur Bridge: The implementation of an innovative deicing technology," *J. Cold Reg. Eng.*, 2008.

Leiva-Padilla, P.; Moreno-Navarro, F.; Iglesias, G.; Rubio-Gamez, M.C. A Review of the Contribution of Mechanomutable Asphalt Materials Towards Addressing the Upcoming Challenges of Asphalt Pavements. *Infrastructures* 2020, 5, 23.

DOI: <https://doi.org/10.3390/infrastructures5030023>

[44] M. Vila-Cortavitarte, D. Jato-Espino, A. Tabakovic, and D. Castro-Fresno, "Optimizing the valorization of industrial by-products for the induction healing of asphalt mixtures," *Constr. Build. Mater.*, vol. 228, p. 116715, Dec. 2019.

[45] D. Eisenberg and K. E. Warner, "Effects of snowfalls on motor vehicle collisions, injuries, and fatalities," *Am. J. Public Health*, 2005.

[46] H. M. Willmert, J. D. Osso, M. R. Twiss, and T. A. Langen, "Winter road management effects on roadside soil and vegetation along a mountain pass in the Adirondack Park, New York, USA," *J. Environ. Manage.*, 2018.

[47] M. O. Rivett et al., "Highway deicing salt dynamic runoff to surface water and subsequent infiltration to groundwater during severe UK winters," *Sci. Total Environ.*, 2016.

[48] X. Shi, M. Akin, T. Pan, L. Fay, Y. Liu, and Z. Yang, "Deicer Impacts on Pavement Materials: Introduction and Recent Developments," *Open Civ. Eng. J.*, 2009.

[49] National Highway Traffic Safety Administration (NHTSA), "Preliminary statement of policy concerning automated vehicles," 2013.

[50] K. Wang and G. Akar, "Effects of neighborhood environments on perceived risk of self-driving: evidence from the 2015 and 2017 Puget Sound Travel Surveys," *Transportation (Amst.)*, vol. 46, no. 6, pp. 2117–2136, 2019.

[51] T. Litman, "Autonomous Vehicle Implementation Predictions: Implications for Transport Planning," *Transp. Res. Board Annu. Meet.*, 2014.



© 2020 by the authors. Submitted for possible open access publication under the terms and conditions of the Creative Commons Attribution (CC BY) license (<http://creativecommons.org/licenses/by/4.0/>).

Anexo 2. "Analysis of the mechanical response of asphalt materials manufactured with metallic fibres under the effect of magnetic fields".

Este anexo contiene la **versión del manuscrito preparado por la autora** y que fue publicado en el Journal de "Smart Materials and Structures" (JIF: 3.613, JCR: Q1 en categoría "Instruments & Instrumentation", "Materials Science"). El acceso al documento publicado, debe realizarse a través del DOI de la publicación: <https://doi.org/10.1088/1361-665X/ab5762>

Este documento corresponde al **primer artículo de este compendio** y desarrolla el primer objetivo definido para esta tesis doctoral:

Comprobar que el aumento en el valor de módulo que se produce por la activación de campos magnéticos en ligantes asfálticos mecanomutables, puede ser escalado a morteros asfálticos mecanomutables, para el desarrollo de materiales inteligentes que pueden adaptar su capacidad mecánica durante su puesta en servicio.

Leiva-Padilla, P., Moreno-Navarro, F., Iglesias-Salto, G., & Rubio-Gamez, M. C. (2019). Analysis of the mechanical response of asphalt materials manufactured with metallic fibres under the effect of magnetic fields. *Smart Materials and Structures*, 29(1), 015033.

DOI: <https://doi.org/10.1088/1361-665X/ab5762>

Analysis of the mechanical response of asphalt materials manufactured with metallic fibres under the effect of magnetic fields

P. Leiva-Padilla², F. Moreno-Navarro², G. Iglesias-Salto³ and M. C. Rubio-Gamez⁴

¹pleiva@ugr.es, Laboratory of Construction Engineering of the University of Granada (LabIC.UGR), Granada, Spain

²fmoreno@ugr.es, Laboratory of Construction Engineering of the University of Granada (LabIC.UGR), Granada, Spain

³iglesias@ugr.es, Department of Applied Physics of the University of Granada, Granada, Spain

⁴mcrubio@ugr.es, Laboratory of Construction Engineering of the University of Granada (LabIC.UGR), Granada, Spain

Abstract.

Mechanomutable Asphalt Materials (MAMs) are being developed as a key contribution towards the evolution of Smart Roads. MAMs are composed of a matrix of asphalt materials modified with metallic fibres that can be activated with magnetic fields. By controlling the physical domain of the magnetic fields, it is possible to manage the mechanical performance of MAMs, and consequently transform the pavement into a smart structure that is capable of reacting efficiently to the requirements of traffic and weather. This paper describes the results obtained from a study conducted using a resonance frequency test to evaluate the mechanical performance of the dynamic modulus of various sizes of specimens of MAM mortars under the activation of various intensities of magnetic field. MAM mortars containing two different quantities of metallic fibres were used to manufacture specimens of two different sizes that were evaluated under various temperatures. The findings indicate that the dynamic modulus of the MAMs is affected by both the intensity of the magnetic field applied and the fibre content, but not by the size of the specimen, therefore, just the two first aforementioned variables should be considered in the design of MAMs for the construction of smart roads.

Keywords: mechanomutable asphalt materials, MAM, smart materials, smart roads

1. Introduction

Through the years, the infrastructure for roads has undergone a continuous process of evolution, starting from the Roman and rustic roads, through to high-capacity roads (highways), and eventually leading to the sustainable and smart roads that are currently under development. These smart roads represent a new concept in which roads are regarded as more than simply a means of

Leiva-Padilla, P., Moreno-Navarro, F., Iglesias-Salto, G., & Rubio-Gamez, M. C. (2019). Analysis of the mechanical response of asphalt materials manufactured with metallic fibres under the effect of magnetic fields. *Smart Materials and Structures*, 29(1), 015033.

DOI: <https://doi.org/10.1088/1361-665X/ab5762>

transporting goods and services, but are infrastructures that provide extra value to the investment made in constructing them.

Sustainable and smart roads are able to integrate all the disruptive changes that are required by the production of autonomous vehicles and can help in the management of the infrastructure in real-time. One of the main tasks related to the development of smart roads is the generation of new technologies and new materials for use in future pavements. In this regard, Mechanomutable Asphalt Materials (MAMs) are currently being developed [1]-[4]. These materials are composed of a bituminous matrix with iron micro-particles that can be activated with external magnetic fields to induce mechanical changes within the materials. These materials can increase their stiffness and perform elastically when a magnetic field is activated, which can help them to better support the loads transferred to the pavement (reducing the impact caused by such loads and extending the service life of the pavement).

Although other previous studies have examined the use of metallic materials (without magnetic fields) for modifying conventional asphalt materials, these have focused primarily on evaluating their mechanical performance against fatigue [5], energy to fracture [6], susceptibility to develop permanent deformation [6], [7], susceptibility to moisture damage [7], [8], and healing capacity [8]-[12]. However, none of these studies have explored the mechanical performance produced in these materials for the activation of magnetic fields.

Similarly, the studies reporting the use of magnetic fields in asphalt materials modified with metallic materials are mainly directed towards generating a self-healing mechanism by the induction of heat in coils [10], [12]-[17]. Consequently, the development of MAMs can introduce a new research field of considerable application potential. Nonetheless, the benefits of using these materials have only been tested at binder scale and under controlled magnetic fields in laboratory [1]. In this sense, and further reinforcing this research, no study has been reported in which aggregates are present or when the direction of the magnetic field has not been controlled, as might be expected when applying the asphalt mortar under real service conditions.

Therefore, this research is focused on evaluating the possibility of transferring the results obtained in mechanomutable asphalt binders to mechanomutable asphalt mortars in order to assess the influence of aggregates (which are more elastic and rigid materials that can impede or minimize the effect of the magnetic field) on the effect induced by magnetic fields in the material. In addition, during this study, the effects of non-controlled and non-directed magnetic fields are studied (since it is not easy to manipulate magnetic fields in real life).

2. Methodology

2.1. Materials

Following previous studies conducted with mechanomutable asphalt binders where recycled materials were studied [3], the metallic materials used in this study were steel fibres obtained by the recycling of end-of-life vehicle tires (which increases both the cost-effectiveness and the sustainability of incorporating these modifiers into the traditional asphalt materials). The steel

Leiva-Padilla, P., Moreno-Navarro, F., Iglesias-Salto, G., & Rubio-Gamez, M. C. (2019). Analysis of the mechanical response of asphalt materials manufactured with metallic fibres under the effect of magnetic fields. *Smart Materials and Structures*, 29(1), 015033.

DOI: <https://doi.org/10.1088/1361-665X/ab5762>

fibres used had an irregular shape, with lengths ranging from 3.3 mm to 83.3 mm and diameters from 0.2 mm to 0.6 mm. Considering that previous studies [7], [10], [12] related to the use of this kind of metallic fibres in bituminous mixtures agreed that high dosages (around 4-10% and more) are prone to form clusters and therefore regions with non-homogeneous distribution (which are also difficult to compact), it was proposed to manufacture mortars with percentages of 0%, 5% and 11% of metallic fibres by aggregate substitution (see Figure 1), in combination with a conventional asphalt binder B50/70 (with a penetration of 65 mm at 25°C based on the EN 1426 [18], a softening point of 51°C based on the EN 1427 [19], and a Fraass fragility of -8°C according to EN 12593 [20]) and limestone sand with a maximum size of 6 mm (Figure 1), to manufacture the three mortars evaluated in this study (Table 1). After the mechanical study of the material, the amount of bitumen selected to manufacture the mortars was 8% (over the total weight of the mixture).

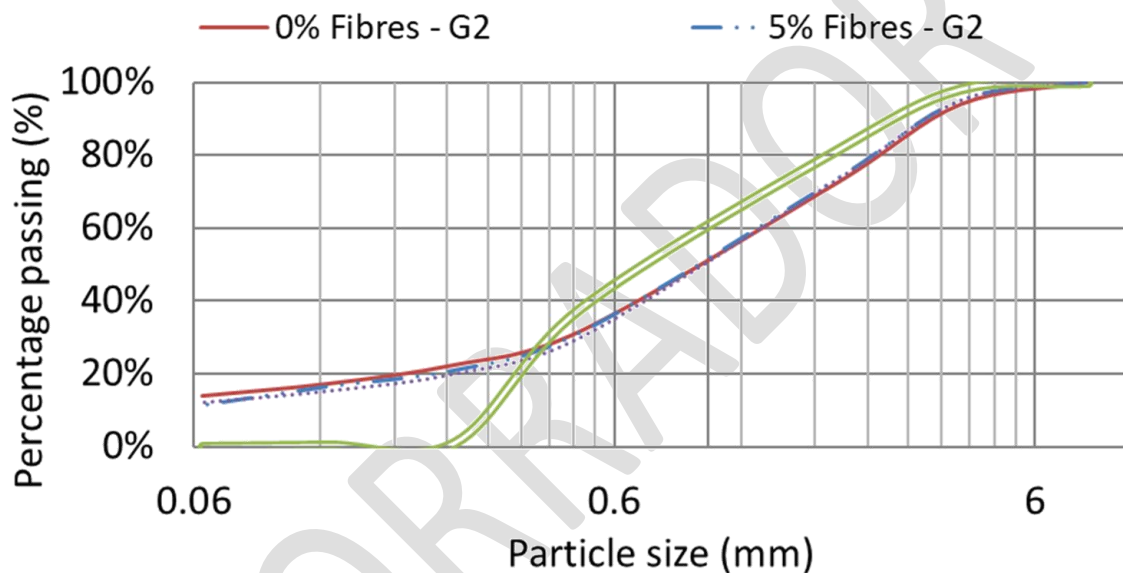


Figure 1. Size distribution of the mortars used in the study

Table 1. Mechanomutable asphalt mortars studied

| Name | Type of binder matrix | Metallic fibre content by substitution of aggregates (%) |
|------------|-----------------------|--|
| M – 0%MF | B 50/70 | 0 |
| M – 5% MF | B 50/70 | 5 |
| M – 11% MF | B 50/70 | 11 |

Leiva-Padilla, P., Moreno-Navarro, F., Iglesias-Salto, G., & Rubio-Gamez, M. C. (2019). Analysis of the mechanical response of asphalt materials manufactured with metallic fibres under the effect of magnetic fields. *Smart Materials and Structures*, 29(1), 015033.

DOI: <https://doi.org/10.1088/1361-665X/ab5762>

Based on these formulations, prismatic specimens of two different heights (8 cm and 12 cm, see Figure 2) were manufactured from a block of asphalt mixture compacted using a laboratory roller compactor, to analyse the effect of the geometry of the material under the action of the magnetic field. The corresponding densities of the specimens by type of mixture are shown in Figure 3, which by Analysis of Variance (ANOVA, in order to make a multiple comparison of the average values) at 95% of confidence establishes the null hypothesis of equality and therefore can be considered the same (which avoids the introduction of other, new variables into the study carried out).

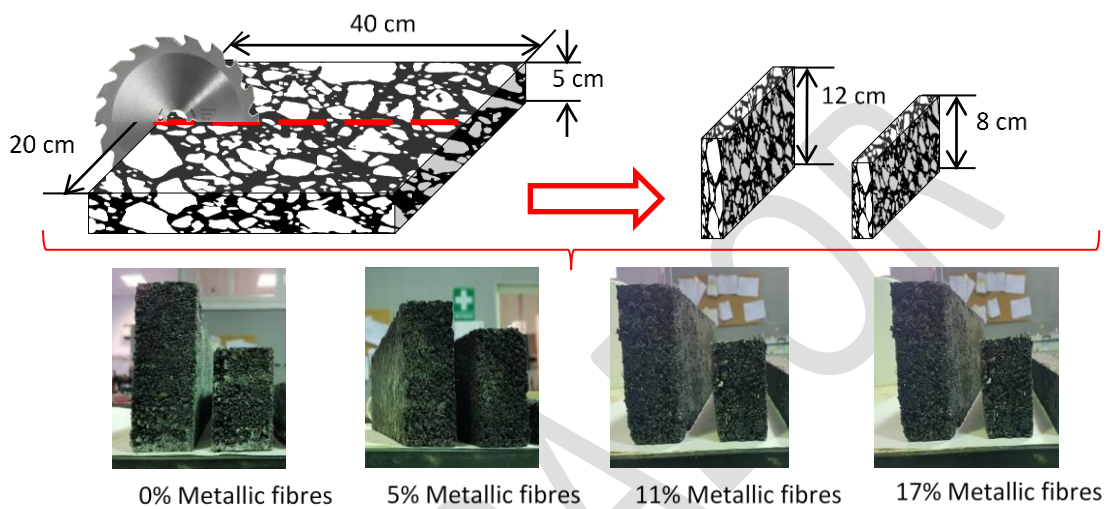


Figure 2. Geometrical configuration used in the specimens

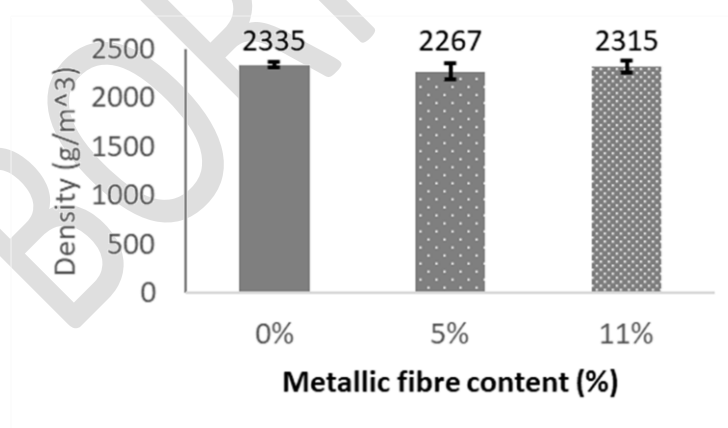


Figure 3. Average density of the mechanomutable asphalt mortars studied.

Leiva-Padilla, P., Moreno-Navarro, F., Iglesias-Salto, G., & Rubio-Gamez, M. C. (2019). Analysis of the mechanical response of asphalt materials manufactured with metallic fibres under the effect of magnetic fields. *Smart Materials and Structures*, 29(1), 015033.

DOI: <https://doi.org/10.1088/1361-665X/ab5762>

2.2. Methods

The performance of each one of the two specimens manufactured with the defined mortars was characterized through the dynamic modulus obtained from the Resonant Frequency Test. The equipment used for the Resonant Frequency Test is composed of a precision accelerometer, a ball hammer, a rubber pad, and a main body acquisition and display unit connected to a Picoscope (Figure 4). The Picoscope was used to extract the complete signal of accelerations produced by the impact of the hammer. As shown in Figure 4, the study evaluated the resonance frequency and the corresponding dynamic modulus of the mortars, by varying the sizes and fibre content of the specimens, as well as, the intensities (based on the separation of the magnet) of non-controlled and non-directed magnetic fields at two different temperatures (25°C and 45°C).

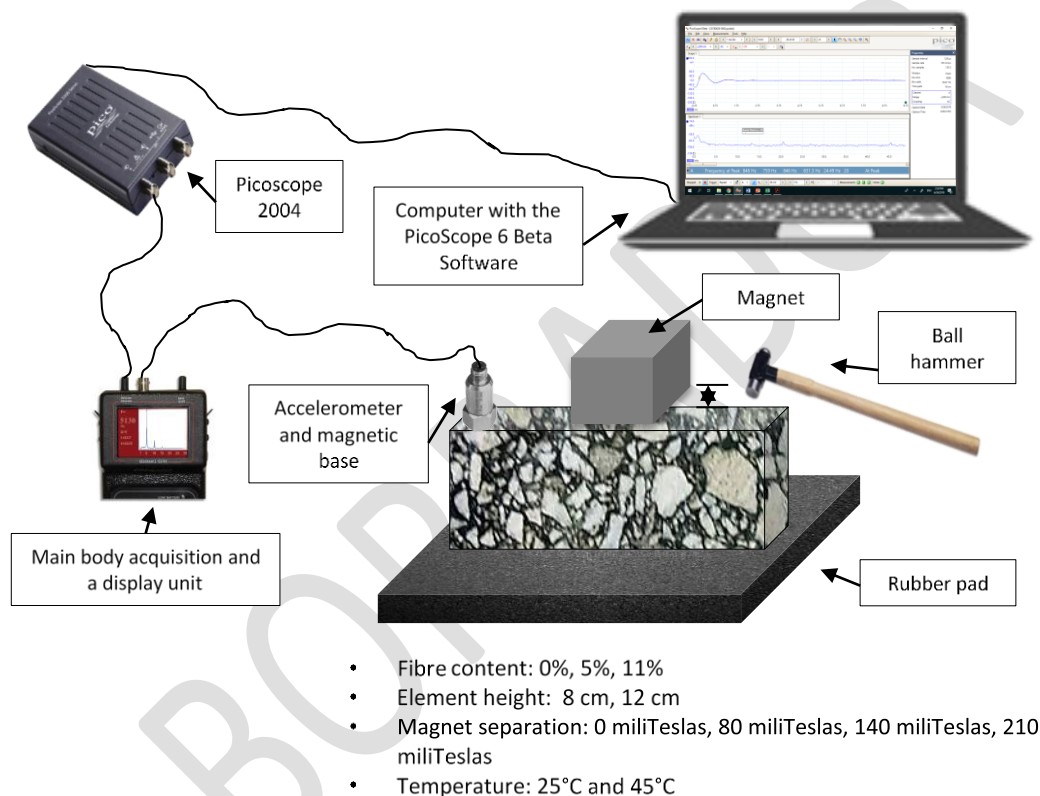


Figure 4. Sketch of the configuration used for the Resonant Frequency Test

The resonance frequency corresponds to the calculated peak of the Fast Fourier Transformation (FFT) to the frequency domain, of the time domain signal measured [21]. The transversal mode of vibration was used on the specimens before and after the activation of the magnetic field, in order to obtain the corresponding resonance frequency value for determining the corresponding modulus through Equation 1 [22] and the change produced in this value by the presence of the metallic fibres and the activation of magnetic fields.

Leiva-Padilla, P., Moreno-Navarro, F., Iglesias-Salto, G., & Rubio-Gamez, M. C. (2019). Analysis of the mechanical response of asphalt materials manufactured with metallic fibres under the effect of magnetic fields. *Smart Materials and Structures*, 29(1), 015033.

DOI: <https://doi.org/10.1088/1361-665X/ab5762>

$$E = 0.965 * 10^{-6} \left(\frac{l^3}{b * h^3} \right) * R * W * f_n^2 \quad \text{Equation 1}$$

Where E is the modulus of the material, l is the length of the specimen, b is the width of the specimen, h is the height of the specimen, R is a factor that relates to the length of the specimen and the radius, W is the weight of the specimen and f_n is the resonance frequency.

It is important to mention that, a good correlation between the modulus values obtained in this study and the modulus values obtained in the Indirect Tensile test (IT) has already been demonstrated [23-25]. In this respect, several previous studies [26-29] had attributed the dissipation of energy obtained, due to temperature increase, to the damping component of the viscoelastic performance of the asphalt concrete material and had calculated the corresponding master curves, with the results of similar resonance frequency tests. Because of this, and in order to determine the effect of temperature in the mechanical response of the materials studied, it was decided to carry out the tests at intermediate (25 °C) and high (45 °C) temperatures, avoiding low temperatures (which would require high magnetic fields that are expensive and are not easy to produce at the scale of laboratory, to show any appreciable difference in the material properties).

3. Results and Discussion

In order to describe the effect of the activation of magnetic fields in MAMs, Figure 5 shows the dynamic modulus values obtained when a magnetic field of 210 mT is activated, in comparison with the values of a control specimen without their activation. These results indicate that the rates of increase in the dynamic modulus values went from from 0.81 GPa/°C to 0.92 GPa/°C (15% higher), whilst the dynamic modulus values, per mT, decreased from 0.012 GPa/mT to 0.0016 GPa/mT (the 0.13 part), with a temperature increase from 25°C to 45°C.

Leiva-Padilla, P., Moreno-Navarro, F., Iglesias-Salto, G., & Rubio-Gamez, M. C. (2019). Analysis of the mechanical response of asphalt materials manufactured with metallic fibres under the effect of magnetic fields. *Smart Materials and Structures*, 29(1), 015033.

DOI: <https://doi.org/10.1088/1361-665X/ab5762>

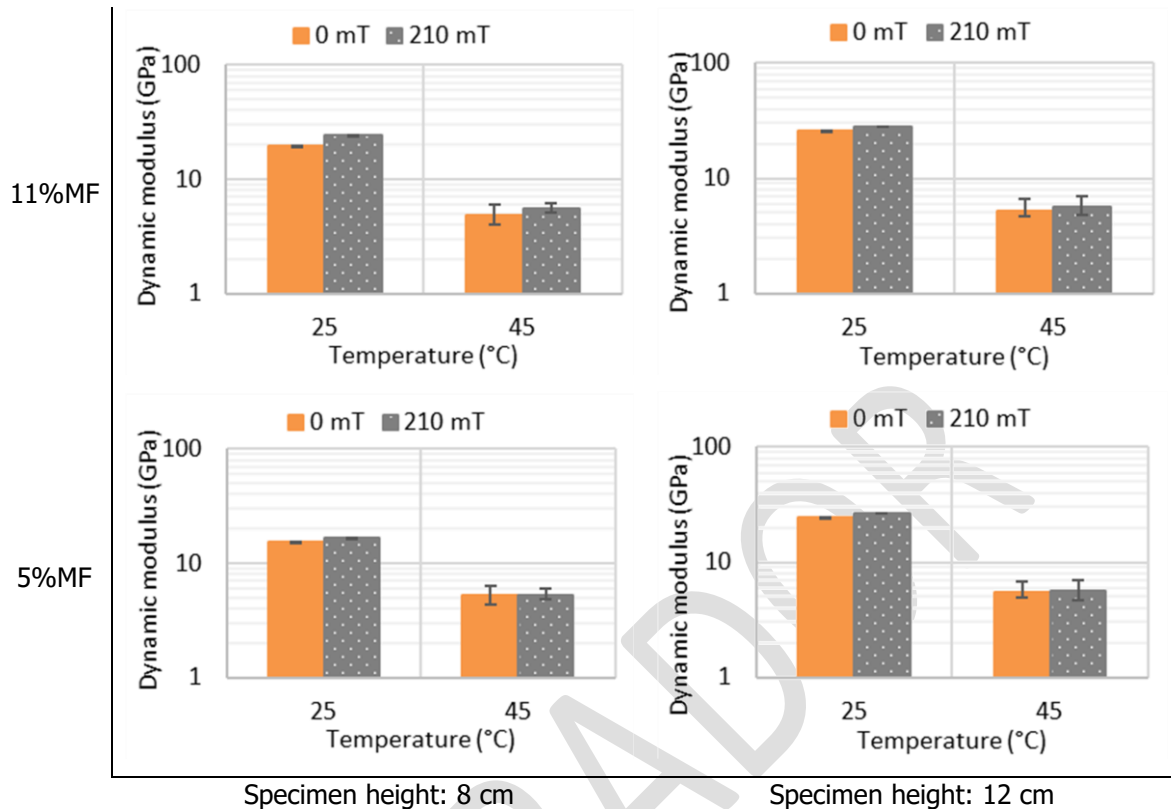


Figure 1. Influence of temperature and 210 mT of magnetic field.

Figure 6 summarizes the results obtained from analysing the percentage increase in the value of the dynamic modulus according to specimen height, when a magnetic field of 210 mT is applied, at temperature values of 25°C and 45°C. Despite there being higher increments at 45°C, dynamic modulus values are 76% lower and more variable than the values obtained at 25°C. From the Multivariate Analysis of Variance (MANOVA, extension of the Analysis of Variance ANOVA, for the simultaneous comparison of the dynamic modulus at two test temperatures, with and without the activation of magnetic fields for two different specimen sizes) of this data, it is concluded that, with 95% confidence (that is, with a p value set at < 0.05) the specimen height has no significant effect on the value of the dynamic modulus at a temperature of 25°C, whilst it has a significant influence at 45°C. A complementary paired t-test was conducted to explore the differences between the values of the dynamic modulus with and without an activated magnetic field (for each specimen height and percentage of metallic fibre). The t-test revealed, with 95% confidence, that applying a magnetic field of 210 mT leads to significant changes in the dynamic modulus values of the MAM mortars (these values becoming higher, according to the pattern of results obtained).

Leiva-Padilla, P., Moreno-Navarro, F., Iglesias-Salto, G., & Rubio-Gamez, M. C. (2019). Analysis of the mechanical response of asphalt materials manufactured with metallic fibres under the effect of magnetic fields. *Smart Materials and Structures*, 29(1), 015033.

DOI: <https://doi.org/10.1088/1361-665X/ab5762>

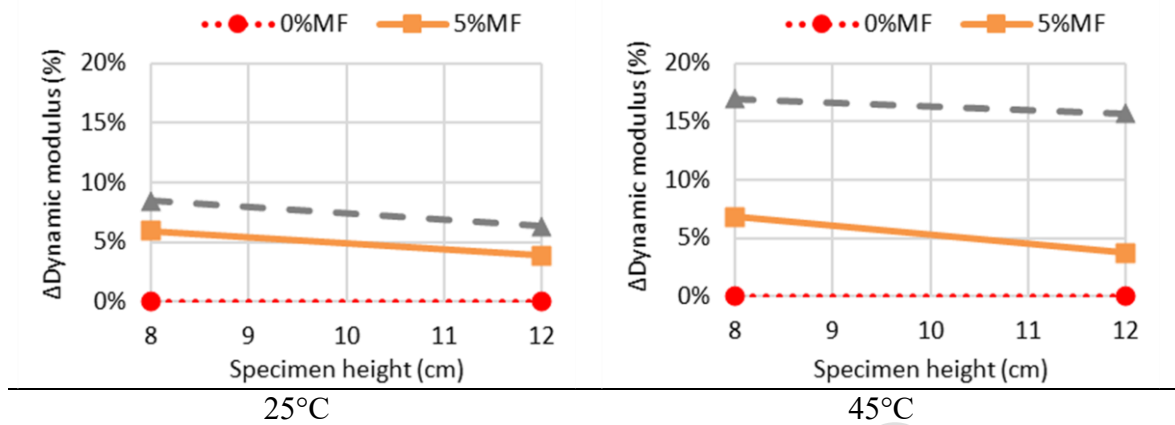


Figure 6. Influence of specimen height on the increment in dynamic modulus of MAM when applying a magnetic field of 210 mT.

The results obtained from a deeper analysis, in which the intensity of the magnetic field was varied, are shown in Figure 7. As the intensity of the applied magnetic field is increased, the value of the dynamic modulus also increases. In order to know whether the applied intensity was sufficient to generate significant differences according to the content of metallic fibres, a MANOVA was conducted on the data displayed in Figure 7. This analysis revealed that, with 95% confidence, there are significant differences in the rate of increase of the dynamic modulus according to both the fibre content and the change in the value of the magnetic fields applied.

Leiva-Padilla, P., Moreno-Navarro, F., Iglesias-Salto, G., & Rubio-Gamez, M. C. (2019). Analysis of the mechanical response of asphalt materials manufactured with metallic fibres under the effect of magnetic fields. *Smart Materials and Structures*, 29(1), 015033.

DOI: <https://doi.org/10.1088/1361-665X/ab5762>

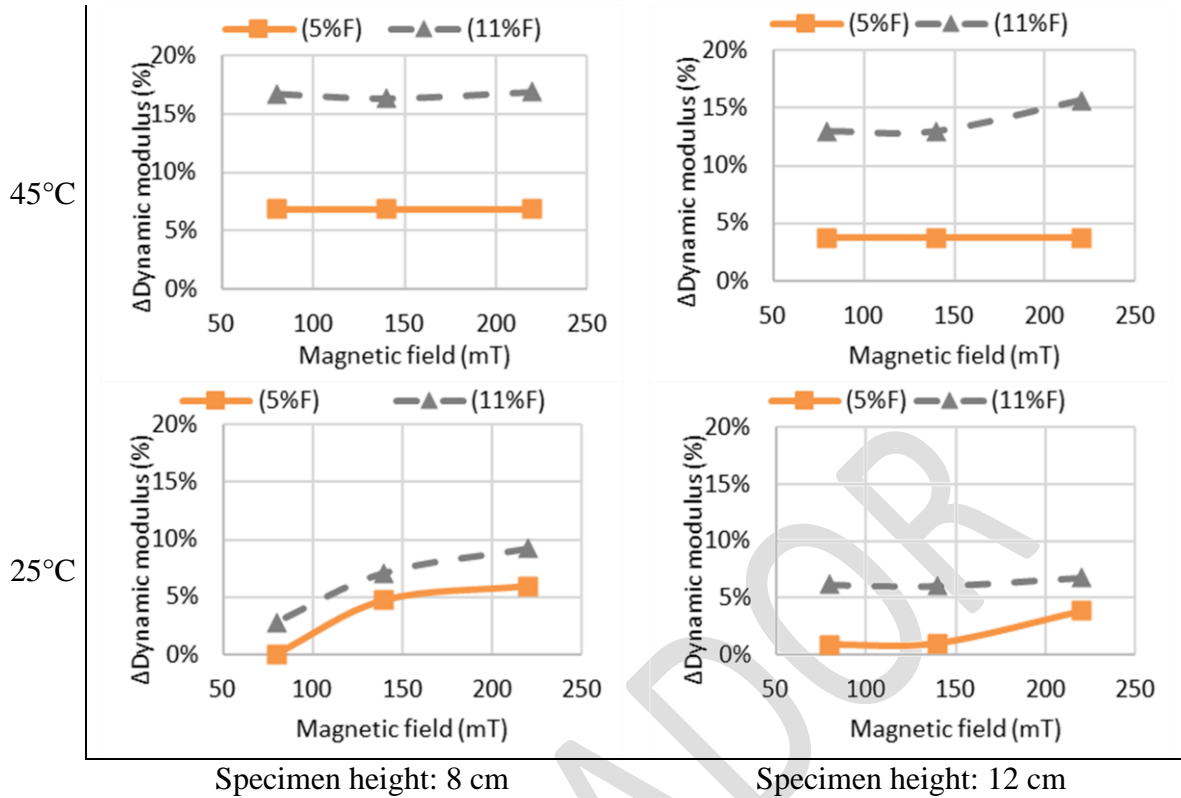


Figure 7. Influence of the intensity of magnetic field on the modulus of MAMs.

Finally, despite the densities of the manufactured specimens being statistically the same, Figure 8 shows the increase in the dynamic modulus obtained according to the density values. As expected, when the density increases, the dynamic modulus increases but this effect becomes less considerable as test temperature increases. In addition, it should be highlighted that regardless of the density of the specimen, the activation of the magnetic fields increases the values of the dynamic modulus of the material (which demonstrate the viability of mechanomutable materials).

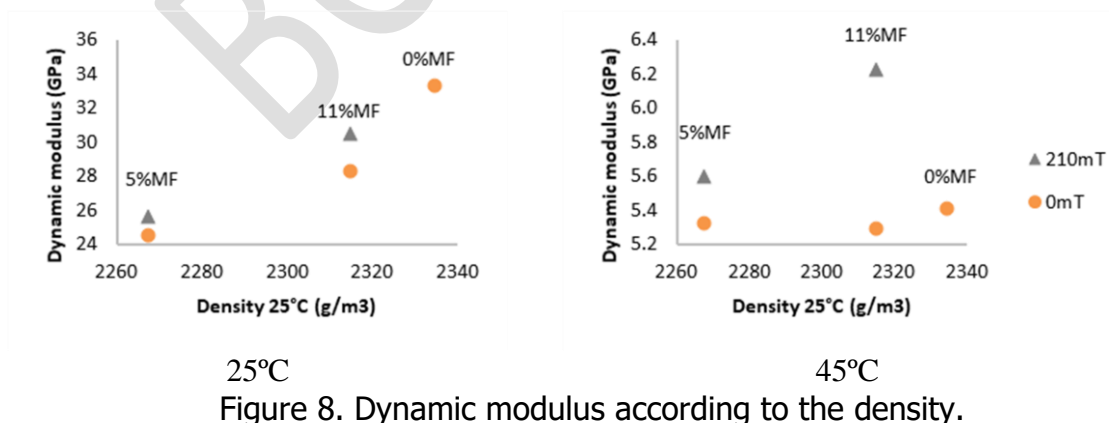


Figure 8. Dynamic modulus according to the density.

Leiva-Padilla, P., Moreno-Navarro, F., Iglesias-Salto, G., & Rubio-Gamez, M. C. (2019). Analysis of the mechanical response of asphalt materials manufactured with metallic fibres under the effect of magnetic fields. *Smart Materials and Structures*, 29(1), 015033.

DOI: <https://doi.org/10.1088/1361-665X/ab5762>

4. Summary of Findings and Conclusions

This paper summarizes the results obtained from a study analysing the mechanical response of asphalt materials manufactured with metallic fibres under the effect of magnetic fields. Two different sizes of specimens with two different quantities of metallic fibres were evaluated when applying three different intensities of magnetic field at temperatures of 25°C and 45°C. On the basis of the results obtained, the following conclusions can be drawn:

1. Even though aggregates affect the capacity of magnetic fields to change the dynamic modulus of the mechanomutable asphalt materials, it has been confirmed that the activation of magnetic fields can increase the dynamic modulus values of the material. The significance of this increase depends on the intensity of the magnetic field applied and the content of fibre used, while specimen height has no impact. This indicates that greater changes in the mechanical properties could be achieved by increasing the magnetic field and the quantity of metallic materials used. Therefore, when designing these materials, the dosage of metallic particles and magnetic field to be used should be adapted to the weather and load conditions in order to guarantee the adequate performance of the pavement at high temperatures, but without affecting its performance at intermediate and low temperatures.
2. Regardless of the fact that the activation of magnetic fields produced a higher absolute value in dynamic modulus at 45°C, a higher rate of increase in dynamic modulus values, per °C and mT applied, were obtained at 25°C. Showing that there is a greater effect of the activation of magnetic fields at 25°C, when the movement of the metallic fibres is hindered to a greater extent.
3. Although the magnetic fields that can be applied in real-life practice have the limitation of being non-controlled and non-directed, it is possible to generate changes in the mechanical performance of mechanomutable asphalt mortars. Therefore, the intensities of a magnetic field that can be potentially applied in practice should be considered in order to optimize the use of this technology. Given these considerations, the work presented here will be extended to the study of other metallic materials, asphalt mixtures, and magnetic fields.

Acknowledgments

The research presented in this paper was carried out as part of the H2020-MSCA-ETN-2016. This project has received funding from the European Union's H2020 Programme for research, technological development, and demonstration under grant agreement number 721493.

Leiva-Padilla, P., Moreno-Navarro, F., Iglesias-Salto, G., & Rubio-Gamez, M. C. (2019). Analysis of the mechanical response of asphalt materials manufactured with metallic fibres under the effect of magnetic fields. *Smart Materials and Structures*, 29(1), 015033.

DOI: <https://doi.org/10.1088/1361-665X/ab5762>

References

- [1] F. Moreno-Navarro, G. R. Iglesias, and M. C. Rubio-Gámez, “Development of mechanomutable asphalt binders for the construction of smart pavements,” *Mater. Des.*, 2015.
- [2] F. Moreno-Navarro, G. R. Iglesias, and M. C. Rubio-Gámez, “Experimental evaluation of using stainless steel slag to produce mechanomutable asphalt mortars for their use in smart materials,” *Smart Mater. Struct.*, 2016.
- [3] F. Moreno-Navarro, G. R. Iglesias, and M. C. Rubio-Gámez, “Mechanical performance of mechanomutable asphalt binders under cyclic creep and recovery loads,” *Constr. Build. Mater.*, 2016.
- [4] [F. Moreno-Navarro, G. R. Iglesias, and M. C. Rubio-Gámez, “Encoded asphalt materials for the guidance of autonomous vehicles,” *Autom. Constr.*, 2019.
- [5] H. Zhao, S. Zhong, X. Zhu, and H. Chen, “High-efficiency heating characteristics of ferrite-filled asphalt-based composites under microwave irradiation,” *J. Mater. Civ. Eng.*, 2017.
- [6] Z. Chen, S. Wu, J. Wen, M. Zhao, M. Yi, and J. Wan, “Utilization of gneiss coarse aggregate and steel slag fine aggregate in asphalt mixture,” *Constr. Build. Mater.*, 2015.
- [7] Á. García, E. Schlangen, M. van de Ven, and Q. Liu, “Electrical conductivity of asphalt mortar containing conductive fibers and fillers,” *Constr. Build. Mater.*, 2009.
- [8] Z. Wang, C. Xu, S. Wang, J. Gao, and T. Ai, “Utilization of magnetite tailings as aggregates in asphalt mixtures,” *Constr. Build. Mater.*, 2016.
- [9] N. Nabian and M. M. Khabiri, “Mechanical and moisture susceptibility properties of HMA containing ferrite for their use in magnetic asphalt,” *Constr. Build. Mater.*, 2016.
- [10] Y. Pamulapati, M. A. Elseifi, S. B. Cooper, L. N. Mohammad, and O. Elbagalati, “Evaluation of self-healing of asphalt concrete through induction heating and metallic fibers,” *Constr. Build. Mater.*, 2017.
- [11] K. Zhang, X. Gao, Q. Zhang, T. Li, H. Chen, and X. Chen, “Preparation and microwave absorption properties of asphalt carbon coated reduced graphene oxide/magnetic CoFe₂O₄ hollow particles modified multi-wall carbon nanotube composites,” *J. Alloys Compd.*, 2017.
- [12] A. González, J. Norambuena-Contreras, L. Storey, and E. Schlangen, “Effect of RAP and fibers addition on asphalt mixtures with self-healing properties gained by microwave radiation heating,” *Constr. Build. Mater.*, 2018.
- [13] Á. García, E. Schlangen, M. Van De Ven, and D. Van Vliet, “Induction heating of mastic containing conductive fibers and fillers,” *Mater. Struct. Constr.*, 2011.
- [14] Á. García, E. Schlangen, M. Van De Ven, and Q. Liu, “A simple model to define induction heating in asphalt mastic,” *Constr. Build. Mater.*, 2012.
- [15] B. Gómez-Meijide, H. Ajam, P. Lastra-González, and A. Garcia, “Effect of air voids content on asphalt self-healing via induction and infrared heating,” *Constr. Build. Mater.*, 2016.
- [16] H. Ajam, P. Lastra-González, B. Gómez-Meijide, and Á. García, “Self-healing of dense asphalt concrete by two different approaches: Electromagnetic induction and infrared radiation,” *RILEM Bookseries*, 2016.
- [17] B. Gómez-Meijide, H. Ajam, A. Garcia, and S. Vansteenkiste, “Effect of bitumen properties in the induction healing capacity of asphalt mixes,” *Constr. Build. Mater.*, 2018.
- [18] Asociación Española de Normalización y Certificación, EN 1426 Bitumen and Bituminous Binders (Determination of Needle Penetration). .
- [19] Asociación Española de Normalización y Certificación, EN 1427 Bitumen and Bituminous Binders (Determination of the Softening Point).” . .
- [20] Asociación Española de Normalización y Certificación, EN 12593 Bitumen and bituminous binders (Determination of the Fraass breaking point). .

Leiva-Padilla, P., Moreno-Navarro, F., Iglesias-Salto, G., & Rubio-Gamez, M. C. (2019). Analysis of the mechanical response of asphalt materials manufactured with metallic fibres under the effect of magnetic fields. *Smart Materials and Structures*, 29(1), 015033.

DOI: <https://doi.org/10.1088/1361-665X/ab5762>

- [21] G. Kweon and Y. Richard Kim, "Determination of asphalt concrete complex modulus with impact resonance test," in *Transportation Research Record*, 2006.
- [22] ASTM Standard C215, "Standard Test Method for Fundamental Transverse , Longitudinal , and Torsional Resonant Frequencies of Concrete Specimens," ASTM standard. 2008.
- [23] N. Ryden, "Resonant frequency testing of cylindrical asphalt samples," *Eur. J. Environ. Civ. Eng.*, 2011.
- [24] A. Gudmarsson, N. Ryden, and B. Birgisson, "Determination of the frequency dependent dynamic modulus for asphalt concrete beams using resonant acoustic spectroscopy," *RILEM Bookseries*, 2012.
- [25] R. Tauste, F. Moreno-Navarro, R. Gallego, and M. C. Rubio-Gámez, "Analysis of the sensitivity of the impact resonance frequency test as a tool to determine the elastic properties of bituminous materials," *Mater. Constr.*, 2017.
- [26] I. Boz, "The Impact of Specimen Size and Void Content on the Impact Resonance Testing of Asphalt Concrete," in *Transportation Research Board 93rd Annual Meeting*. January 12-16, Washington, D.C., 2014.
- [27] A. Gudmarsson, N. Ryden, H. Di Benedetto, and C. Sauzéat, "Complex modulus and complex Poisson's ratio from cyclic and dynamic modal testing of asphalt concrete," *Constr. Build. Mater.*, 2015.
- [28] I. Boz, K. Bekiroglu, M. Solaimanian, P. Tavassoti-Kheiry, and C. Lagoa, "Validation of Model Order Assumption and Noise Reduction Method for the Impact Resonance Testing of Asphalt Concrete," *J. Nondestruct. Eval.*, 2017.
- [29] A. Bekele, B. Birgisson, N. Ryden, and A. Gudmarsson, "Slow dynamic diagnosis of asphalt concrete specimen to determine level of damage caused by static low temperature conditioning," in *AIP Conference Proceedings*, 2017.

Anexo 3. "Interpretation of the Magnetic Field Signals Emitted by Encoded Asphalt Pavement Materials".

Este anexo contiene la **versión del manuscrito preparado por la autora** y que fue publicado en el Journal de "Sustainability" (JIF: 2.592, JCR: Q1 en categoría "Environmental/Ecology". El acceso al documento publicado debe realizarse a través del DOI de la publicación: <https://doi.org/10.3390/su12187300>

Este documento corresponde al **segundo artículo de este compendio** y desarrolla el segundo objetivo definido para esta tesis doctoral:

Caracterizar la forma en que la altura de medición, la distancia de medición y la velocidad de aproximación del vehículo, pueden afectar la señal magnética emitida por morteros asfálticos codificados, que podrían asistir en el guiado de los vehículos.

Leiva-Padilla, P., Moreno-Navarro, F., Iglesias, G., & Rubio-Gamez, M. (2020). Interpretation of the Magnetic Field Signals Emitted by Encoded Asphalt Pavement Materials. *Sustainability*, 12(18), 7300.

DOI: <https://doi.org/10.3390/su12187300>

Article

Interpretation of the Magnetic Field Signals Emitted by Encoded Asphalt Pavement Materials

Paulina Leiva-Padilla^{1,*}, Fernando Moreno-Navarro², Guillermo Iglesias³ and M^a Carmen Rubio-Gamez⁴

¹ Laboratory of Construction Engineering of the University of Granada (LabIC.UGR), Granada, Spain; pleiva@ugr.es

² Laboratory of Construction Engineering of the University of Granada (LabIC.UGR), Granada, Spain; fmoreno@ugr.es

³ Department of Applied Physics of the University of Granada, Spain; iglesias@ugr.es

⁴ Laboratory of Construction Engineering of the University of Granada (LabIC.UGR), Granada, Spain; mcrubio@ugr.es

* Correspondence: pleiva@ugr.es

Received: date; Accepted: date; Published: date

Abstract: Asphalt materials modified with different types and dosages of magnetically responsive materials can emit patterns of magnetic signals easily detectable by magnetic field sensors. These patterns could be used to encode roads and improve infrastructure-to-vehicle (I2V)/road-to-vehicle (R2V) communications. In this sense, this paper presents a laboratory study addressed to analyze the magnetic field signals emitted by encoded asphalt specimens manufactured with various dosages of steel fibers. The analysis consisted in the evaluation of the influence of three parameters: (1) the height of placement of the magnetic field sensors, (2) the approach speed of the encoded specimen/vehicle and (3) the distance from signal detection. Results show that, for each one of the parameters evaluated, there is a limit value below which it is possible to work with the magnetic signal emitted by the encoded samples. A proof-of-concept was used to validate the results obtained.

Keywords: encoded asphalt materials, smart roads, road-to-vehicle, infrastructure-to-vehicle.

1. Introduction

Five main benefits have been outlined from the implementation of autonomous vehicles (AV) [1]. The first benefit is related to the improvement of road safety [2],[3] in terms of collision prevention between vehicles and infrastructure elements, pre-detection of vehicle malfunction and monitoring of the driver status during transit. The second benefit refers to easy driving and parking [4], which is associated with a reduction in fatigue, stress, and difficulties for the user. The third benefit is linked to operational efficiency [5], [6] as a result of reductions in fuel costs, insurance rates, and travel time. And the fourth and fifth benefits are related to multitasking [5], [6] and social advantages for users [2], [3], [5], [6]. For example, taking a break from driving, enjoying entertainment or an increase in work productivity, and reducing traffic congestion and fuel emissions, as well as improving the mobility of disabled or elderly people, and children.

Leiva-Padilla, P., Moreno-Navarro, F., Iglesias, G., & Rubio-Gamez, M. (2020). Interpretation of the Magnetic Field Signals Emitted by Encoded Asphalt Pavement Materials. *Sustainability*, 12(18), 7300.

DOI: <https://doi.org/10.3390/su12187300>

The concerns identified with AVs relate to the vehicle's performance in bad weather conditions [4], safety issues linked to the vehicle's response to unexpected situations during driving [4], [5], [7] (i.e. the interaction with other self-driving vehicles and system failures), and privacy and security issues related to the occurrence of system failures [3], [4] (i.e. errors or problems from hacking and violation of privacy). Additional concerns include the increase in the production and maintenance costs of the vehicles [5], [7] and the social challenges [4], [5], [7] related to the legal liability associated with the ethical dilemma or social non-consensus produced by the use of these technologies. Furthermore, the definition of insurance policies and the difficulty of elderly or disabled people to use them also raise concerns.

In this sense, the work of the stakeholders within this industry is of utmost importance. Automotive manufactures and information technology companies in the United States and Europe have made considerable investments in the development of vehicle-to-everything communications (V2X) in the last 40 years [1], [8]. The latest AV vehicle models are equipped with camera-based systems, geographic positioning systems (GPS), inertial navigation systems (INS), high precision maps to identify obstacles, sensing technologies among them LIDAR, RADAR, ultrasonic and infrared sensors, as well as technologies already being implemented in conventional vehicles such as adaptive cruise control, lane assist, front collision warning, etc. [2], [9], [10]. This set of autonomous travel technologies are used to feed machine learning, big data, virtual reality, and other techniques to enhance the reliability of AVs [10]–[14].

Additionally, many government agencies and academia research centers in the United States and several European and Asian countries [1] have been working on infrastructure-to-vehicle (I2V)/road-to-vehicle (R2V) communications through investment in research, along with improvements in laws and regulations to promote the development of intelligent transportation infrastructure (ITS). Some of these systems are already used for the design and simulation of intelligent traffic at real intersections [15]–[17], as well as, the implementation of Roadside Smart Devices (RSDs), which are composed of a large number of sensing devices in the road with short-range wireless communication for monitoring the physical phenomena happening in the road structure, as well as communicating with the vehicles [18]–[20]. Additional examples also include a hybrid between the visible light communication (VLC) and radio frequency (RF) systems [21]–[24], to offer longer distance transmissions and improved I2V.

In this respect, encoded asphalt materials are part of a recent solution for further assisting AV guidance, which consists of encoding part of the pavement structure by modifying asphalt mixtures with magnetically responsive materials [9], [25], [26]. This technique consists of producing certain magnetic field signals detectable by sensors installed in the vehicle. Previous studies [9] have already demonstrated that it is possible to codify asphalt materials using metallic particles (preferably with high iron content) and that the code established in this way is sufficiently sensitive to be read from regular magnetic field sensors. As a further step in the development of these encoded materials, the aim of this study is to analyze how pavement-vehicle interaction and vehicle speed influences the AV signal reception.

2. Materials and Methods

2.1. Materials

The capability of an encoded asphalt material to emit a magnetic field signal depends on the type of magnetically responsive material used in its manufacture. A previous study made by the authors [9] confirmed that steel fibres, thanks to their higher iron content, emit better magnetic field signals than steel slags. In this sense, the encoded materials selected for this study were manufactured with various dosages of steel fibres obtained from recycled end-of-life vehicle tires. The signals emitted by these encoded

Leiva-Padilla, P., Moreno-Navarro, F., Iglesias, G., & Rubio-Gamez, M. (2020). Interpretation of the Magnetic Field Signals Emitted by Encoded Asphalt Pavement Materials. *Sustainability*, 12(18), 7300.

DOI: <https://doi.org/10.3390/su12187300>

materials can be detected by sensors installed in vehicles and could act as a form of code to communicate the characteristics of a pavement (maximum speed, left or right turn in carriageway, type of road, etc.) (Figure 1). Therefore, based on this concept, there are unlimited codification possibilities to provide real-time information to the vehicles.

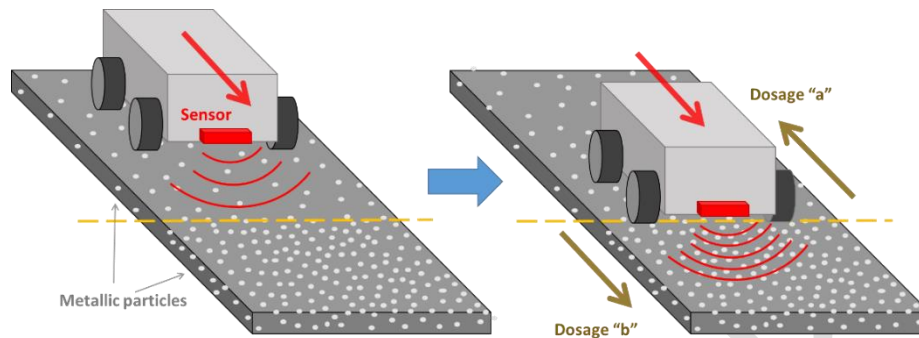


Figure 1. Characteristics of the pavements that can interact with sensors installed in the vehicles.

Figure 2 shows the steel fibers used, which were the smallest sizes obtainable from recycled tire plants. Their average lengths and diameters sizes were among 0.3 cm and 1.0 cm, and 0.15 cm and 0.30 cm, respectively. These fibers were used to manufacture mortar specimens of size 12 cm x 8 cm x 2 cm, with percentages of 5%, 11% and 17% of steel fibers. The size of the steel fibers and the specimens used were selected to represent three main characteristics:

- Firstly, to create elements with a high concentration of steel fibers, which is required for magnetic field detection.
- Secondly, the fabrication of practical elements, which can be easily placed inside the surface course of existing pavements with minimal processing.
- Thirdly, the reduction in fiber grouping during mixing. This was achieved by preheating the fibers and incorporating them after the aggregates but before the asphalt binder in the mixing process. A discontinuous granulometry was used for the asphalt mixture, with fine aggregates (maximum size of 6 mm) and a rich content of asphalt binder (8%).

The asphalt binder used is a B50/70, with a penetration of 65 mm at 25 °C based on the EN 1426, a softening point of 51 °C based on the EN 1427, and a Fraass fragility of -8 °C according to EN 12593.

Leiva-Padilla, P., Moreno-Navarro, F., Iglesias, G., & Rubio-Gamez, M. (2020). Interpretation of the Magnetic Field Signals Emitted by Encoded Asphalt Pavement Materials. *Sustainability*, 12(18), 7300.

DOI: <https://doi.org/10.3390/su12187300>

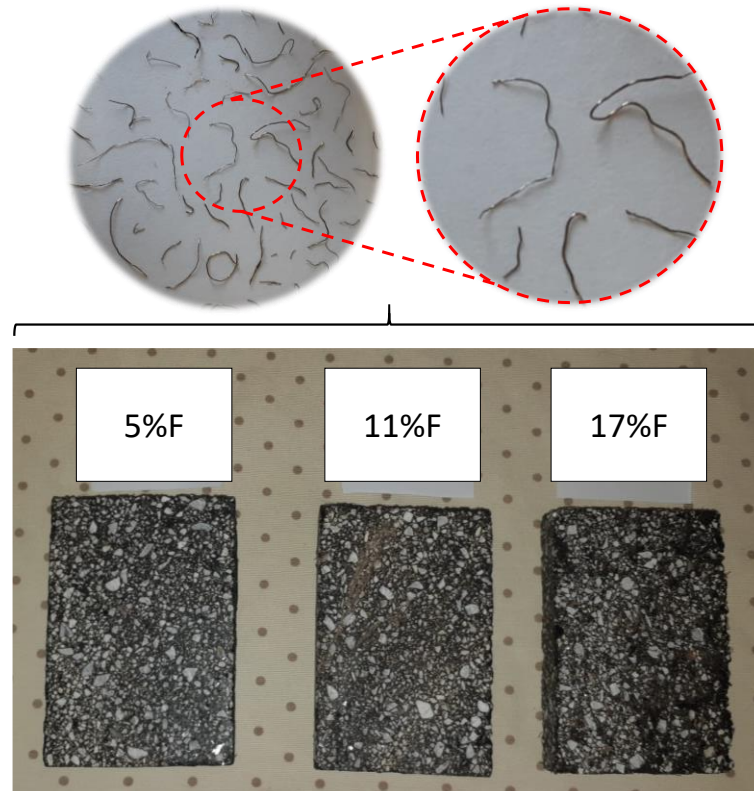


Figure 2. Steel fibres and the encoded asphalt samples used in the study.

2.2. Methods

Given that the encoded asphalt materials are an emerging technology, which is still in the early stages of development, standardized test protocols to evaluate the magnetic signal emitted by these materials are not yet defined. In this sense, and also considering the conditions associated with the use of these materials inside the autonomous vehicle industry (for example, speed of approximation, the proper placement of the sensors, etc), a novel test protocol was designed for this research study.

This test protocol required the design and manufacture of the system as shown in Figure 3, which is composed of three main parts: (1) data measurement device, (2) data acquisition and emission device (via wireless) and (3) data capture and processing software.

Leiva-Padilla, P., Moreno-Navarro, F., Iglesias, G., & Rubio-Gamez, M. (2020). Interpretation of the Magnetic Field Signals Emitted by Encoded Asphalt Pavement Materials. *Sustainability*, 12(18), 7300.

DOI: <https://doi.org/10.3390/su12187300>

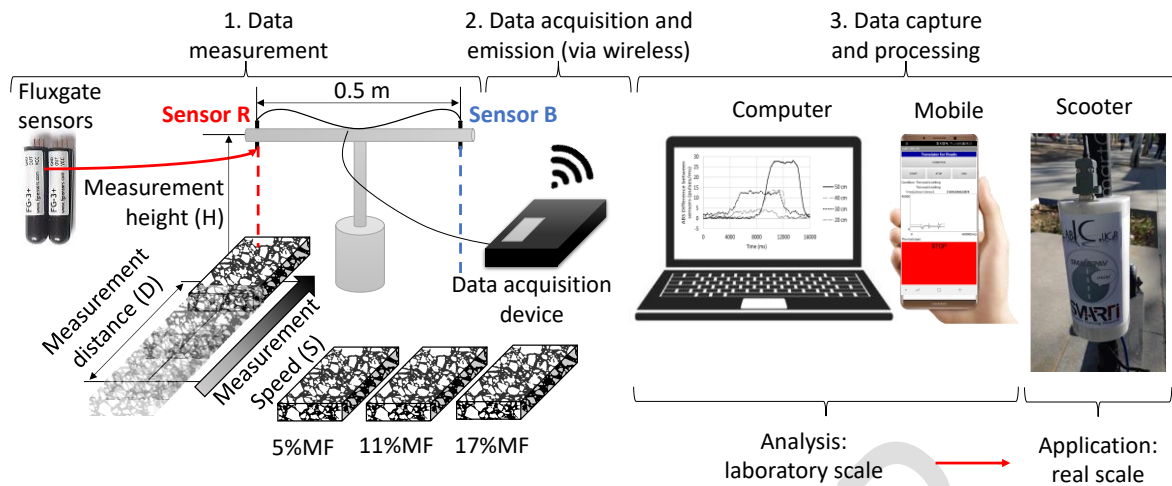


Figure 3. System manufactured for the study.

As shown in Figure 4, the first part consists of a base with two sensors separated at 0.5 m from each other in order to configure a horizontal gradiometer device. This horizontal gradiometer is capable of perceiving the vertical displacement of both sensors, where the field strength of the encoded specimen just in one of them. In this sense, it is possible to isolate the effect of the encoded specimen by scaling the measured values obtained from each sensor. The magnetic field sensors used are fluxgate sensors FG-3+, which operate in the range of ± 50 microteslas. The output is a 5-volt rectangular pulse with a period/frequency directly proportional to the field strength. This device was designed to measure the magnetic field signal emitted by the encoded samples according to three types of analysis shown in Figure 4:

- Analysis 1. Height influence: variation of the magnetic field strength depending on the height ($H = 0.05$ m, 0.1 m, 0.3 m and 0.4 m).
- Analysis 2. Speed influence: variation of the magnetic field strength depending on the approach speed of the encoded sample ($S = 0.1$ m/s, 0.2 m/s and 0.4 m/s).
- Analysis 3. Closer distance influence: variation of the magnetic field strength depending on the closer distance to the sensor (CD). As shown in Figure 4, the CD (dashed lines) depends on the measurement distance (D : Position 1= 0.250 m, Position 2= 0.125 m and Position 3= 0 m) and the height of measurement ($H = 0.1$ m).

Leiva-Padilla, P., Moreno-Navarro, F., Iglesias, G., & Rubio-Gamez, M. (2020). Interpretation of the Magnetic Field Signals Emitted by Encoded Asphalt Pavement Materials. *Sustainability*, 12(18), 7300.

DOI: <https://doi.org/10.3390/su12187300>

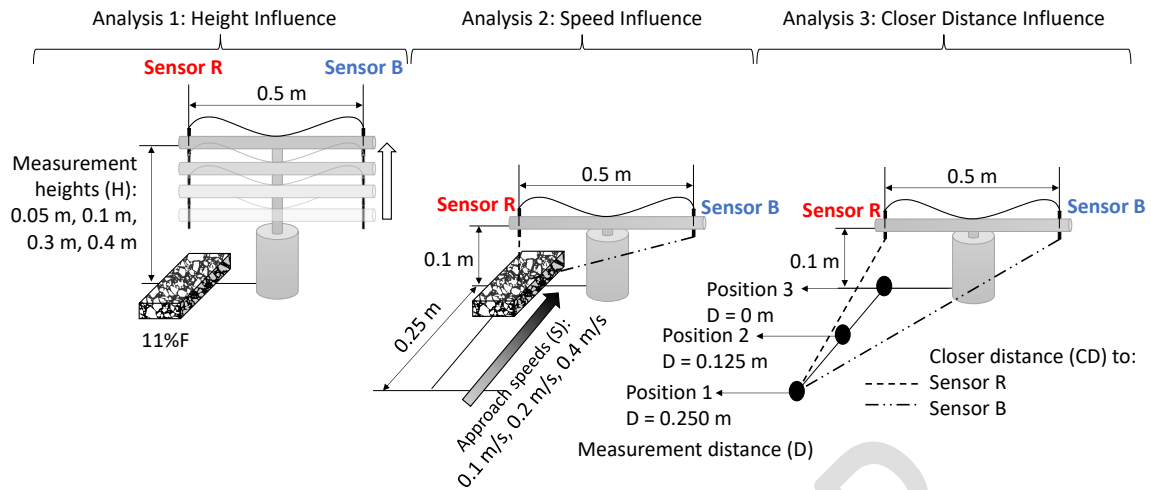


Figure 4. Process of analysis defined for this study

The second part corresponds to the acquisition device responsible for the collection and emission of the data measured by the magnetic field sensors. As can be seen in Figure 5, this device was developed in Arduino, which is characterized to be an open access hardware and software platform, commonly used for the proposal of electronic prototypes addressed to multidisciplinary and multi-technology projects. Due to the range of frequency of the FG-3+ being higher than the range of commonly processed data by the Arduino UNO board, a PCB was designed (printed circuit board) in a shield format, which contains a frequency divisor and a Bluetooth module (Arduino HC06), to ensure the correct measurement of the data, as well as its wireless emission to the third part of the system.

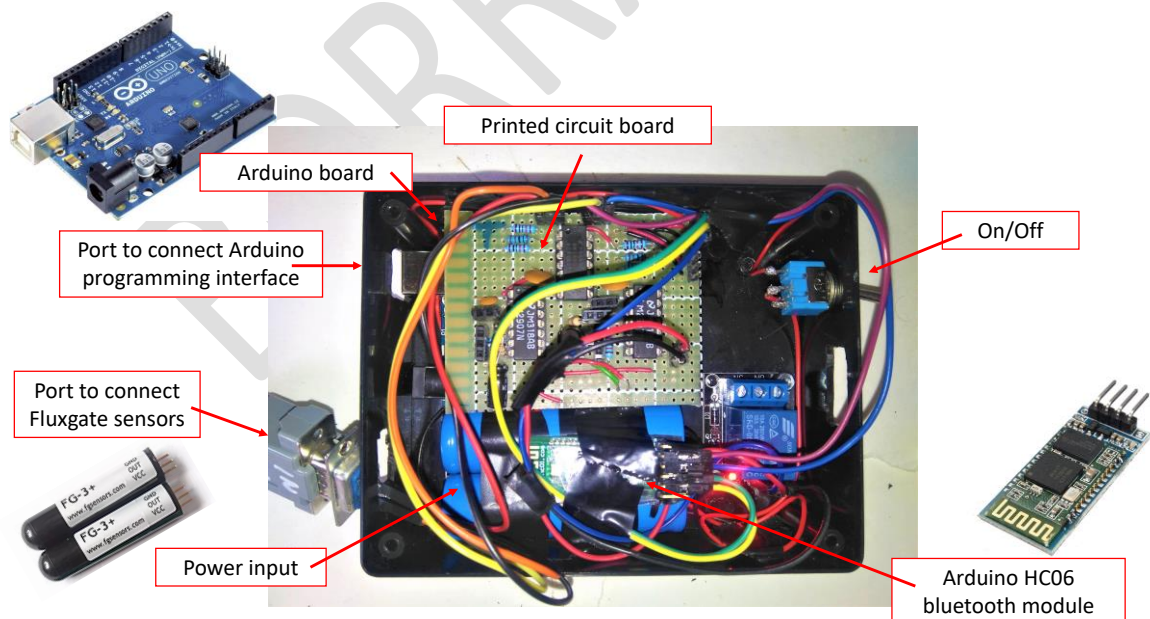
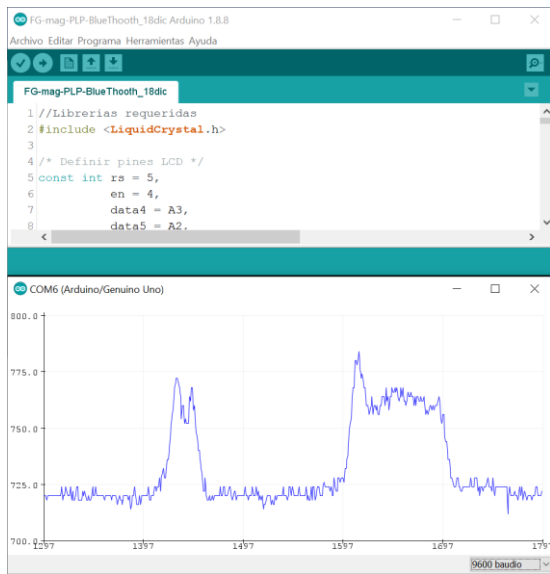


Figure 5. Details of the electronic components of the acquisition device

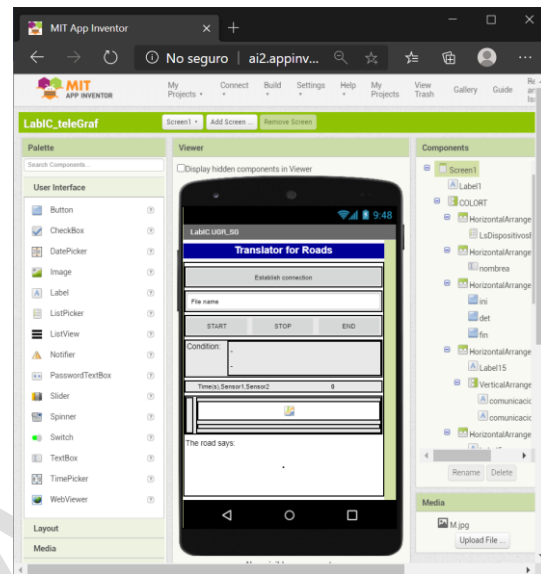
Leiva-Padilla, P., Moreno-Navarro, F., Iglesias, G., & Rubio-Gamez, M. (2020). Interpretation of the Magnetic Field Signals Emitted by Encoded Asphalt Pavement Materials. *Sustainability*, 12(18), 7300.

DOI: <https://doi.org/10.3390/su12187300>

The third part of the system involves the capturing and processing of the data, which will provide the final instructions that are proposed to help vehicle guidance. As shown in Figure 6a, the open-source Arduino Software (IDE) was used to upload instructions to the Arduino UNO board and to extract the data required during the experiment. Additionally, Figure 6b shows a mobile application (LabIC-SG) developed to capture and visualize data. This application was designed and programmed using the MIT App Inventor intuitive, visual programming environment developed by the Massachusetts Institute of Technology (MIT).



(a) Arduino IDE software



(b) MIT APPinventor platform

Figure 6. Software used and created for the data capture and processing

In order to test the functioning of the system, a 4-step proof of concept (PoC) was developed, as shown in Figure 7, for an electric scooter. Step 1, Step 2 and Step 3 are related with the design, manufacture and assembly of the sensor installed in the electric scooter and the test track with the encoded plates. Step 4 is the final stage, which tests the correct functioning of the system.

Leiva-Padilla, P., Moreno-Navarro, F., Iglesias, G., & Rubio-Gamez, M. (2020). Interpretation of the Magnetic Field Signals Emitted by Encoded Asphalt Pavement Materials. *Sustainability*, 12(18), 7300.

DOI: <https://doi.org/10.3390/su12187300>

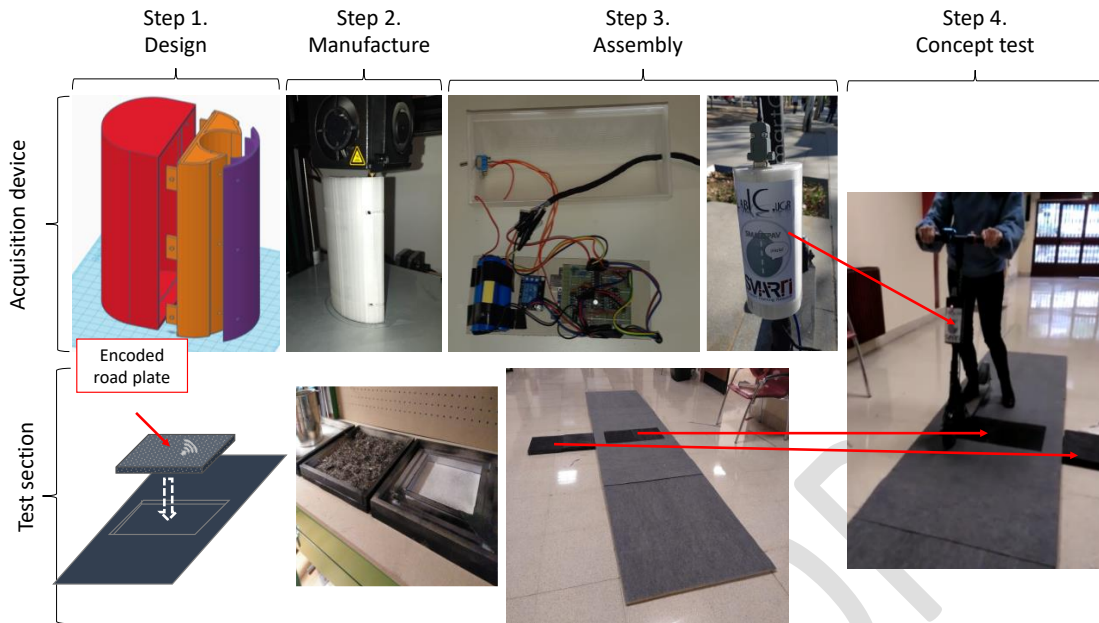


Figure 7. Four-step proof of concept.

3. Results

Figure 8 summarizes the maximum frequencies obtained for the specimen of 11%MF, when the measurement height (H) of the sensor is increased. As can be observed, as H is increased, the frequency of detection (kHz: pulses/ms) in Sensor R is reduced, tending to a constant value of 718 kHz at the highest H (0.4 m) value, which means that the sensor does not recognize the specimen anymore. Therefore, the sensors should be positioned at measurement heights lower than approximately 0.11 m.

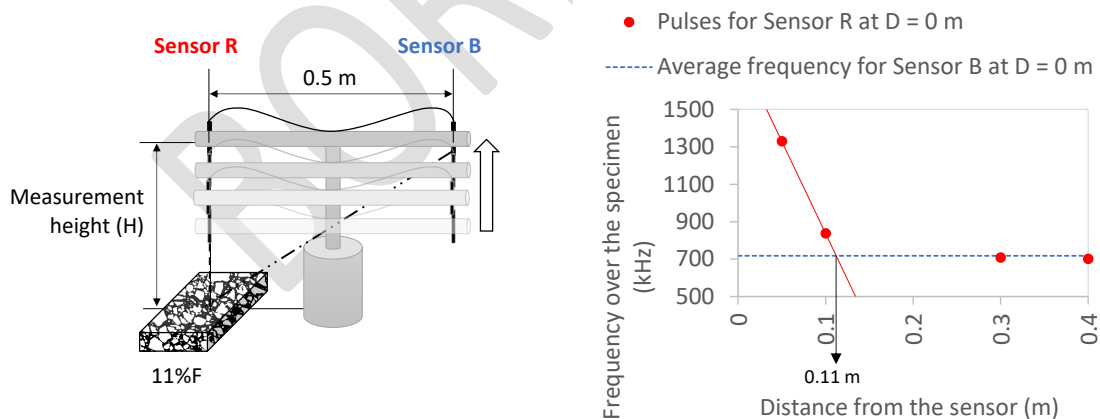


Figure 8. Influence of the measurement height (H).

Figure 9 shows the recorded frequency values at varying approach speeds, with $H = 0.1\text{m}$ and at a measurement distance of 0 m. As can be seen, when the approach speed is increased, the recorded signal between both sensors is reduced. However, the frequencies could be increased by increasing the amount

Leiva-Padilla, P., Moreno-Navarro, F., Iglesias, G., & Rubio-Gamez, M. (2020). Interpretation of the Magnetic Field Signals Emitted by Encoded Asphalt Pavement Materials. *Sustainability*, 12(18), 7300.

DOI: <https://doi.org/10.3390/su12187300>

of magnetic material. It is important to remark that, the values of the frequencies obtained are dependent on the electronic capacities of the sensors used.

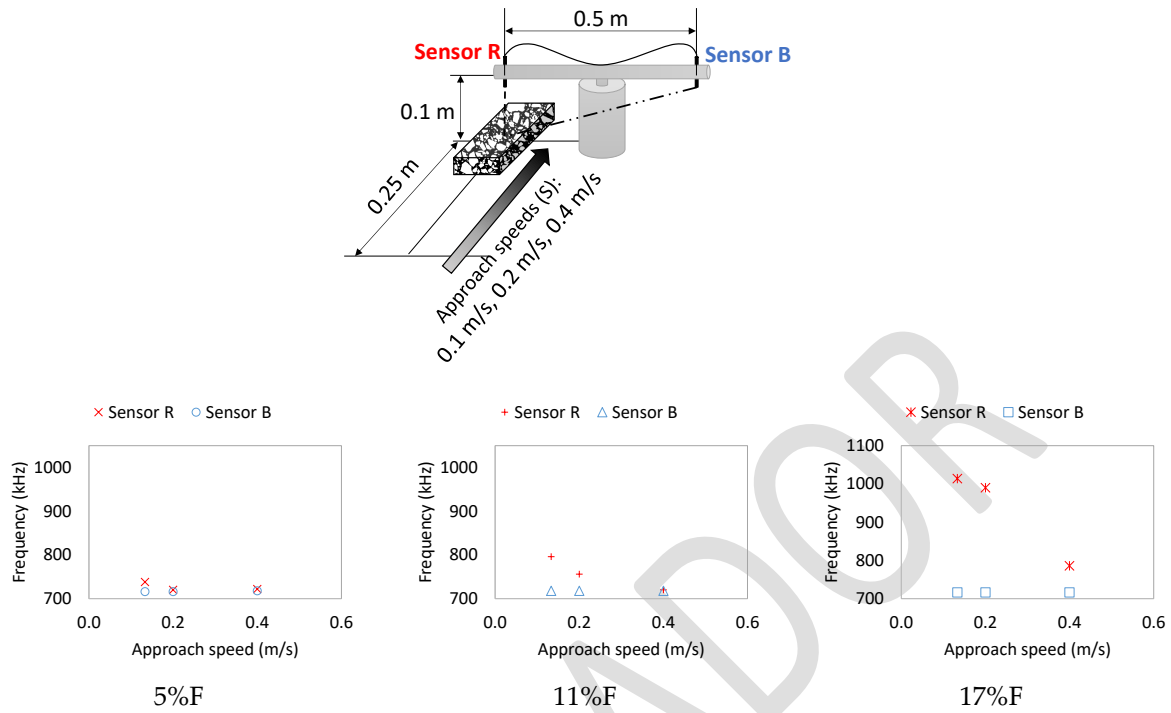


Figure 9. Influence of the measurement speed (S) at measurement distance = 0 m.

Considering the same approach speeds evaluated in Figure 9, and in order to evaluate the capacity of localization of the device, the three specific positions for measuring frequency were selected, as shown in Figure 10. Results showed that, similar to the case of the variation of the measurement height (Figure 8), the closer the specimens are to the sensor (smaller CD), the higher the frequency values obtained. Once again, these values are dependent on the travel speed and the content of steel fibers used in the encoded specimens.

Leiva-Padilla, P., Moreno-Navarro, F., Iglesias, G., & Rubio-Gamez, M. (2020). Interpretation of the Magnetic Field Signals Emitted by Encoded Asphalt Pavement Materials. *Sustainability*, 12(18), 7300.

DOI: <https://doi.org/10.3390/su12187300>

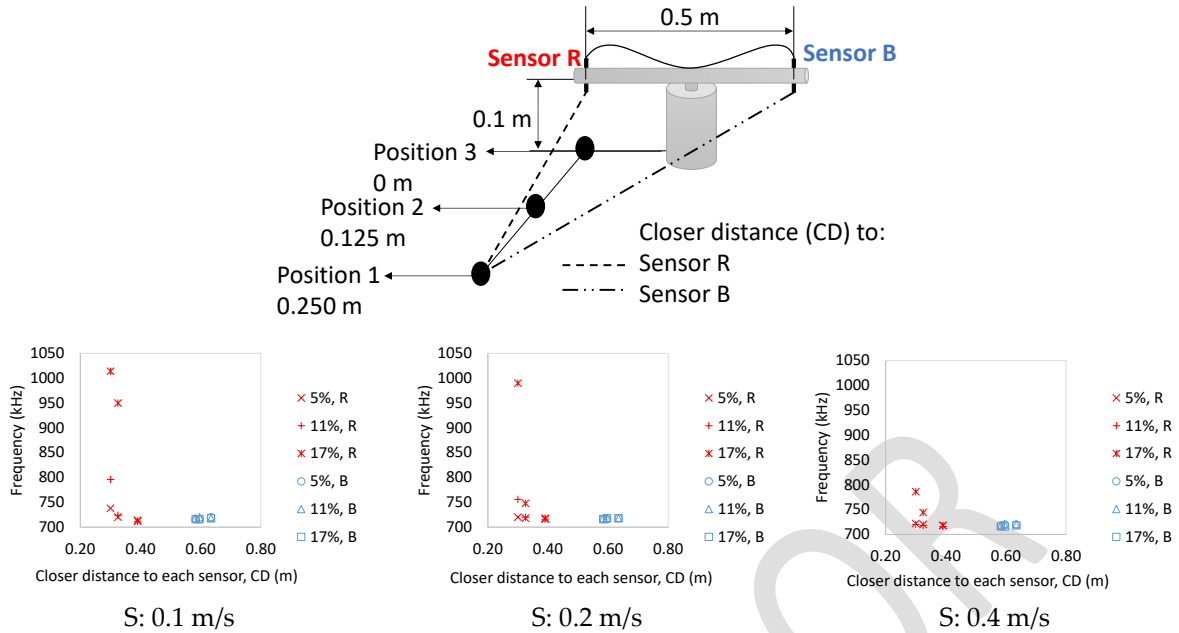


Figure 10. Influence of the closer distance to each sensor.

Finally, an encoded plate with 11%F was manufactured and was placed in the test section to define a proof-of-concept with a binary instruction of activation/deactivation for an electric scooter. As can be seen in Figure 11, over the 740 kHz (3.65 V) the device installed in the scooter sends a high voltage message to deactivate and stop the electric scooter.

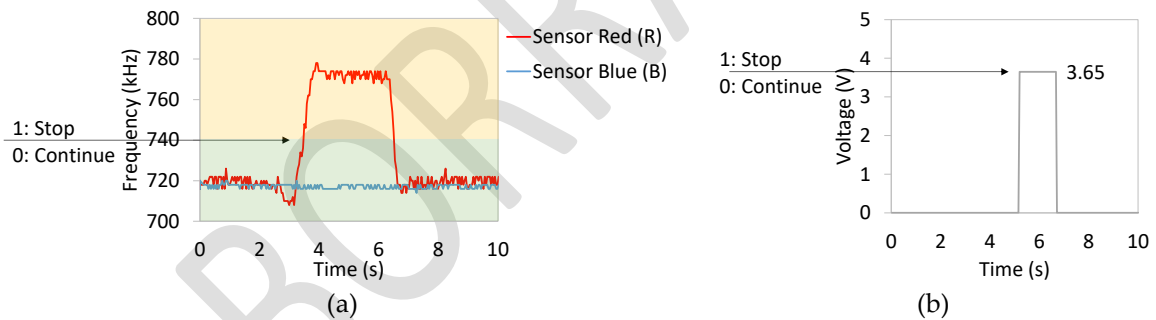


Figure 11. Proof of concept based on binary activation for 11%F.

4. Discussion

In the line with the aim of this study, the results presented have shown that there is an interaction between the encoded asphalt materials and the AV. This interaction is truly influenced by three variables studied, assessed with three different experiments, defined in this study's testing protocol.

In Analysis 1 it was demonstrated that there is a maximum limit related with the placement height of the magnetic field sensors. Over this limit value, the magnetic field sensors placed in the vehicle were not capable of detecting the magnetic field signal emitted by the encoded asphalt materials. Therefore, recognizing that the magnetic field signal of these materials depends on the type and dosage of the

Leiva-Padilla, P., Moreno-Navarro, F., Iglesias, G., & Rubio-Gamez, M. (2020). Interpretation of the Magnetic Field Signals Emitted by Encoded Asphalt Pavement Materials. *Sustainability*, 12(18), 7300.

DOI: <https://doi.org/10.3390/su12187300>

magnetically responsive material used in their manufacture [9], as well as, the detection capacity of the magnetic field sensors [27]–[29], the limit of this variable could be readjusted according to the requirements of the system.

In the Analysis 2 it was shown that, as the approach speed of the encoded specimen increases (which in real life would be the approach speed of the vehicle), the detection capacity of the magnetic field sensors is decreased. However, and aligned with the discussion of Analysis 1, it was confirmed that with a higher dosage of magnetically responsive material, the encoded asphalt materials' capacity to be detected by the magnetic field sensors was better.

In the Analysis 3 it was determined that inside a distance of 0.4 m around the magnetic field, the signal of the encoded asphalt samples started to be detected. This means that there is an area of influence and time of detection before and after passing over the encoded area.

Finally, as a step towards the possible use of this technology in a real scale application, the end of the results section showed a successful implementation of a PoC developed with these materials. This achievement validates the use of encoded asphalt pavements for enhancing vehicle-infrastructure transit, which could have significant safety and operational benefits for AVs.

In this context, encoded asphalt materials could prove to be one of the required strategies to help increase the reliability of AV implementation. Road conditions, for example traffic accidents, works on public roadways, environmental conditions, etc., are part of the challenges proposed to be addressed by Level 3 and 4 in the scale of automation of the United States National Highway Traffic Safety Administration [30]. Therefore, keeping in mind that important investments and efforts that have been made by automotive manufacturers and information technology companies over the last few years, the development of more research related to the communication road-to-vehicle is still necessary to contribute to a real success in the implementation of AV. For example, and specifically related to encoded asphalt materials, further research could address the evaluation of the external noise in the signal, other materials that could potentially be used in the modification of the road, or alternative devices that can produce similar signals during their installation (i.e. electromagnets, plates with high density of magnetically responsive materials, etc.).

5. Conclusions

The present paper represents an additional step within a research project aiming to develop a new generation of encoded asphalt materials which could be used for the guidance of autonomous vehicles. Based on the results obtained, the following conclusions can be drawn:

- The magnetic field signal emitted by encoded asphalt materials depends on the height of placement of the sensor, the vehicle approach speed and horizontal distance of the encoded asphalt specimens.
- A proof-of-concept validates the possible use of the encoded asphalt materials inside the required protocols to reach a more reliable implementation of AVs. This tool could be used in future work related to the development of this technology.
- Encoded asphalt materials, and their associated technologies, could greatly support road-to-vehicle communications and better help the successful implementation of AVs.

Supplementary Materials: There are no supplementary materials for this paper.

Author Contributions: All authors have contributed to the current paper. Conceptualization, Paulina Leiva-Padilla, Fernando Moreno-Navarro and Guillermo Iglesias; Formal analysis, Paulina Leiva-Padilla; Funding acquisition, Fernando Moreno-Navarro and M^a Carmen Rubio-Gamez; Investigation, Paulina Leiva-Padilla, Fernando Moreno-

Leiva-Padilla, P., Moreno-Navarro, F., Iglesias, G., & Rubio-Gamez, M. (2020). Interpretation of the Magnetic Field Signals Emitted by Encoded Asphalt Pavement Materials. *Sustainability*, 12(18), 7300.

DOI: <https://doi.org/10.3390/su12187300>

Navarro, Guillermo Iglesias and M^a Carmen Rubio-Gamez; Methodology, Paulina Leiva-Padilla, Fernando Moreno-Navarro and Guillermo Iglesias; Project administration, Fernando Moreno-Navarro and M^a Carmen Rubio-Gamez; Resources, Fernando Moreno-Navarro; Supervision, Fernando Moreno-Navarro and Guillermo Iglesias; Writing – original draft, Paulina Leiva-Padilla; Writing – review & editing, Fernando Moreno-Navarro and M^a Carmen Rubio-Gamez. All authors have read and agreed to the published version of the manuscript.

Funding: The research presented in this paper was carried out as part of the H2020-MSCA-ETN-2016. This project has received funding from the European Union's H2020 Programme for research, technological development, and demonstration under grant agreement number 721493.

Conflicts of Interest: The authors declare no conflict of interest. The funders had no role in the design of the study; in the collection, analyses, or interpretation of data; in the writing of the manuscript, or in the decision to publish the results.

References

1. M.-K. Kim, J.-H. Park, J. Oh, W.-S. Lee, and D. Chung, "Identifying and prioritizing the benefits and concerns of connected and autonomous vehicles: A comparison of individual and expert perceptions," *Res. Transp. Bus. Manag.*, p. 100438, Mar. 2020.
2. S. A. Bagloee, M. Tavana, M. Asadi, and T. Oliver, "Autonomous vehicles: challenges, opportunities, and future implications for transportation policies," *J. Mod. Transp.*, 2016.
3. C. Hohenberger, M. Spörrle, and I. M. Welpel, "Not fearless, but self-enhanced: The effects of anxiety on the willingness to use autonomous cars depend on individual levels of self-enhancement," *Technol. Forecast. Soc. Change*, vol. 116, pp. 40–52, Mar. 2017.
4. M. König and L. Neumayr, "Users' resistance towards radical innovations: The case of the self-driving car," *Transp. Res. Part F Traffic Psychol. Behav.*, vol. 44, pp. 42–52, Jan. 2017.
5. D. Howard, "Public Perceptions of Self-driving Cars: The Case of Berkeley, California," *MS Transp. Eng.*, 2014.
6. P. Bansal, K. M. Kockelman, and A. Singh, "Assessing public opinions of and interest in new vehicle technologies: An Austin perspective," *Transp. Res. Part C Emerg. Technol.*, vol. 67, pp. 1–14, Jun. 2016.
7. Y. Ro and Y. Ha, "A Factor Analysis of Consumer Expectations for Autonomous Cars," *J. Comput. Inf. Syst.*, vol. 59, no. 1, pp. 52–60, 2019.
8. J. Van Brummelen, M. O'Brien, D. Gruyer, and H. Najjaran, "Autonomous vehicle perception: The technology of today and tomorrow," *Transp. Res. Part C Emerg. Technol.*, vol. 89, pp. 384–406, Apr. 2018.
9. F. Moreno-Navarro, G. R. Iglesias, and M. C. Rubio-Gámez, "Encoded asphalt materials for the guidance of autonomous vehicles," *Autom. Constr.*, vol. 99, pp. 109–113, Mar. 2019.
10. D. Fényes, B. Németh, P. Gáspár, and M. Asszonyi, "Possibilities of vehicle state estimation using big data approaches," in *Proceedings of the Mini Conference on Vehicle System Dynamics, Identification and Anomalies*, 2019, vol. 2019-Novem, pp. 395–401.
11. C. S. Arvind and J. Senthilnath, *Autonomous Vehicle for Obstacle Detection and Avoidance Using Reinforcement Learning*, vol. 1048. 2020.
12. J. Guo et al., "A Novel Method of Radar Modeling for Vehicle Intelligence," *SAE Int. J. Passeng. Cars - Electron. Electr. Syst.*, vol. 10, no. 1, 2017.
13. S. Lee et al., "Intelligent traffic control for autonomous vehicle systems based on machine learning," *Expert Syst. Appl.*, vol. 144, p. 113074, Apr. 2020.
14. P. Koopman and M. Wagner, "Autonomous Vehicle Safety: An Interdisciplinary Challenge," *IEEE Intell. Transp. Syst. Mag.*, vol. 9, no. 1, pp. 90–96, 2017.
15. O. Grembek, A. Kurzhanskiy, A. Medury, P. Varaiya, and M. Yu, "Making intersections safer with I2V communication," *Transp. Res. Part C Emerg. Technol.*, vol. 102, pp. 396–410, May 2019.

Leiva-Padilla, P., Moreno-Navarro, F., Iglesias, G., & Rubio-Gamez, M. (2020). Interpretation of the Magnetic Field Signals Emitted by Encoded Asphalt Pavement Materials. *Sustainability*, 12(18), 7300.

DOI: <https://doi.org/10.3390/su12187300>

16. A. S. M. Bakibillah, M. A. S. Kamal, C. P. Tan, T. Hayakawa, and J.-I. Imura, "Event-Driven Stochastic Eco-Driving Strategy at Signalized Intersections from Self-Driving Data," *IEEE Trans. Veh. Technol.*, vol. 68, no. 9, pp. 8557–8569, 2019.
17. A. Buzachis, A. Celesti, A. Galletta, M. Fazio, G. Fortino, and M. Villari, "A multi-agent autonomous intersection management (MA-AIM) system for smart cities leveraging edge-of-things and Blockchain," *Inf. Sci. (Ny)*, vol. 522, pp. 148–163, Jun. 2020.
18. H. Teng et al., "A novel code data dissemination scheme for Internet of Things through mobile vehicle of smart cities," *Futur. Gener. Comput. Syst.*, vol. 94, pp. 351–367, May 2019.
19. H. Teng, W. Liu, T. Wang, A. Liu, X. Liu, and S. Zhang, "A Cost-Efficient Greedy Code Dissemination Scheme Through Vehicle to Sensing Devices (V2SD) Communication in Smart City," *IEEE Access*, vol. 7, pp. 16675–16694, 2019.
20. H. Teng, W. Liu, T. Wang, X. Kui, S. Zhang, and N. N. Xiong, "A Collaborative Code Dissemination Schemes through Two-Way Vehicle to Everything (V2X) Communications for Urban Computing," *IEEE Access*, vol. 7, pp. 145546–145566, 2019.
21. M. M. A. Momen, H. A. Fayed, M. H. Aly, N. E. Ismail, and A. Mokhtar, "An efficient hybrid visible light communication/radio frequency system for vehicular applications," *Opt. Quantum Electron.*, vol. 51, no. 11, 2019.
22. M. A. Vieira, M. Vieira, P. Louro, and P. Vieira, "Cooperative vehicular communication systems based on visible light communication," *Opt. Eng.*, vol. 57, no. 7, 2018.
23. Y. H. Kim and Y. H. O. Chung, "Experimental demonstration of highway I2V using visible light communications," *Appl. Opt.*, vol. 55, no. 22, pp. 5840–5845, 2016.
24. R. A. Gheorghiu, I. Bădescu, and R. S. Timnea, "Infrastructure to vehicle communications using inductive loops," *WSEAS Trans. Commun.*, vol. 13, pp. 596–605, 2014.
25. P. Leiva-Padilla, F. Moreno-Navarro, G. R. Iglesias, and M. C. Rubio-Gómez, "Analysis of the mechanical response of asphalt materials manufactured with metallic fibres under the effect of magnetic fields," *Smart Mater. Struct.*, 2019.
26. P. Leiva-Padilla, F. Moreno-Navarro, and G. Iglesias, "A Review of the Contribution of Mechanomutable Asphalt Materials Towards Addressing the Upcoming Challenges of Asphalt Pavements," *Infrastructures*, 2020.
27. J. Li, Y. Wang, X. Zhang, C. Ji, and J. Shi, "Sensitivity and Resolution Enhancement of Coupled-Core Fluxgate Magnetometer by Negative Feedback," *IEEE Trans. Instrum. Meas.*, 2019.
28. M. Zhi, L. Tang, and D. Qiao, "Design and analysis of miniature tri-axial fluxgate magnetometer," *Mod. Phys. Lett. B*, vol. 31, no. 5, 2017.
29. D. Rühmer, P. Shanmuganathan, F. Ludwig, and M. Schilling, "Spatial and field resolution of wire-wound fluxgates in magnetic dipole fields," *Sensors Actuators, A Phys.*, 2012.
30. NHTSA, "Preliminary Statement of Policy Concerning Automated Vehicles," 2013.



© 2020 by the authors. Submitted for possible open access publication under the terms and conditions of the Creative Commons Attribution (CC BY) license (<http://creativecommons.org/licenses/by/4.0/>).

Anexo 4. “Thermal characterization of electroconductive layers for anti-icing and de-snowing applications on roads”.

Este anexo contiene **la carta de aceptación del artículo**: "Thermal characterization of electroconductive layers for anti-icing and de-snowing applications on roads", que pronto será publicado en el Journal "Road Materials and Pavements Design" (JIF: 2.582, JCR: Q2 en categorías "Construction & Building Technology", "Engineering, Civil", "Materials Science, Multidisciplinary" y "Engineering").

Este documento corresponde al **tercer artículo de este compendio** y desarrolla el tercer objetivo definido para esta tesis doctoral:

Determinar los cambios de temperatura que pueden ser producidos por la activación de campos magnéticos variables, en morteros asfálticos confeccionados con diferentes contenidos de materiales electroconductivos, como mecanismo para la transferencia de temperatura al pavimento.

Leiva-Padilla, P., Moreno-Navarro, F., Iglesias-Salto, G., & Rubio-Gamez, M. C. (2020). Thermal characterization of electroconductive layers for anti-icing and de-snowing applications on roads. *Road Materials and Pavements Design*, (por publicar).

DOI: por publicar.

18/9/2020

Webmail UGR - Road Materials and Pavement Design - Decision on Manuscript ID RMPD-19-12-36.R3

Asunto Road Materials and Pavement Design - Decision on Manuscript ID RMPD-19-12-36.R3
De Road Materials and Pavement Design
<onbehalf@manuscriptcentral.com>
Destinatario <pleiva@ugr.es>
Responder a <gtebaldi@unipr.it>
Fecha 2020-09-17 21:28



Ref: Thermal characterization of electroconductive layers for anti-icing and de-snowing applications on roads

Dear Mrs Leiva-Padilla,

our reviewers considered your answers and they checked the adjustments that you made on your paper and following their recommendations it is now accepted in the present form for publication in Road Materials and Pavement Design. We are pleased to inform you that it will now be forwarded to the publisher for copy editing and typesetting.

You will receive proofs for checking, and instructions for transfer of copyright in due course.

The publisher also requests that proofs are checked through the publisher's tracking system and returned within 48 hours of receipt.

Thank you for your contribution to Road Materials and Pavement Design and we look forward to receiving further submissions from you.

Sincerely,

Professor Gabriele Tebaldi
Editor in Chief of Road Materials and Pavement Design
gtebaldi@unipr.it

Anexo 5. "Recovery capacity of electroconductive asphalt mortars under the influence of magnetic fields".

Este anexo contiene la **versión del manuscrito preparado por la autora** y que fue publicado en el Journal “*Materials Today Communications*” (JIF: 2.678, JCR: Q2 en categoría “Materials Science, Multidisciplinary”). El acceso al documento publicado, debe realizarse a través del DOI de la publicación: <https://doi.org/10.1016/j.mtcomm.2020.101527>

Este documento corresponde al **cuarto artículo de este compendio** y desarrolla el tercer objetivo definido para esta tesis doctoral:

Determinar los cambios de temperatura que pueden ser producidos por la activación de campos magnéticos variables, en morteros asfálticos confeccionados con diferentes contenidos de materiales electroconductivos, como mecanismo para la transferencia de temperatura al pavimento.

Leiva-Padilla, P., Moreno-Navarro, F., Iglesias-Salto, G., & Rubio-Gamez, M. C. (2020). Recovery capacity of electroconductive asphalt mortars under the influence of magnetic fields. *Materials Today Communications*, 101527.

DOI: <https://doi.org/10.1016/j.mtcomm.2020.101527>

Recovery capacity of electroconductive asphalt mortars under the influence of magnetic fields

P. Leiva-Padilla¹, F. Moreno-Navarro², G. Iglesias-Salto³ and M. C. Rubio-Gamez⁴

¹pleiva@ugr.es, Laboratory of Construction Engineering of the University of Granada (LabIC.UGR), Granada, Spain.

²fmoreno@ugr.es, Laboratory of Construction Engineering of the University of Granada (LabIC.UGR), Granada, Spain.

³iglesias@ugr.es, Department of Applied Physics of the University of Granada, Granada, Spain.

⁴mcrubio@ugr.es, Laboratory of Construction Engineering of the University of Granada (LabIC.UGR), Granada, Spain.

P. Leiva Padilla (pleiva@ugr.es)

Abstract.

The self-healing capacity of electroconductive asphalt materials can be enhanced by the use of induction heating. The highest enhancement of this self-healing capacity is produced in the early stages of the fatigue life of the material. During the early stages of the fatigue life, micro-cracks appear in the mastics/mortars that compose the asphalt mixture. In this sense, by the use of micromechanics, it could be possible to study the mastics/mortars to characterize the healing performance of asphalt mixtures under induction heating treatments. This study evaluates the recovery capacity of electroconductive asphalt mortars (EM), after multiple applications of induction heating and rest periods. In order to use a representation of materials that can be produced on-site, the EM were manufactured with the smallest sizes of metallic fibres obtained from the recycling process of vehicle tires at the end of their useful life. Results showed that half of the recovery capacity of the EM was produced by the effect of induction heating and the remainder by the effect of rest periods. This recovery capacity generates an extension in the fatigue life of the EM, which along with the use of a high asphalt content (higher than 7%) and fine aggregates (less than 9.5 mm), provides the conditions to use the EM in the construction of interlayer systems. The use of EM as interlayer systems, additionally to delay the reflection of cracks in the surface layers of the pavement, seems to represent a safe strategy to introduce their use on-site.

Keywords: electroconductive asphalt mortars; rest periods; induction heating; enhanced healing capacity

5. Introduction

One of the main distresses suffered by flexible pavements during their service life is in the form of fatigue cracking. These appear as a result of the dynamic demands of traffic and the road's external environment, particularly due to temperature and moisture changes. The application of appropriate and effective maintenance strategies designed to prevent or delay the time required for cracks to appear in the surface layer, can extend the service life of the road and reduce the asset's long-term economic costs, regarding the number of maintenance actions and the need for road closures.

The fatigue failure mechanism for the surface layer of asphalt pavements can be explained through a three-phase sequence. In Phase 1 the stiffness of the material decreases rapidly via biased effects (non-linearity, heating, and thixotropy), in Phase 2 micro-cracks appear as a consequence of fatigue damage produced by

Leiva-Padilla, P., Moreno-Navarro, F., Iglesias-Salto, G., & Rubio-Gamez, M. C. (2020). Recovery capacity of electroconductive asphalt mortars under the influence of magnetic fields. *Materials Today Communications*, 101527.

DOI: <https://doi.org/10.1016/j.mtcomm.2020.101527>

traffic and weather conditions as temperature changes and ageing, and in Phase 3 the micro-cracks grow and gradually interconnect to generate the macro-cracks, resulting in the failure of the material [1][2][3].

Modern self-repairing/self-healing maintenance strategies [4], [5] employed to repair pavement cracks have focused on considering the natural self-repairing/self-healing capacity of the asphalt materials [6], to extend the service life of the flexible pavement. The self-repairing/self-healing capacity of a material can be defined as “the ability to substantially return to an initial, proper operating state or condition prior to the exposure to a dynamic environment by making the necessary adjustments to restore to normality and/or the ability to resist the formation of irregularities and/or defects” [7].

It has been demonstrated that asphalt mixtures have the capacity to recover part of their initial structural conditions under the application of rest periods prior to the appearance of significant damage in the pavement can be considered a self-healing [8]–[11]. In fact, it has been observed that the cracks developed during winter can disappear by summer, due to the softening of the asphalt caused by higher temperatures [12]. In this sense, rest period and temperature have been found to be the most influential conditions associated with the self-healing of asphalt mixtures [4]. These key variables have been the basis of previous research work, where it has been found that the self-healing capacity of asphalt mixtures can actually be artificially enhanced by the application of heat by induction [13]–[15] and microwaves [13], [14], [16].

In the case of induction heating, the asphalt materials should be modified with imbedded electrically conductive materials. Electrically conductive materials in presence of a time-varying magnetic fields, produced by alternating current, have the capacity to develop Foucault currents, and consequently energy losses in the form of heat, via the Joule effect [17]. In order to propose suitable temperature conditions for the healing of cracks, some previous studies [18], [19] found that the optimal temperatures to heal fatigue damage is at the asphalt binder’s softening point temperature. The softening point temperature has been defined for some studies [18], as the transition temperature where the viscosity of the material characterizes a near-Newtonian fluid behaviour. Therefore the asphalt is able to move and fill the cracks, via capillarity flow [18][20]–[22].

Mechanomutable Asphalt Materials (MAMs) is a recent term given to asphalt materials modified with magnetically and electrically responsive materials (MERMs), under the effect of magnetic fields [23]–[25]. MERMs already used to modify asphalt materials include carbon fibres, steel fibres, steel wool, graphite, graphene, carbon black, steel slag, carbonyl iron powder, ferrite, magnetite, and conductive polymer polyaniline [6], [15], [23], [25]–[32]. Firstly, studies specifically related with the evaluation of MAMs were addressed to consider the changes in the dynamic modulus produced when a stress field is generated in the internal structure of the MAMs by the movement of ferromagnetic attracted by static magnetic fields [23], [24], [33]. Subsequently, other studies with the same materials are trying to propose them to encode the roads, in order to use them to help in a safer implementation of the autonomous vehicles [34].

However, these studies have been focused on exploring the healing capacity of asphalt mixtures and mastics. Recognizing that fatigue cracks propagate through the asphalt mortar and failure rarely occurs in the aggregate, this study focuses on the analysis of the healing capacity of Electroconductive Asphalt Mortars (EM) subjected to fatigue failure tests and treated with multiple cycles of induction heating and rest periods.

The EM studied get their electroconductive properties via the use of metallic fibres obtained from the end of life vehicle tires. The use of this type of steel fibres along to promote the use of recycling practices and cheaper solutions of manufacturing, intends to consider the smallest particle sizes obtained from the end

Leiva-Padilla, P., Moreno-Navarro, F., Iglesias-Salto, G., & Rubio-Gamez, M. C. (2020). Recovery capacity of electroconductive asphalt mortars under the influence of magnetic fields. *Materials Today Communications*, 101527.

DOI: <https://doi.org/10.1016/j.mtcomm.2020.101527>

processing of these materials in recycling plants. All this with the purpose to propose practical solutions to make possible the use of steel fibres on-site.

Aligned with the aim to propose practical solutions, the EM studied were enriched with asphalt to help in the manufacturing process of these materials and to provide an asphalt layer with the characteristics of a moisture barrier and stress relief system. The strategic placement of these kinds of systems as intermediate layers inside the asphalt layers of the pavement, are ideal to avoid the sharp and pointy characteristic of the steel fibres at the surface of the pavement.

6. Methodology

6.1. Materials

As is shown in Figure 1, the mortars studied in this work are considered to be a dense mixture (sand-bitumen type), with a sand maximum particle size of 6 mm. The asphalt binder used was a B50/70, with a penetration of 65 mm at 25 °C based on the EN 1426, a softening point of 51 °C based on the EN 1427, and a Fraass fragility of -8 °C according to EN 12593. In order to produce a mortar with a high content of binder, with the aim to build an intermediate layer that can delay the propagation of cracks to the surface of the pavement, the proportion of binder used was 7% over the total weight of the mixture.

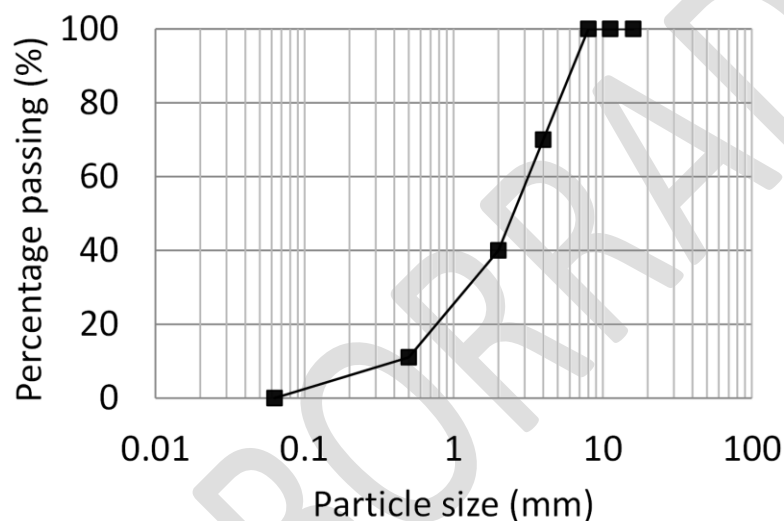


Figure 1. Granulometric curve of the EM studied

The study considered the evaluation of the mortars without and with metallic fibres obtained from recycled end-of-life vehicle tires, with the aim to promote recycling practices in the construction of flexible pavements. In order to ensure the most homogeneous size distribution between the solid materials in the mortar and the metallic fibres, the recycling plant was requested to process them to the smallest size possible. As shown in Figure 2 from taking a sample of 50 metallic fibres obtained from this plant, an average length of 4.8 mm (coefficient of variation: 4.8 mm), with an average diameter of 0.3 mm (coefficient of variation: 0.3 mm) was obtained. The length and the diameter of each fibre were recorded through the analysis of a scaled (with a calliper) microscope-produced image.

Leiva-Padilla, P., Moreno-Navarro, F., Iglesias-Salto, G., & Rubio-Gamez, M. C. (2020). Recovery capacity of electroconductive asphalt mortars under the influence of magnetic fields. *Materials Today Communications*, 101527.

DOI: <https://doi.org/10.1016/j.mtcomm.2020.101527>

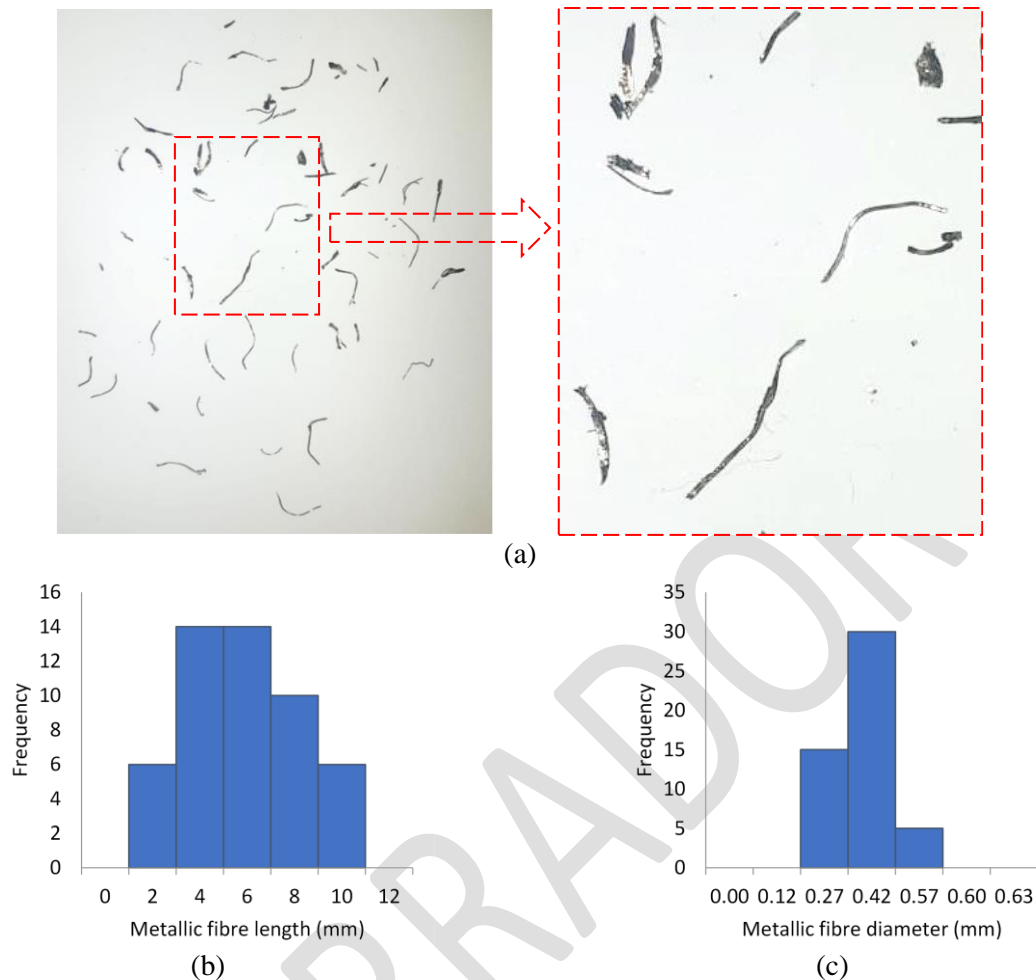


Figure 2. Metallic fibres obtained from the selected tire recycling plant (a) sample, (b) length and (c) diameter

The corresponding proportion of fibres added was 5% by weight substitution of the aggregate, by following recommendations obtained in previous studies [35] and verified during the manufacturing process of this study, to avoid the inhomogeneous distribution of fibres. The metallic fibres were preheated and mixed with the aggregates during the manufacturing process in order to avoid heat loss, as well as, the grouping of fibres during mixing. The mixture obtained was compacted to reach ~0% air voids using a gyratory compactor to produce a cylinder of 100 mm in diameter and 40 mm in height.

The cylinder was cut into 8.6 ± 1 mm wide slices, as shown in Figure 3. Due to the slices varying in length and also considering that the samples should be taken from the area inside the cylinder, each picture was then cut into areas of 30 mm x 90 mm (blue border square in Figure 3). The distribution of the metallic fibres was then verified, via the image processing shown in Figure 4. This consisted in scaling the image to digitalize the x and y position of each metallic fibre. As it is also shown in Figure 4, the content of metallic fibres in the surface of the slices vary from 84 to 114, with an average value of 96 and a coefficient of variation of 13%, which means the distribution of the metallic fibres can be considered homogenous inside the cylinder.

Leiva-Padilla, P., Moreno-Navarro, F., Iglesias-Salto, G., & Rubio-Gamez, M. C. (2020). Recovery capacity of electroconductive asphalt mortars under the influence of magnetic fields. *Materials Today Communications*, 101527.

DOI: <https://doi.org/10.1016/j.mtcomm.2020.101527>

Finally, as shown in Figure 3, the 8.6 mm slices were cut into prismatic specimens with dimensions of 8.6 ± 1 mm x 8.6 ± 1 mm x 50 ± 1 mm. The dimensions of the specimens were selected by following the recommendations of the producer of the equipment of testing, which is a Dynamic Mechanical Analyser (DMA), and ASTM D4065, which mentions a length of at least 50 mm for the thickness and a width that depends on the complex modulus of the material. In this sense, after initial tests and also considering the length size of the metallic fibres, 8.6 mm was selected as the 90th percentile, for the length and width of the specimen.

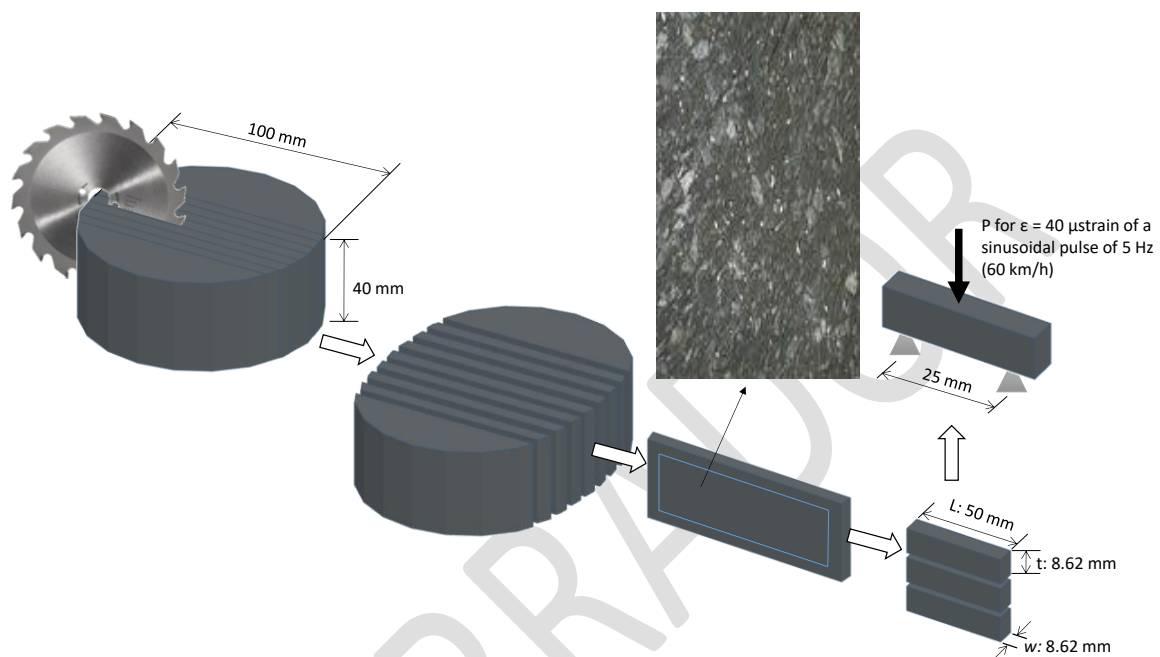


Figure 3. Cutting process of the specimens studied

Leiva-Padilla, P., Moreno-Navarro, F., Iglesias-Salto, G., & Rubio-Gamez, M. C. (2020). Recovery capacity of electroconductive asphalt mortars under the influence of magnetic fields. *Materials Today Communications*, 101527.

DOI: <https://doi.org/10.1016/j.mtcomm.2020.101527>

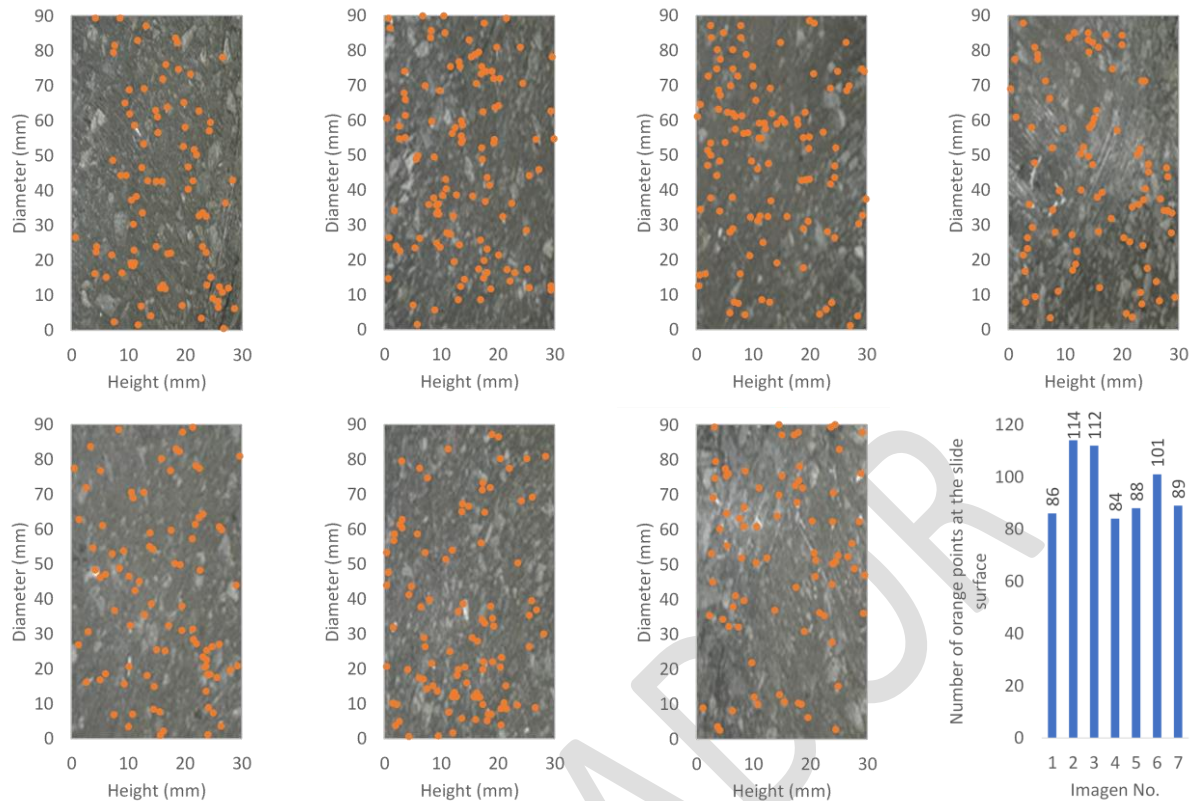


Figure 4. Distribution of the metallic fibres on the surface of 8.6 mm width slices obtained from the Superpave compacted cylinder.

6.2. Methods

6.2.1. Equipment and configuration used during testing

In order to follow the aim of the study, a Dynamic Mechanical Analyser (DMA, Figure 5) equipment was used to evaluate the mechanical properties of the EM of this study. The DMA is an equipment designed to evaluate the mechanical properties of plastics, elastomers-rubber, composites, fibres-textiles, and metals, through using specimens of small sizes, which means reductions in costs of the experimental plan. This equipment has been used in previous studies to evaluate the asphalt mixtures [36]–[39], from the evaluation of asphalt mastics and mortars. Particularly in this study, the DMA was used in a fatigue 3-point bending beam mode of load, under two configurations of testing, at a constant temperature of 35°C. Both configurations of testing are explained step by step in the following sections.

Figure 6a shows the induction heating system setup used. The working frequency resulted from the coupling between the conductors and the capacitors of this system was 20 kHz with a power of the generator of 1400 W. As shown in Figure 6b, the coil is placed at a distance of 15 mm from the surface of the specimen, to produce a magnetic field of 10 mT in the centre of the specimen. This magnetic field helps to reach the selected healing temperature (approx. 60°C), 2.5 min of induction heating (Figure 6c) were applied as healing process.

Leiva-Padilla, P., Moreno-Navarro, F., Iglesias-Salto, G., & Rubio-Gamez, M. C. (2020). Recovery capacity of electroconductive asphalt mortars under the influence of magnetic fields. *Materials Today Communications*, 101527.

DOI: <https://doi.org/10.1016/j.mtcomm.2020.101527>

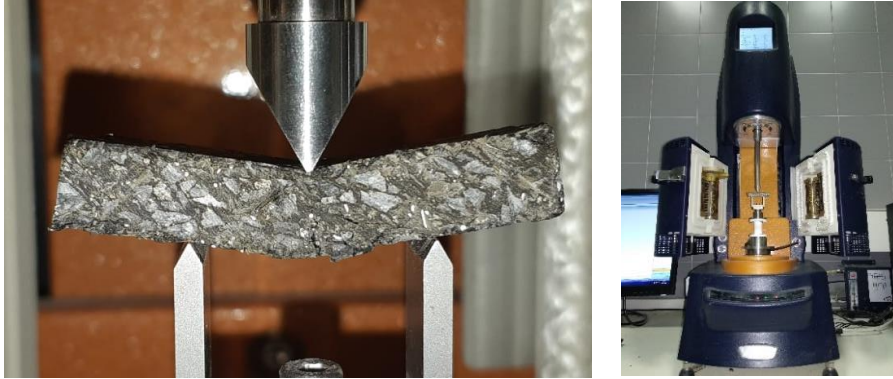
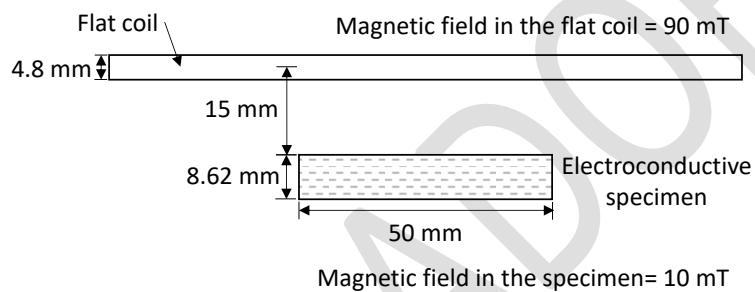


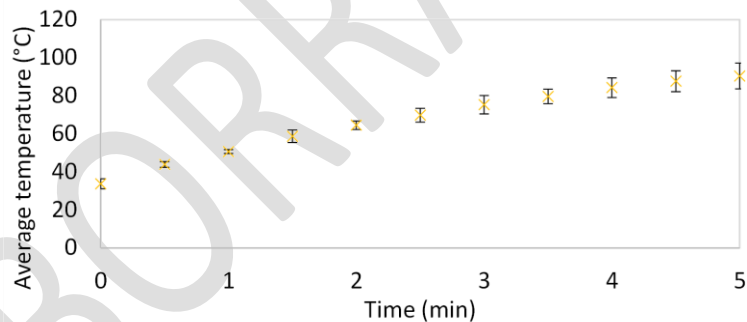
Figure 5. Dynamical Mechanical Analyzer used in the study



(a)



(b)



(c)

Figure 6. Induction heating system used (a) assembly, (b) details of the lateral view and (c) temperature reached according to the time of induction heating.

Leiva-Padilla, P., Moreno-Navarro, F., Iglesias-Salto, G., & Rubio-Gamez, M. C. (2020). Recovery capacity of electroconductive asphalt mortars under the influence of magnetic fields. *Materials Today Communications*, 101527.

DOI: <https://doi.org/10.1016/j.mtcomm.2020.101527>

6.2.2. Test 1. Healing effect after fatigue cracking failure

Test 1 was comprised the following steps, which were applied to 3 specimens for each test condition undertaken:

- Step 1: Execution of the fatigue 3-point bending test with sinusoidal displacements for an amplitude of 40 μm and frequency of 5 Hz until reaching the fatigue cracking failure, considered as the macrocracking appearance in the specimen.
- Step 2: Once the fatigue cracking failure of the specimen has been reached, 2.5-min of induction heating is applied. It is important to remark that the treatment was applied at the end of the fatigue life of the specimen, therefore the surfaces around the crack were not in contact anymore. Therefore, it was necessary to manually straighten the specimen to correctly re-join the cracked surfaces before applying the treatment.
- Step 3: Application of a 1h rest period, to reach laboratory temperature, 25°C.
- Step 4: Execution of the fatigue 3-point bending test over the same specimen but after the treatment, as well as, the determination of the following parameters:
 - %Healing_AreaT1 (Equation 1 and Figure 7a): mechanical recovery determined as the ratio of the A : area between the curve of the modulus, and the fatigue cracking failure [40], for the test b : before and a : after the application of the treatment.
 - %F_{ext}T1 (Equation 2 and Figure 7b): extension of fatigue life determined as the ratio between the N : number of cycles $bT1$: before and $aT1$: after the application of the treatment.
 - S - N curve: Stress vs Number of cycles curve for the condition before treatment.

$$\%Healing_AreaT1 = \frac{A_a}{A_b} * 100 \quad \text{Equation 1}$$

$$\%F_{ext}T1 = \frac{N_{aT1}}{N_{bT1}} * 100 \quad \text{Equation 2}$$

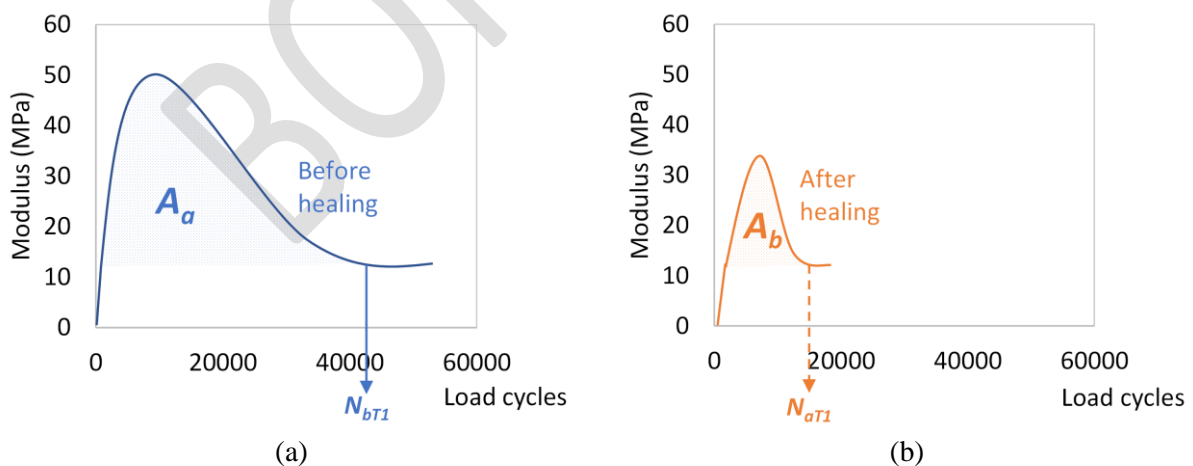


Figure 7. Schematic representation of the parameters used to determine healing in terms of the (a) area and (b) fatigue life extension

Leiva-Padilla, P., Moreno-Navarro, F., Iglesias-Salto, G., & Rubio-Gamez, M. C. (2020). Recovery capacity of electroconductive asphalt mortars under the influence of magnetic fields. *Materials Today Communications*, 101527.

DOI: <https://doi.org/10.1016/j.mtcomm.2020.101527>

6.2.3. Test 2. Healing effect before and during fatigue cracking failure

Test 2 comprised of the following steps, which were applied to 3 specimens for each test condition tested:

- Step 1, 3, 5 and 7: Application of 15000 cycles in the fatigue 3-point bending test, which corresponds to the number of cycles where the EM leaves the zone of low-cycle fatigue strength. The zone of low-cycle fatigue strength, was determined from the curve of cycles vs modulus before the treatment, obtained in Test 1. This zone represents the data after the maximum strength, but before the zone of high-cycle fatigue, where it is possible to determine the Wohler line of the material.
- Step 2, 4 and 6: Application of the treatment: (1) rest periods and (2) induction heating plus rest periods.
- Step 8: Evaluation of the percentage of healing using the energy approach and the corresponding extension of fatigue life:
 - *%Healing_AreaT2* (Equation 3 and Figure 8): mechanical recovery quantified as the ratio between the A_{aT2} : area under the curve modulus vs load cycle after each corresponding treatment, in reference to the A_{bT1} : area under the curve modulus vs load cycle before treatment in the Test 1 for 15000, 30000, 45000 and 60000 load cycles. The energy in this case was determined by the same procedure followed in Test 1.
 - *S-N curve*: Stress vs Number of cycles curves of both treatments applied.

$$\%Healing_AreaT2 = \frac{A_{aT2} - A_{bT1}}{A_{bT1}} * 100 \quad \text{Equation 3}$$

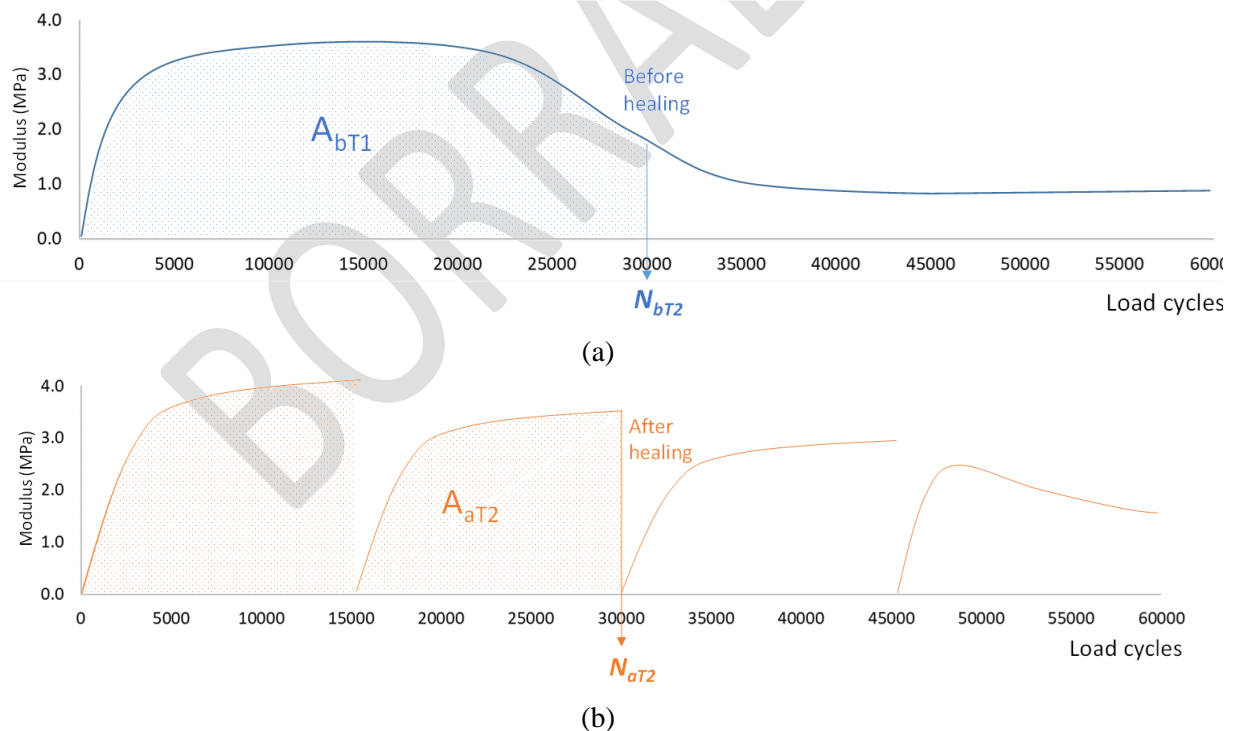


Figure 8. Schematic representation of the parameters used to determine healing in terms of the (a) area and (b) fatigue life extension

Leiva-Padilla, P., Moreno-Navarro, F., Iglesias-Salto, G., & Rubio-Gamez, M. C. (2020). Recovery capacity of electroconductive asphalt mortars under the influence of magnetic fields. *Materials Today Communications*, 101527.

DOI: <https://doi.org/10.1016/j.mtcomm.2020.101527>

7. Results and Discussion

In the first test, the values of the average modulus obtained for the specimens without and with metallic fibres (in this case, before and after the application of the treatment) are shown in Figure 9. As can be seen, even though the addition of metallic fibres reduces the value of the maximum average modulus of the asphalt mixture, the fatigue life is increased by 8%. Additionally, for the specimens with metallic fibres, it is shown just a little recovery of the average modulus by the application of induction heating treatment. This result was specifically obtained as a consequence of the straightening of the specimen, which ensured the contact of the cracked surfaces and therefore allowed the healing.

The area under each one of the curves is shown in Figure 10, as well as the corresponding percentage of healing produced and the extension of the fatigue life of the specimens, which are 14% and 19%. The paired t-test conducted to compare the results before and after the treatment revealed that with 95% confidence ($P\text{-value} < 2.4E-5$) the values differ and therefore the material had only recovered a little part of its original condition.

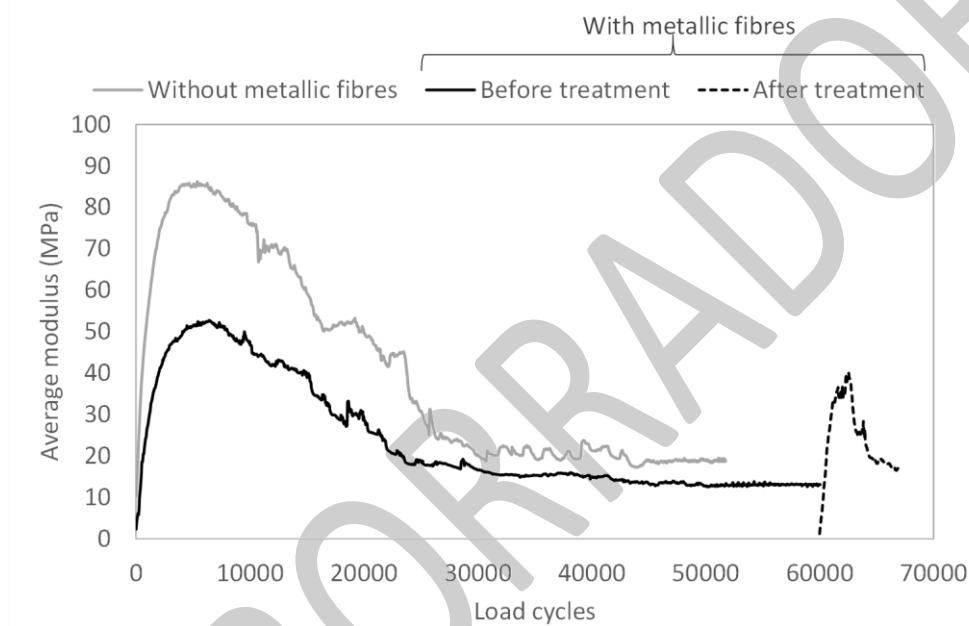


Figure 9. Average modulus values according to the load cycles for Analysis 1

Leiva-Padilla, P., Moreno-Navarro, F., Iglesias-Salto, G., & Rubio-Gamez, M. C. (2020). Recovery capacity of electroconductive asphalt mortars under the influence of magnetic fields. *Materials Today Communications*, 101527.

DOI: <https://doi.org/10.1016/j.mtcomm.2020.101527>

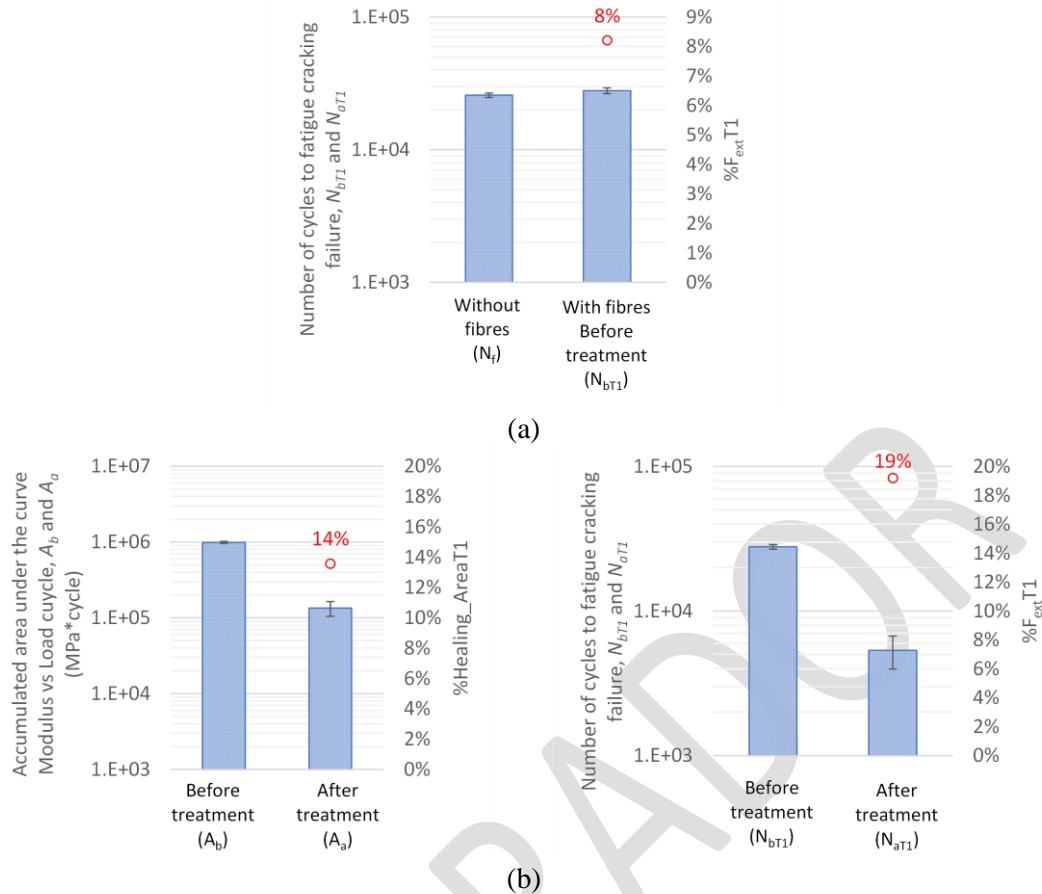
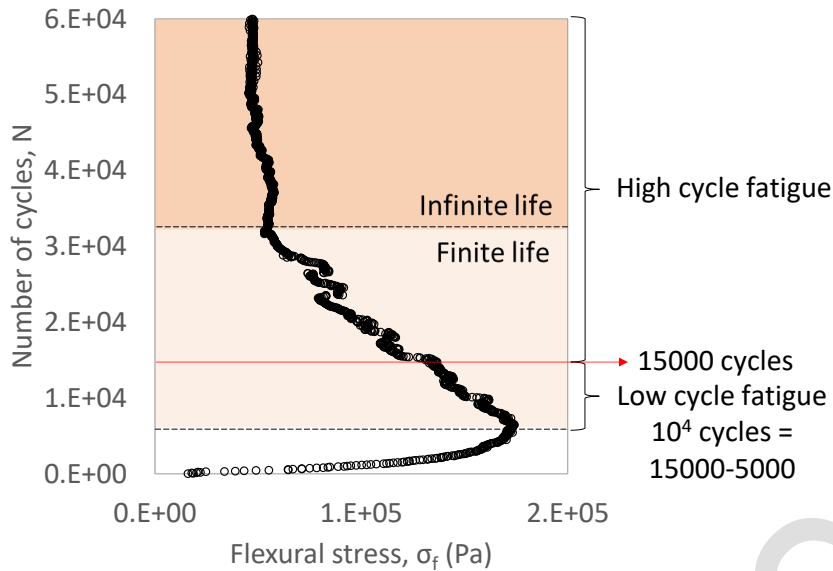


Figure 10. Average values of Analysis 1, (a) fatigue life extension by adding fibres and (b) Healing and fatigue life extension by induction heating

The flexural stress for each number of cycles curve (S-N curve) of the data before treatment is shown in Figure 11. Through the Low Cycle Fatigue (LCF) area, which was identified as 10^4 cycles after the material has reached its maximum strength value (15000 cycles - 5000 cycles), there was determined the number of cycles of the material for a specific flexural stress value, during the finite fatigue life, which is a proper moment to apply treatments. In this sense, considering that microcracks mainly happens before the LCF, it was determined 15000 cycles as the proper fatigue life moment when to apply the preventive treatment in Test 2.

Leiva-Padilla, P., Moreno-Navarro, F., Iglesias-Salto, G., & Rubio-Gamez, M. C. (2020). Recovery capacity of electroconductive asphalt mortars under the influence of magnetic fields. *Materials Today Communications*, 101527.

DOI: <https://doi.org/10.1016/j.mtcomm.2020.101527>



(a)

Figure 11. Stress-Number of cycles data for EM before treatment for Test 1 (35°C and 5Hz)

Figure 12 shows the normalized values of the average modulus for every 15000 cycles of load for the condition before (continuous line) and after (dashed lines) each treatment. As the figure shows, the curves tend to be flattened with the number of cycles applied, as might be predicted by the damage produced during testing.

The calculation of the area under each one of the curves is shown in Figure 13, along with the corresponding percentage of recovery ($\%Healing_AreaT2$) after each application of treatment. As it is possible to see in Figure 13a in the case of the treatment with Rest Periods, the percentages of healing are 14%, 19% and 16%, this means that 14% of the recovery was reached in the first time of application of Rest periods. Due to these percentages are calculated from the accumulated areas under the curve of modulus, just a 5% of healing, resulted from 19% minus 14%, is produced in the second application of the treatment. For the third application of the treatment, there was a loss of 5% in the total healing reached, going back to an accumulated percentage of healing of 14%.

In the case of the combination of Induction heating and Rest periods, the percentages of healing displayed in Figure 13b were 25%, 29% and 32%. This implies that the combination of Induction heating and Rest periods produces 11% of more healing than only Rest periods. Additionally, the second application of the treatment produced an additional 4% of healing, and the third application a 3% more for a total healing of 32%.

From the results obtained from both treatments, it is observed that most of the healing was obtained during the microcrack phase, which corresponds to the first application of the treatments. As well, by looking at the difference between the percentage values at the end of the test, half of the accumulated healing recovered have been due to the effect of induction heating and a half to the rest periods. An ANOVA conducted to compare the results revealed that with 95% confidence, both treatments produce significant healing (P-

Leiva-Padilla, P., Moreno-Navarro, F., Iglesias-Salto, G., & Rubio-Gamez, M. C. (2020). Recovery capacity of electroconductive asphalt mortars under the influence of magnetic fields. *Materials Today Communications*, 101527.

DOI: <https://doi.org/10.1016/j.mtcomm.2020.101527>

value = $7.2E-4$), which is significantly different at each time the treatment was applied (P-value = $2.9E-3$). The Honest Significant Difference test reveals that each treatment produced a significant recovery by itself (P-value = $6.1E-3$), without any significant additional recovery during the second and third application of the treatment, which correspond to the macrocrack level (P-value = $2.7E-3$).

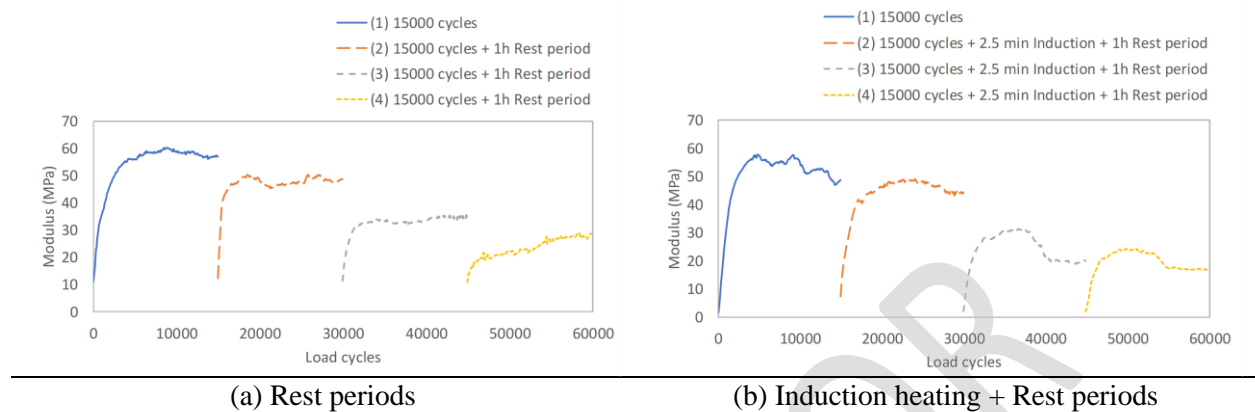


Figure 12. Normalized values of the average modulus per cycle for Analysis 2

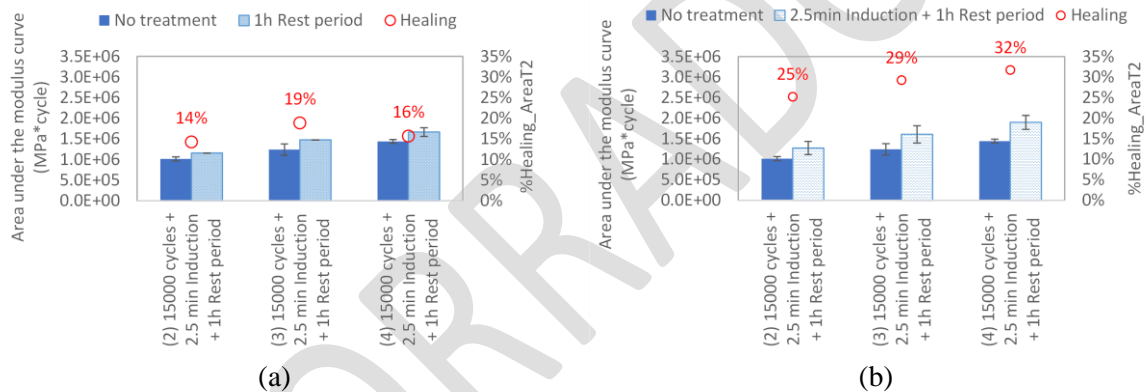


Figure 13. Healing for the treatments: (a) Rest periods and (b) Induction heating + Rest periods

Figure 14 shows the S-N data for each treatment. By comparing both lines with the material without treatment in Figure 11, at flexural stress of 0.16 MPa, selected to have an easy point to compare the curves, the fatigue cycles are 17% higher for Rest periods treatments and 40% higher for Induction heating plus Rest periods. Therefore, the application of both treatments produces an extension in the fatigue life of the specimen.

Leiva-Padilla, P., Moreno-Navarro, F., Iglesias-Salto, G., & Rubio-Gamez, M. C. (2020). Recovery capacity of electroconductive asphalt mortars under the influence of magnetic fields. *Materials Today Communications*, 101527.

DOI: <https://doi.org/10.1016/j.mtcomm.2020.101527>

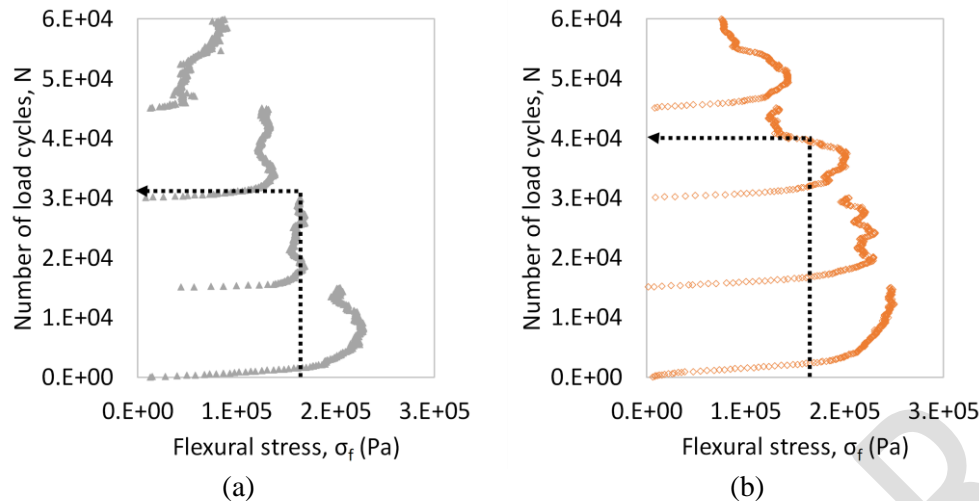


Figure 14. Stress range S-N data for EM for Test 2 (35°C and 5Hz) (a) Rest periods and (b) Induction heating + Rest periods

8. Conclusions

The present study evaluated the recovery capacity to fatigue cracking of EM, after the application of two different treatments along the fatigue life of the material: 1) rest periods and 2) induction heating plus rest periods. The key conclusions that can be drawn from this work are as follows:

- The application of multiple treatments along the fatigue life of the specimen along with the determination of the LCF to determine the first application of them, allows to understand that most of the healing can be enhanced during the microcrack phase of testing. This is mainly due to the small size of the cracks in this phase, which can be easily sealed at temperatures over the softening point of the asphalt binder, followed by a rest period to allow the binder flow and fill the crack. Recognizing that the increase in temperature produced in EM is directly dependent on the time of application of a changing magnetic field, and that a specific temperature the flow of the binder is produced, the healing could be optimised by considering both parameters during the design of the treatment to apply.
- Despite the application of induction heating at the macrocrack stage can enhance the healing capacity of EM, the contribution obtained is considerably low in comparison to the one reached at the microcrack stage.
- The smallest steel fibres obtained from recycling plants and rich content of asphalt binder, allows the production of homogeneous enough EM to be used in the construction of stress relief asphalt interlayer systems of flexible pavements. The stress relief asphalt interlayer systems are characterized to be very thin (between 20 mm and 30 mm) high flexible asphalt mixture layers, composed by fine aggregates (less than 9.5 mm) and high contents of asphalt (higher than 7%). These conditions give to the interlayers the capacity to absorb part of the vertical and horizontal movements of the cracked surfaces, reducing the shear stresses in the interface and finally delaying the reflection of cracks. Additionally, due to the high content of asphalt used in its production, these systems also work as a moisture barrier, which protects the existing pavement structure from water damage.
- Future recommended research work includes the evaluation of alternative materials such as graphene, carbon nanotubes, steel slag, and ferrite filler, amongst others. Moreover, the effect of ageing, moisture damage, and the corresponding optimum times to design the pavement

Leiva-Padilla, P., Moreno-Navarro, F., Iglesias-Salto, G., & Rubio-Gamez, M. C. (2020). Recovery capacity of electroconductive asphalt mortars under the influence of magnetic fields. *Materials Today Communications*, 101527.

DOI: <https://doi.org/10.1016/j.mtcomm.2020.101527>

management system required along service life would need to be considered. As a final step, a field test track would be needed to validate and adjust the results for the final design and construction guidelines for the proper placement of these materials.

Acknowledgments

The research presented in this paper was carried out as part of the H2020-MSCA-ETN-2016. This project has received funding from the European Union's H2020 Programme for research, technological development, and demonstration under grant agreement number 721493.

The research is also part of the NARESPAV project, which has been financed by the "European Regional Development Fund" (ERDF), managed by the State Program of Research, Development and Innovation Oriented to the Challenges of Society within the framework of the State Plan for Scientific and Technical Research and Innovation 2013-2016 (2016 call), with number RTC-2016-5154-4.

References

- [1] H. Di Benedetto, Q. T. Nguyen, and C. Sauzéat, "Nonlinearity, heating, fatigue and thixotropy during cyclic loading of asphalt mixtures," *Road Mater. Pavement Des.*, 2011.
- [2] F. Moreno-Navarro and M. C. Rubio-Gómez, "A review of fatigue damage in bituminous mixtures: Understanding the phenomenon from a new perspective," *Constr. Build. Mater.*, vol. 113, pp. 927–938, Jun. 2016.
- [3] H. Di Benedetto, C. De La Roche, H. Baaj, A. Pronk, and R. Lundström, "Fatigue of bituminous mixtures," *Mater. Struct. Constr.*, 2004.
- [4] F. Moreno-Navarro, M. Sol-Sánchez, and M. C. Rubio-Gómez, "Exploring the recovery of fatigue damage in bituminous mixtures: the role of healing," *Road Mater. Pavement Des.*, 2015.
- [5] P. Ayar, F. Moreno-Navarro, M. Sol-Sánchez, and M. C. Rubio-Gómez, "Exploring the recovery of fatigue damage in bituminous mixtures: the role of rest periods," *Mater. Struct. Constr.*, 2018.
- [6] A. Tabaković and E. Schlangen, "Self-healing technology for asphalt pavements," in *Advances in Polymer Science*, 2016.
- [7] H. Fischer, "Self-repairing material systems—a dream or a reality?," *Nat. Sci.*, 2010.
- [8] S. Shen, X. Lu, Y. Zhang, and R. Lytton, "Fracture and Viscoelastic Properties of Asphalt Binders During Fatigue and Rest Periods," *J. Test. Eval.*, 2014.
- [9] P. Ayar, F. Moreno-Navarro, and M. C. Rubio-Gómez, "The healing capability of asphalt pavements: A state of the art review," *J. Clean. Prod.*, 2016.
- [10] Q. Lv, W. Huang, X. Zhu, and F. Xiao, "On the investigation of self-healing behavior of bitumen and its influencing factors," *Mater. Des.*, 2017.
- [11] D. Sun, G. Sun, X. Zhu, F. Ye, and J. Xu, "Intrinsic temperature sensitive self-healing character of asphalt binders based on molecular dynamics simulations," *Fuel*, 2018.
- [12] Q. Liu, Á. García, E. Schlangen, and M. van de Ven, "Induction healing of asphalt mastic and porous asphalt concrete," *Constr. Build. Mater.*, vol. 25, no. 9, pp. 3746–3752, Sep. 2011.
- [13] J. Norambuena-Contreras and A. Garcia, "Self-healing of asphalt mixture by microwave and induction heating," *Mater. Des.*, vol. 106, pp. 404–414, Sep. 2016.
- [14] S. Xu, A. García, J. Su, Q. Liu, A. Tabaković, and E. Schlangen, "Self-Healing Asphalt Review: From Idea to Practice," *Advanced Materials Interfaces*. 2018.
- [15] M. Vila-Cortavitarte, D. Jato-Espino, A. Tabakovic, and D. Castro-Fresno, "Optimizing the valorization of industrial by-products for the induction healing of asphalt mixtures," *Constr. Build. Mater.*, vol. 228, p. 116715, Dec. 2019.

Leiva-Padilla, P., Moreno-Navarro, F., Iglesias-Salto, G., & Rubio-Gamez, M. C. (2020). Recovery capacity of electroconductive asphalt mortars under the influence of magnetic fields. *Materials Today Communications*, 101527.

DOI: <https://doi.org/10.1016/j.mtcomm.2020.101527>

- [16] B. Shu et al., “Synthesis and properties of microwave and crack responsive fibers encapsulating rejuvenator for bitumen self-healing,” *Mater. Res. Express*, 2019.
- [17] Á. García, E. Schlangen, M. van de Ven, and Q. Liu, “A simple model to define induction heating in asphalt mastic,” *Constr. Build. Mater.*, vol. 31, pp. 38–46, Jun. 2012.
- [18] J. Tang, Q. Liu, S. Wu, Q. Ye, Y. Sun, and E. Schlangen, “Investigation of the optimal self-healing temperatures and healing time of asphalt binders,” *Constr. Build. Mater.*, vol. 113, pp. 1029–1033, Jun. 2016.
- [19] H. Li et al., “Study on the gradient heating and healing behaviors of asphalt concrete induced by induction heating,” *Constr. Build. Mater.*, vol. 208, pp. 638–645, May 2019.
- [20] Á. García, “Self-healing of open cracks in asphalt mastic,” *Fuel*, vol. 93, pp. 264–272, Mar. 2012.
- [21] R. N. Traxler, *Asphalt: Its composition, properties, and uses*. 1961.
- [22] Y. Hou, L. Wang, T. Pauli, and W. Sun, “Investigation of the asphalt self-healing mechanism using a phase-field model,” *J. Mater. Civ. Eng.*, 2015.
- [23] F. Moreno-Navarro, G. R. Iglesias, and M. C. Rubio-Gómez, “Development of mechanomutable asphalt binders for the construction of smart pavements,” *Mater. Des.*, vol. 84, pp. 100–109, Nov. 2015.
- [24] P. Leiva-Padilla, F. Moreno-Navarro, G. R. Iglesias, and M. C. Rubio-Gómez, “Analysis of the mechanical response of asphalt materials manufactured with metallic fibres under the effect of magnetic fields,” *Smart Mater. Struct.*, 2019.
- [25] F. Moreno-Navarro, G. R. Iglesias, and M. C. Rubio-Gómez, “Mechanical performance of mechanomutable asphalt binders under cyclic creep and recovery loads,” *Constr. Build. Mater.*, vol. 113, pp. 506–512, Jun. 2016.
- [26] H. Zhao, S. Zhong, X. Zhu, and H. Chen, “High-efficiency heating characteristics of ferrite-filled asphalt-based composites under microwave irradiation,” *J. Mater. Civ. Eng.*, 2017.
- [27] M. M. Karimi, M. K. Darabi, H. Jahanbakhsh, B. Jahangiri, and J. F. Rushing, “Effect of steel wool fibers on mechanical and induction heating response of conductive asphalt concrete,” *Int. J. Pavement Eng.*, 2019.
- [28] A. Menozzi, A. Garcia, M. N. Partl, G. Tebaldi, and P. Schuetz, “Induction healing of fatigue damage in asphalt test samples,” *Constr. Build. Mater.*, vol. 74, pp. 162–168, Jan. 2015.
- [29] L. F. Walubita and A. E. Martin, “Comparison of Fatigue Analysis Approaches for Predicting Fatigue Lives of Hot-Mix Asphalt (HMAC) Mixtures,” *Civ. Eng.*, 2006.
- [30] Q. Liu, E. Schlangen, and M. Van De Ven, “Induction healing of porous asphalt,” *Transp. Res. Rec.*, 2012.
- [31] X. Zhu, Y. Cai, S. Zhong, J. Zhu, and H. Zhao, “Self-healing efficiency of ferrite-filled asphalt mixture after microwave irradiation,” *Constr. Build. Mater.*, vol. 141, pp. 12–22, Jun. 2017.
- [32] M. Skaf, J. M. Manso, Á. Aragón, J. A. Fuente-Alonso, and V. Ortega-López, “EAF slag in asphalt mixes: A brief review of its possible re-use,” *Resour. Conserv. Recycl.*, vol. 120, pp. 176–185, May 2017.
- [33] F. Moreno-Navarro, G. R. Iglesias, and M. C. Rubio-Gómez, “Experimental evaluation of using stainless steel slag to produce mechanomutable asphalt mortars for their use in smart materials,” *Smart Mater. Struct.*, 2016.
- [34] F. Moreno-Navarro, G. R. Iglesias, and M. C. Rubio-Gómez, “Encoded asphalt materials for the guidance of autonomous vehicles,” *Autom. Constr.*, vol. 99, pp. 109–113, Mar. 2019.
- [35] E. Jeoffroy, F. Bouville, M. Bueno, A. R. Studart, and M. N. Partl, “Iron-based particles for the magnetically-triggered crack healing of bituminous materials,” *Constr. Build. Mater.*, vol. 164, pp. 775–782, Mar. 2018.
- [36] D. N. Little and J. C. Petersen, “Unique effects of hydrated lime filler on the performance-related properties of asphalt cements: Physical and chemical interactions revisited,” *J. Mater. Civ. Eng.*, 2005.
- [37] F. Miranda-Argüello, L. Loria-Salazar, J. P. Aguiar-Moya, and P. Leiva-Padilla, *Measurement of G* in fine asphalt mixes: Dynamic mechanical analyzer shear test implementation*, vol. 2507. 2015.

Leiva-Padilla, P., Moreno-Navarro, F., Iglesias-Salto, G., & Rubio-Gamez, M. C. (2020). Recovery capacity of electroconductive asphalt mortars under the influence of magnetic fields. *Materials Today Communications*, 101527.

DOI: <https://doi.org/10.1016/j.mtcomm.2020.101527>

[38] L. Fang, Q. Yuan, D. Deng, Y. Pan, and Y. Wang, "Effect of mix parameters on the dynamic mechanical properties of cement asphalt mortar," *J. Mater. Civ. Eng.*, 2017.

[39] Q. Fu, Y. Xie, G. Long, D. Niu, and H. Song, "Dynamic mechanical thermo-analysis of cement and asphalt mortar," *Powder Technol.*, 2017.

[40] H. Wang, J. Yang, G. Lu, and X. Liu, "Accelerated Healing in Asphalt Concrete via Laboratory Microwave Heating," *J. Test. Eval.*, 2020.

BORRADOR

